REPORT NO.
UC SESM-70-19

STRUCTURES AND MATERIALS RESEARCH
DEPARTMENT OF CIVIL ENGINEERING

# FINITE ELEMENT STUDY OF REINFORCED CONCRETE BEAMS WITH DIAGONAL TENSION CRACKS

by

D. NGO

H. A. FRANKLIN

A. C. SCORDELIS

Report to
National Science Foundation
NSF Grant GK-1809

DECEMBER 1970

COLLEGE OF ENGINEERING
UNIVERSITY OF CALIFORNIA
BERKELEY CALIFORNIA

Structures and Materials Research
Department of Civil Engineering
Division of Structural Engineering
and
Structural Mechanics

Report No. UC SESM 70-19

# FINITE ELEMENT STUDY OF REINFORCED CONCRETE BEAMS WITH DIAGONAL TENSION CRACKS

by

D. Ngo
Junior Specialist

H.A. Franklin
Assistant Specialist

A.C. Scordelis
Professor of Civil Engineering

Prepared under the sponsorship of
National Science Foundation
Grant GK-1809

College of Engineering
Office of Research Services
University of California
Berkeley, California

December 1970

## ABSTRACT

Reinforced concrete beams with varying amounts of cracking are analyzed by a finite element method. Progression of the diagonal crack is simulated and the analysis offers information concerning the state of the stresses at the various cracking stages. Beams with and without web reinforcement are examined and compared for the same cracking conditions. The effects of aggregate interlock, horizontal splitting, and extended shear span are also briefly studied.

The disturbance of the diagonal crack is found to be quite localized and the stresses have a very similar pattern at the early stage of cracking for both beams with and without web reinforcement. But as the diagonal crack progresses, the stress distributions for the two beam types begin to differ more and more from each other.

Part of the behavior found in the finite element analyses can be explained by the concept of "arch" and "beam" actions advanced by various investigators. It is found that the web reinforcement has the additional benefit of limiting the principal tensile stress in the concrete in the vicinity of the crack to a constant maximum level. Two zones in which the web reinforcement are essentially ineffective are shown to exist. Another interesting finding for the beam analyzed is that the aggregate interlock tends to increase, rather than decrease, the dowel shear. An attempt is made to correlate the interrelationship among the diagonal cracking, aggregate interlocking and horizontal splitting, based on the results of the present investigations.

## KEY WORDS

Reinforced concrete beam; diagonal crack; finite element; computer analysis; bond link; dowel shear; dowel tension; effective dowel length; aggregate interlock; horizontal splitting; longitudinal reinforcement; web reinforcement; longitudinal stress; shear stress; principal stresses.

# TABLE OF CONTENTS

# LIST OF FIGURES

# 1. INTRODUCTION

## 1.1 Nature of the Problem

Many attempts have been made in the past several decades to investigate experimentally as well as analytically the behavior of reinforced concrete beams under load. Depsite all of these efforts, a complete understanding of the problem has not yet been fully achieved. The main difficulties may be attributed to the following factors:

a) The inherent nature of the material inhomogeneity and non-linearity of the concrete.

b) The lack of an adequate failure theory for concrete under combined stresses.

c) The intricate interaction between the concrete and the steel.

d) The not yet well-understood nature of the bond force, bond slip, dowel force, and aggregate interlocking.

e) The continuously changing topology of the structure as cracks propagate.

Furthermore, all of these factors are not independent; they are closely interrelated to each other. This fact tends to make the problem even more unamenable to solution, since it is often difficult to single out any one particular factor for individual examination either experimentally or analytically.

However, the need for a rational theory for reinforced concrete members has not been unrecognized as indicated by the extensive research work in this area. Some of this research will be briefly

reviewed in the next section.

This report will deal only with a limited aspect of the overall problem. It will concentrate on the relative contributions of the uncracked concrete section, the dowel action, the aggregate interlock, and the vertical stirrups to the total shear capacity of a reinforced concrete beam with a diagonal tension crack.

## 1.2 Previous Studies

A large portion of the previous research work on reinforced concrete beam problems has been concerned with the question of shear failure. A classical summary of this research has been presented by ACI-ASCE Committee 326 [1]. A more recent account has been given by Bresler and MacGregor [2]. Some of the more recent contributions in the field of reinforced concrete research which are closely related to the subject of the present investigation are briefly reviewed in the following sections.

### 1.2.1 Acharya and Kemp [3]

The contribution of dowel force to the shear carrying capacity of reinforced concrete beams without web reinforcement has been examined by Acharya and Kemp. The stresses at the top of the shear crack were calculated based upon several assumptions (Fig. 1.1). Strain readings were also obtained from actual beam tests. It was found that the effect of the diagonal tension crack was to reduce significantly the depth of the compression zone. By assuming the dowel force to be zero, Acharya and Kemp found that under ultimate load, the calculated combined stress level was too high according to the failure criteria suggested by Bresler and Pister [4] and thus the beams should

have failed at a lower load than found experimentally. This fact led to the conclusion that dowel force should not be neglected in the consideration of shear failure in reinforced concrete beams.

The presence of the dowel force reduces the shear $S_1$ and the moment $M_1$ at a vertical section at the top of the crack (Fig. 1.1). These reduced values are given by the following equations:

$$S_1 = W - D \tag{1.1a}$$

$$M_1 = C_1 h = Wa - De \tag{1.1b}$$

Unfortunately, the magnitude of the dowel force, D, was not measured by Acharya and Kemp. An assumed dowel force of 60% of the total shear W was chosen instead. With this added assumption, the calculated stresses were found to be in better agreement with the available failure criteria.

### 1.2.2 Krefeld and Thurston [5]

A series of 10 interesting tests on the dowel action in reinforced concrete beams were carried out by Krefeld and Thurston. The specially manufactured beam specimens are shown in Fig. 1.2. Nine of the specimens are of the type shown in Fig. 1.2(a), and one of Fig. 1.2(b). In the first type, the applied load is carried by the dowel action alone, thus it permits the evaluation of the effect of bar size and thickness of concrete coverage under the reinforcement on the dowel force carried. The beam of the second type was intended to measure the contribution of the dowel force to the total shear force. It was found that, for beams of the first type, the shear force resisted by the longitudinal reinforcing bars decreased with an increase of distance from the crack to support, and increased with

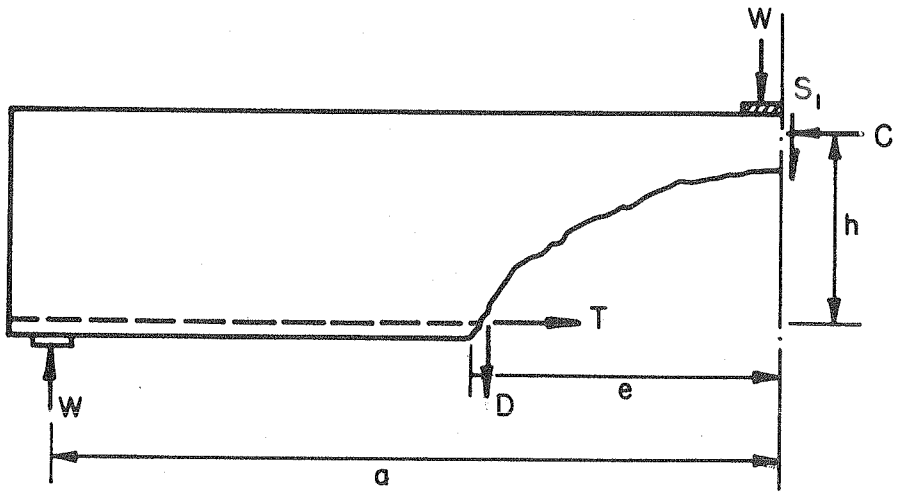


FIG. I.1 BEAM STUDIED BY ACHARYA AND KEMP [3]

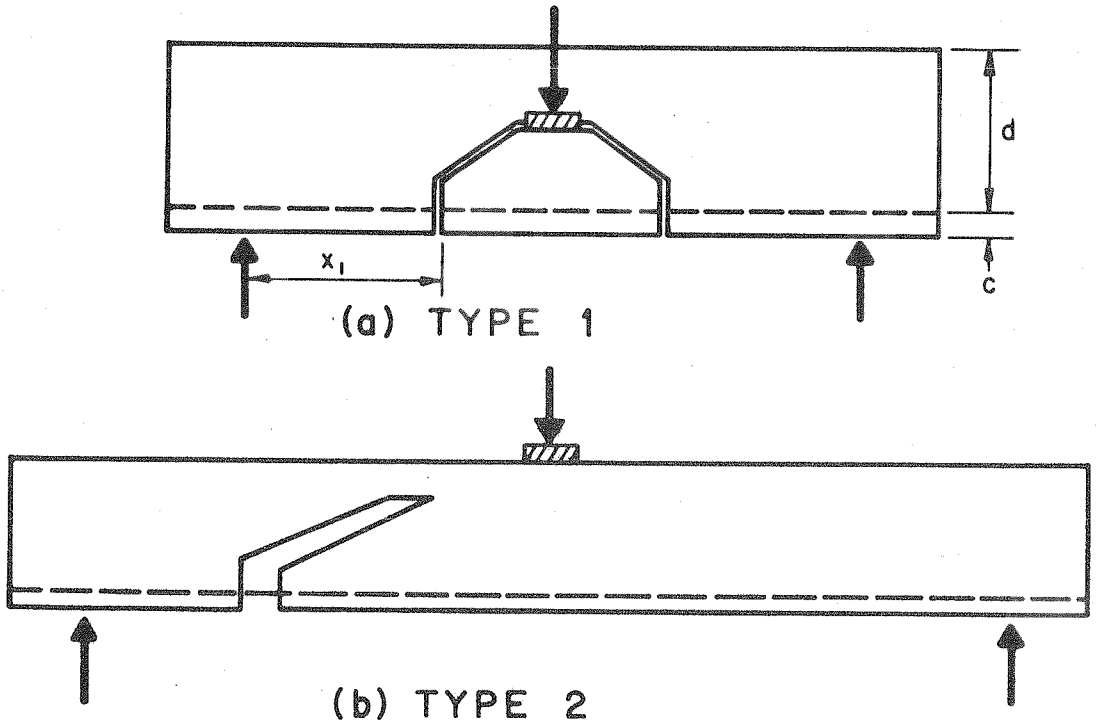


FIG. I.2 BEAMS STUDIED BY KREFELD AND THURSTON [5]

larger concrete coverage. An expression for the dowel shear, $V_1$, was derived by Krefeld and Thurston:

$$V_1 = b\sqrt{f'_c}\ \left[1.3\ \left(1 + \frac{180\ p}{\sqrt{f'_c}}\right)\ c + d\right] \frac{1}{\sqrt{x_1/d}} \qquad (1.2)$$

where c was taken as the distance from the center of the single layer of bars to the bottom surface, and $x_1$ was the distance from the support to the crack section, see Fig. 1.2(a).

In the second type of beam, it was found that the dowel shear increased as the applied load was increased, and reached as high as 65% of total shear in the ultimate condition. This finding is in contradiction to the general belief that the dowel force decreases as the applied load approaches the ultimate condition.

It should be noted that all of the beams tested for dowel force by Krefeld and Thurston may not model actual reinforced concrete beams accurately, because of the nature of the preformed cracks. Particularly in the second beam type where the crack width was too large to be considered realistic. Nevertheless, the results of such tests offer additional insight into the nature of dowel action.

### 1.2.3 MacGregor and Walters [6]

An analytical model was devised by MacGregor and Walters. The beam was assumed to fail after the formation of inclined cracks. The stresses were calculated based upon ordinary beam theory. The iterative calculation procedure was done with the aid of a computer and is best illustrated by the flow diagram in Fig. 1.3. The predicted crack patterns were close to those observed experimentally in specimens tested by Bresler and Scordelis [7]. It was found that the

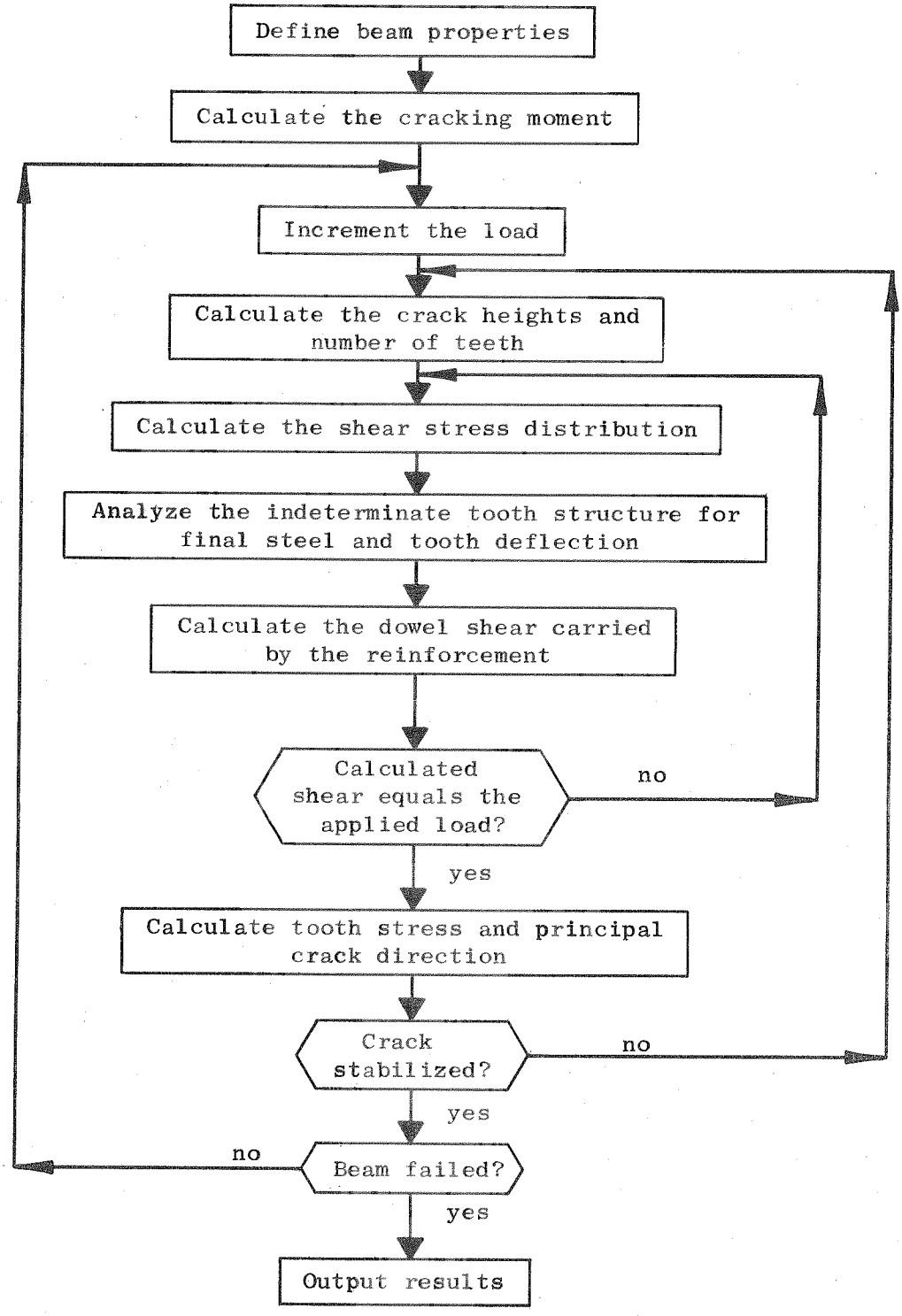


FIG. 1.3 FLOW CHART AFTER MAC GREGOR AND WALTERS [6]

inclined cracking load was affected by the concrete strength in about the same way as indicated by the ACI Code design equation, $v_c = 2\sqrt{f'_c}$ . However, the effect of steel percentage was found to be greater than that suggested by the ACI Code equation, $v_c = 1.9\sqrt{f'_c} + \frac{2500pVd}{M}$ .

In this study, the crack spacing was assumed to be two times the distance from the tensile face of the beam to the centroid of the longitudinal steel reinforcement. Even though it is generally believed that the spacing of flexural cracks influences the diagonal tension cracking load, MacGregor and Walters contended that in the practical range of crack spacing, this effect was not pronounced.

1.2.4 Taylor [8]

Another series of six beam tests were carried out by Taylor. An ingenious method of computing the direct and shear stresses in the compression zone of the reinforced concrete beams was also developed:

$$\tau_{xy} = \int_0^y \frac{\partial \sigma_x}{\partial x}\, dy = \int_0^y \frac{\partial \sigma_x}{\partial M}\,\frac{\partial M}{\partial x}\, dy = \int_0^y E_c\,\frac{\partial \epsilon_x}{\partial M}\, V\, dy \qquad (1.3)$$

where $\tau_{xy}$ is the shear stress; $\frac{\partial \epsilon_x}{\partial M}$ the slope of the $\epsilon_x$ - M plot; $E_c$ the modulus of elasticity of concrete; V the shear due to applied load; and y the distance from the compression face.

By comparing the resulting stresses with the shear-compression failure criteria of Bresler and Pister [4] and of Reeves [9], it was found that the breakdown of the dowel force by horizontal splitting of the concrete along the steel level was a significant cause of the failure of the beams. The dowel force was believed to provide a

significant contribution to the balance of internal moment, and became an important factor in considering shear failure of beams without web reinforcement.

### 1.2.5 Fenwick and Paulay [10]

One of the most comprehensive investigations of the mechanism of shear resistance in concrete beams was recently carried out by Fenwick and Paulay. Particular attention was given to the experimental evaluation of aggregate interlock. The test arrangement used is shown in Fig. 1.4. Influence of the concrete strength $f'_c$, and the crack width c, on the shearing stress $v_{ai}$ transmitted across the crack were studied. From a regressional analysis, the following relationship was developed:

$$v_{ai} = \frac{467}{c} - (8410)\ (0.0225\sqrt{f'_c} - 0.409)\ (\delta_s - 0.0436\ c) \qquad (1.4)$$

where $\delta_s$ is the shear displacement across the crack.

A number of dowel tests were also performed, Fig. 1.5. It was found that the contribution of the dowel section of the flexural reinforcement was greatly influenced by the position of the bars at the time of placing the concrete, and that the dowel action is not likely to resist more than 20% of the bond force in a beam without web reinforcement. Semi-empirical equations were also formulated, which enabled the contribution of the dowel action to be assessed. But this prediction could only be regarded as the upper limit of the dowel action.

### 1.2.6 Gergely [11]

The splitting cracks along the main reinforcement in concrete beams, the dowel action and the influence of the aggregate interlock

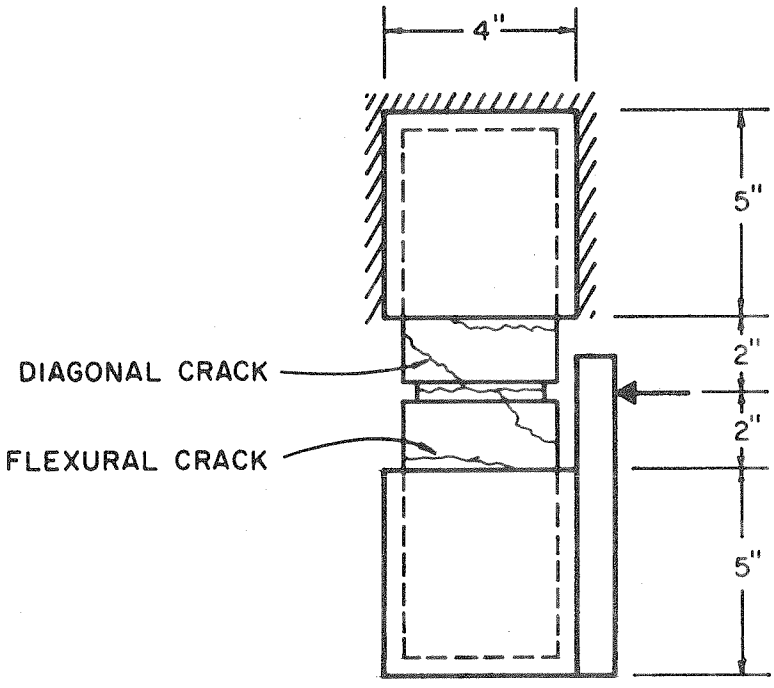


FIG. I.4 TEST ARRANGEMENT FOR AGGREGATE INTERLOCK USED BY FENWICK AND PAULAY [10]

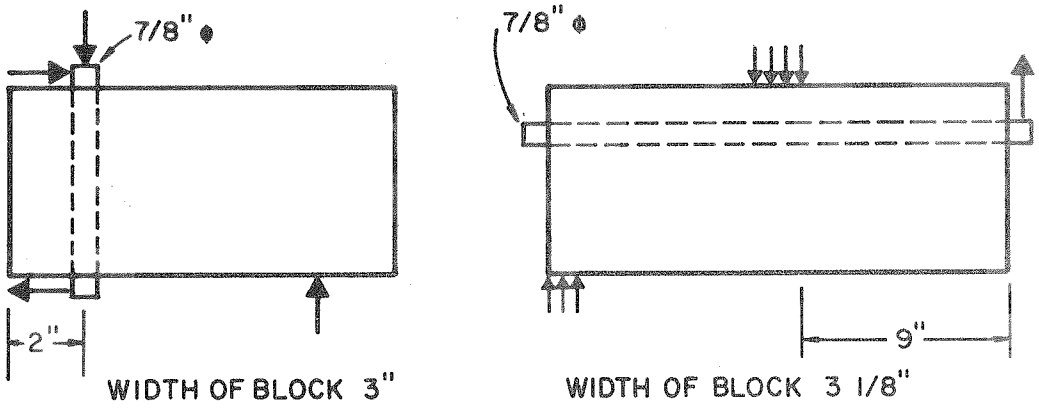


SHORT DOWELS LONG DOWELS

FIG. I.5 TEST ARRANGEMENTS FOR DOWEL FORCE USED BY FENWICK AND PAULAY [10]

were examined by Gergely. Sketches of the experimental set-ups used are shown in Fig. 1.6. A theoretical study utilizing the finite element method was also performed to investigate the splitting stresses at a "beam-end" (Fig. 1.7) under the following four loading conditions: a) pullout; b) pullout and wedging; c) dowel; d) pullout, wedging, and dowel.

It was concluded that the dowel force is the most important factor producing splitting in beams without web reinforcement. However, the dowel capacity of beams was found to be limited. In carrying the external shear, the aggregate interlock contributed about 40 to 60% of the total shear, while the dowel force was about 20 to 25%. The remaining 20 to 30% of the total shear was taken by the compressive concrete block above the crack tip. Attention was also called to the wedging action which caused high circumferential and radial stresses around the reinforcing bars at the transverse cracks. These stresses, together with dowel action, dominated the splitting mechanism.

## 1.3 Dowel Force, Aggregate Interlock, and Bond

From the brief survey presented, it is evident that the contributions of the dowel force and of the aggregate interlock to the total shear carrying capacity of reinforced concrete beams are very important and should not be ignored. However, the conclusions advanced by the various investigators are not in complete agreement with respect to the percentage of total shear carried by dowel action and the amount of aggregate interlock existing in the various cases.

It can be seen that there is no simple method by which the contribution of dowel action and aggregate interlock can be assessed

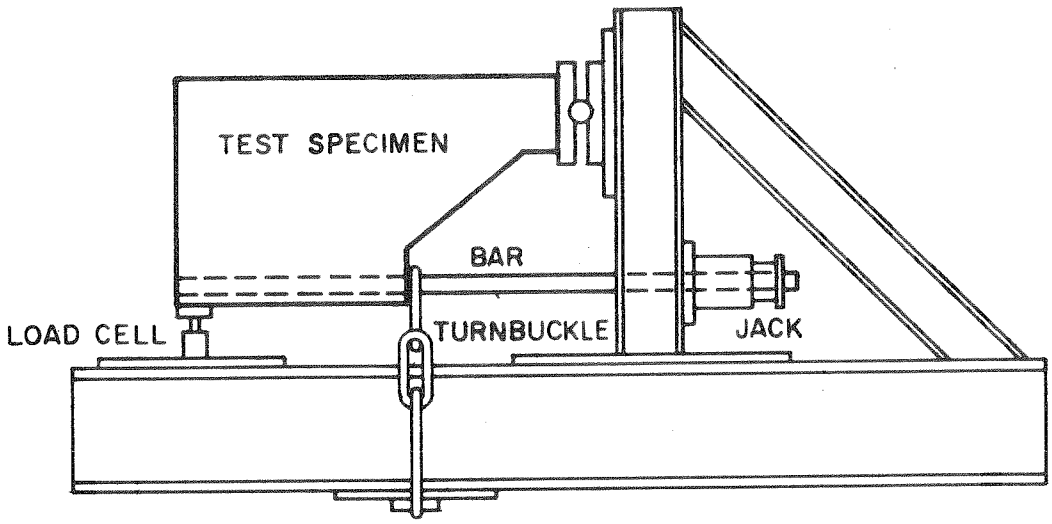


(a) BEAM AND TESTING ARRANGEMENT

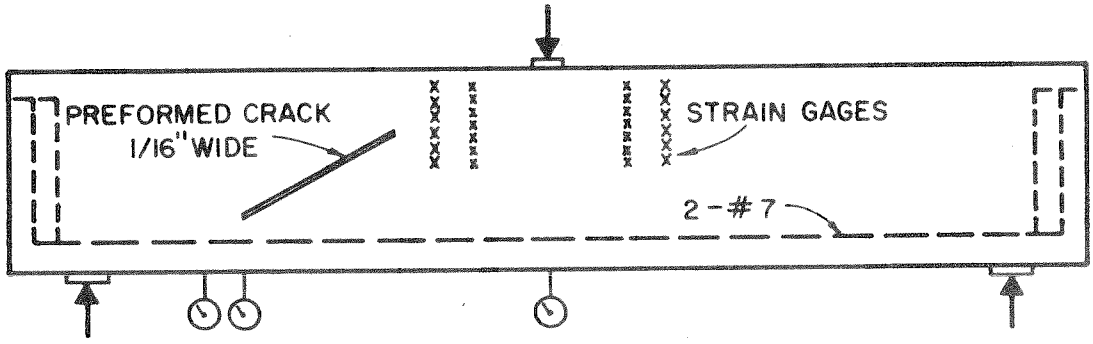


(b) AGGREGATE INTERLOCKING TEST

FIG. I.6 EXPERIMENTAL SETUPS USED BY GERGELY [11]

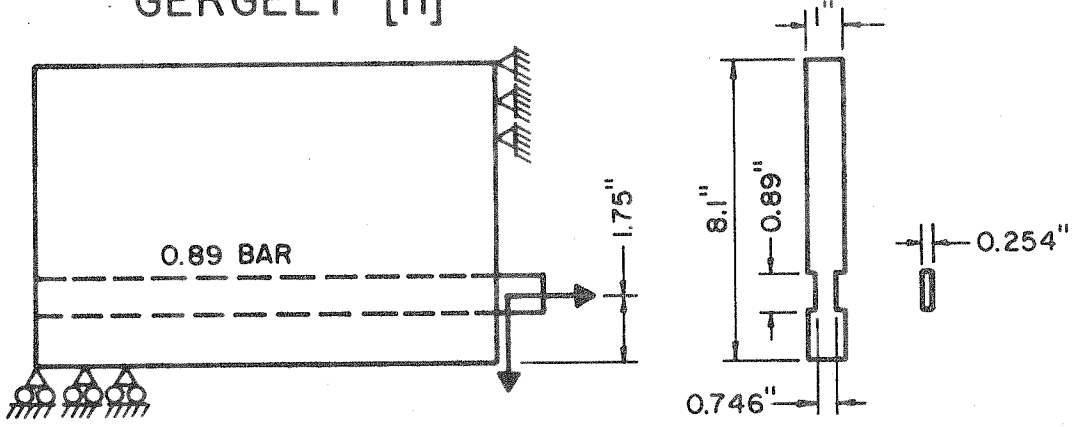


FIG. I.7 MODEL USED FOR ANALYSIS BY GERGELY [11]

experimentally, despite the many ingenious schemes which have been devised. The same can be said about bond stress and bond slip. Furthermore, it is very difficult to experimentally measure these quantities without interfering with the true behavior in a real beam. In addition, the variables affecting these quantities are numerous, and a comprehensive experimental program for the study of all these factors can become an enormous undertaking.

As an alternate and complementary approach to an experimental investigation, theoretical studies may be made using refined analytical models based on the finite element method. Solutions to some problems of particular interest can then be obtained with the aid of a high speed digital computer.

## 1.4 Objective and Scope

This report will present the results of a series of analyses of cracked reinforced concrete beams. A finite element model was employed. Cracks were predefined in a manner closely representing actual cracks observed in an experimental study on a full scale beam specimen.

For the sake of simplicity, all material properties were assumed to be linearly elastic. This assumption may appear to be questionable, especially at the level where the applied load has caused a predominant diagonal tension crack to occur. Nevertheless, the basic response of reinforced concrete beams with a diagonal crack under such an assumption should add to the further understanding of the behavior of cracked reinforced concrete beams.

In the present study, particular attention is given to the contribution of the dowel force and the effect of aggregate interlock. Normal and shearing stresses in concrete will also be examined. The influence of the shear span and splitting along the longitudinal reinforcement will be briefly investigated.

# 2. METHOD OF ANALYSIS

## 2.1 Finite Element Method

The finite element method can be thought of as a numerical procedure by means of which the solution of a problem in continuum mechanics can be approximated by analyzing a structure consisting of an assemblage of finite elements interconnected at a finite number of nodal points, in which selected internal stress or displacement patterns are assumed in the elements to satisfy certain required conditions. With such a discretization, a problem in solid mechanics is transformed into a related problem of an articulated structure which can be readily analyzed by the standard matrix methods of structural analysis. Details of the finite element method can be found in a text by Zienkiewicz and Cheung [12]. Pertinent discussion of the method employed in the present investigation can be found in the reports by Wilson [13], Sandhu et al. [14].

## 2.2 Beam Modeling

Because of the great versatility of the finite element method, application of the method has been extended to the analysis of reinforced concrete beams. The first application was made by Ngo and Scordelis [15], in which a cracked reinforced concrete beam was analyzed assuming it to be linearly elastic. Non-linear analysis of reinforced concrete members has been carried out by Nilson [16], and by Franklin [17], as well as others. Essential features of the finite element model used for reinforced concrete beams are summarized in the following sections.

### 2.2.1 Plane Stress Analysis

One of the basic assumptions made in the present method of investigation is that the behavior of a reinforced concrete beam can be adequately represented in terms of a two-dimensional stress state. Plane stress analysis can then be performed. The reinforcement is assumed to be uniformly distributed across the width of the cross-section. In other words, the steel is transformed into a layer having a width equal to that of the beam, by modifying the modulus of elasticity of the steel, Fig. 2.1. A beam of unit width can then be analyzed by the plane stress method.

### 2.2.2 Bond and Bond Slip

In ordinary reinforced concrete structures, the interaction of the steel reinforcement and the concrete is achieved by means of bond. The mechanism of bond can be attributed to two factors: chemical bond and mechanical interlock between the steel and the concrete. Some investigators believe that chemical bond is destroyed at a quite early stage of loading, and therefore, the mechanical interlock is the prime factor responsible for the composite action between the steel and the concrete. Consequence of this fact is that slippage between the steel and the concrete takes place. This slippage is commonly called bond slip. To simulate this effect, a device called a linkage element was developed by Ngo and Scordelis [15]. These linkage elements connect the nodes of the steel and concrete finite elements. At the same time, they permit a certain degree of relative movement between steel and concrete which represents bond slip, Fig. 2.2. The chief advantage of this type of

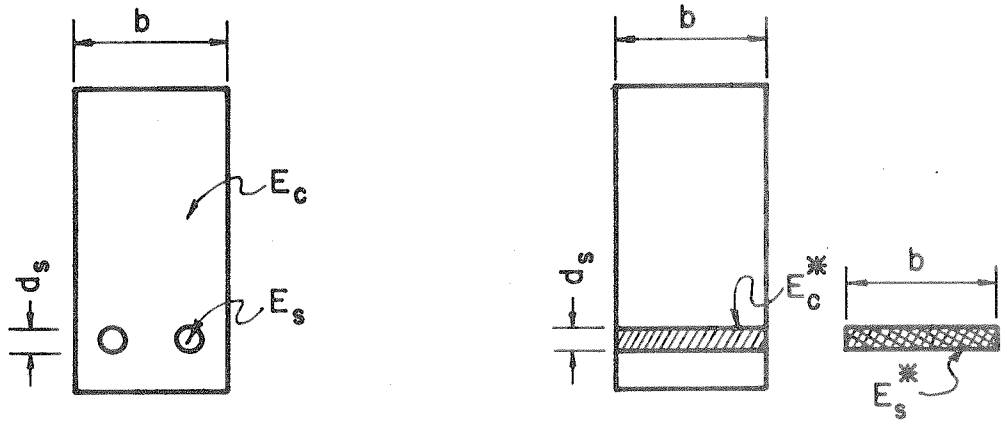


FIG. 2.1 CROSS-SECTIONAL TRANSFORMATION

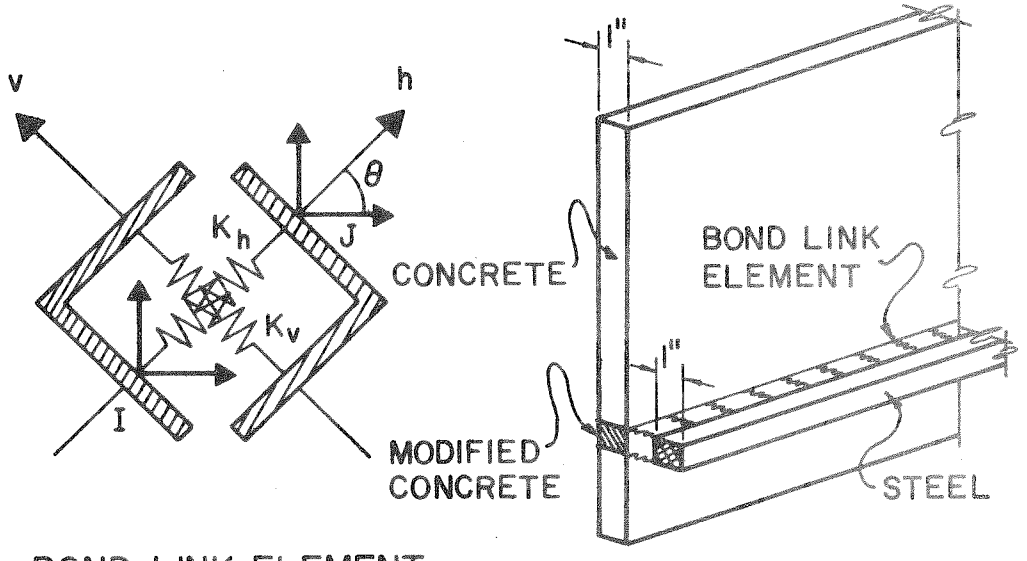


BOND LINK ELEMENT

FIG. 2.2 LINKAGE ELEMENT TO SIMULATE BOND

linkage element is that it has no physical dimensions. Therefore, its presence does not alter the actual geometry of the beam under consideration.

The amount of relative movement or slippage between the steel and the concrete for a given loading condition is, of course, dependent on the stiffnesses $K_h$ and $K_v$ assigned to the linkage elements. These values must reflect the actual bond slip relationship in a real beam. Unfortunately, accurate quantitative information from experimental studies is meager on this subject. Nilson [16] has interpreted the experimental results of Bresler and Bertero [18], and derived a second degree polynomial expression to relate bond force and bond slip. However, to be consistent with the linear analysis to be used in the present study, constant values are assigned to the stiffness $K_h$ and stiffness $K_v$. In other words, a linear bond slip relationship was assumed for the beams under investigation in this report.

### 2.2.3 Representation of Cracks

In the present investigation, the shape and location of the cracks were predefined. The representation of such cracks in a finite element model amounts to nothing more than assigning a separate node on each side of the crack, Fig. 2.3. The width of the cracks is zero when there is no applied load. In other words, the pair of nodes on each side of the cracks have the same coordinates. The ability of varying the topological property (connectivity) without altering the geometrical (shape and size) and physical (E, $\nu$) properties of the beams is another attractive feature of the finite element

model used in this investigation.

### 2.2.4 Aggregate Interlock

The physical meaning of assigning a node on each side of the crack is simply that the finite elements on one side of the crack can move freely with respect to the elements on the other side. For ordinary cracking problems, this representation will suffice. However, cracking in reinforced concrete members is more than a simple separation of physical entities. Transmission of forces and restraint of movements in some directions exist across the crack, due to the aggregate interlocking. The concrete elements on both sides of the cracks are not completely disconnected.

The exact behavior of the aggregate interlocking is still largely unknown. Yet its effect on the dowel action and the overall load carrying capacity of the reinforced concrete beams is important. More experimental evidence is needed. The contribution of Fenwick and Paulay [10] is particularly significant in this respect.

In the finite element modeling of reinforced concrete beams, the aggregate interlock may be simulated by the linkage elements. A linkage element can be attached to the nodes across the crack as shown in Fig. 2.4. A zero stiffness is assigned to $K_v$ normal to the crack, whenever the crack is assumed to be open. However, a similar difficulty is encountered here, as in the case of bond linkage in assigning an appropriate value to the stiffness $K_h$ parallel to the crack to represent the aggregate interlock. Such values cannot be obtained readily experimentally. While this value varies with load, for the sake of simplicity, a constant value was assumed in the present investigation.

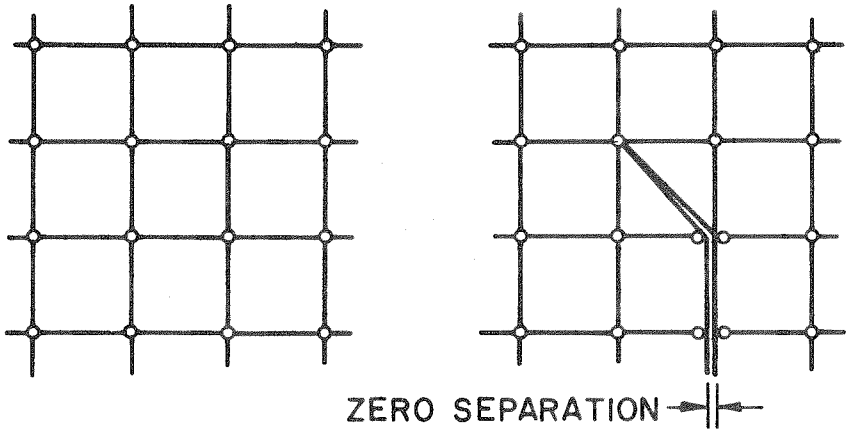


FIG. 2.3 CRACK REPRESENTATION

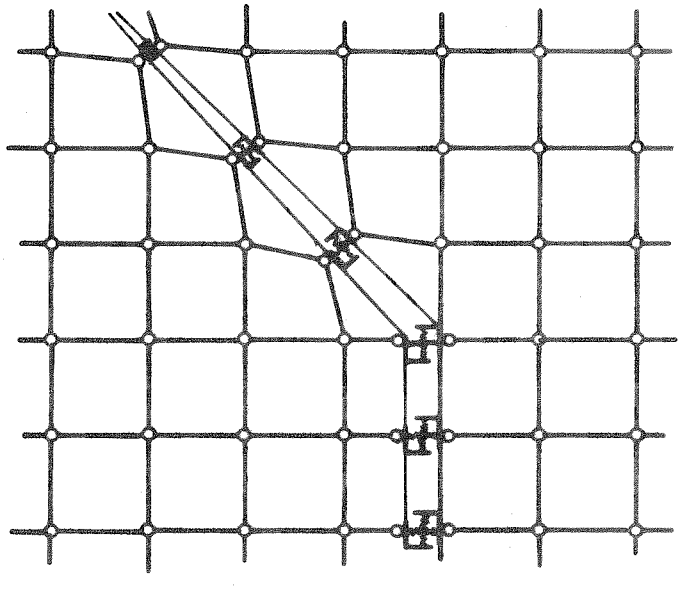

FIG. 2.4 REPRESENTION OF AGGREGATE INTERLOCK

### 2.2.5 Effective Dowel Length

The transverse shear force carried by the longitudinal steel reinforcement at the section through a crack is known as dowel force or dowel shear. By modeling the longitudinal steel reinforcement as a series of two-dimensional finite elements as shown in Fig. 2.5, such dowel force can be obtained directly from a computer analysis. However, attention must be given to the fact that the magnitude of the resulting dowel force depends on many factors. In the present analytical model, a factor of particular importance is the effective dowel length.

The effective dowel length at a cracked section, as indicated in Fig. 2.5, is defined as the gage length between the nodes which are connected to the concrete elements. It is not difficult to see that the stiffness of a particular dowel section is inversely proportional to the effective dowel length.

Physically, the effective dowel length represents the distance in which bonding has been destroyed. Unfortunately, there is no simple way by which the effective dowel length can be determined a priori. In the present investigation, the effective dowel length was taken to be two inches; one inch away from the crack on each side of the cracked section.

### 2.2.6 Web Reinforcement

To simulate web reinforcement or stirrups, one-dimensional bar elements were used. These elements were attached to the nodes as shown in Fig. 2.6. When a crack crossed the bar elements, the connections were omitted for those nodes at the crack. This arrangement is similar to that of effective dowel length, except here the

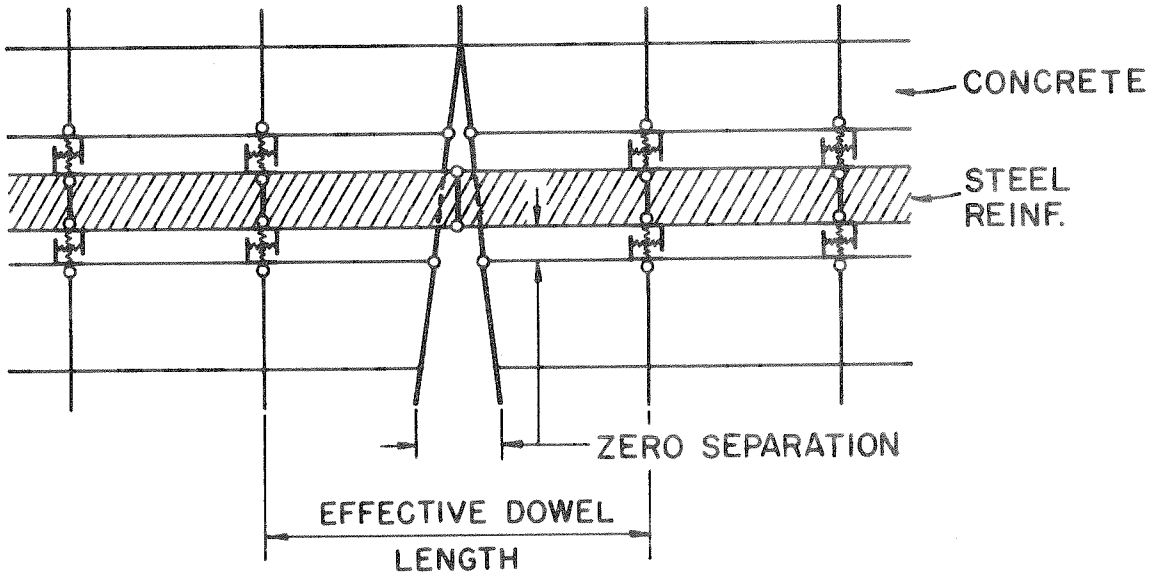


FIG. 2.5 EFFECTIVE DOWEL LENGTH

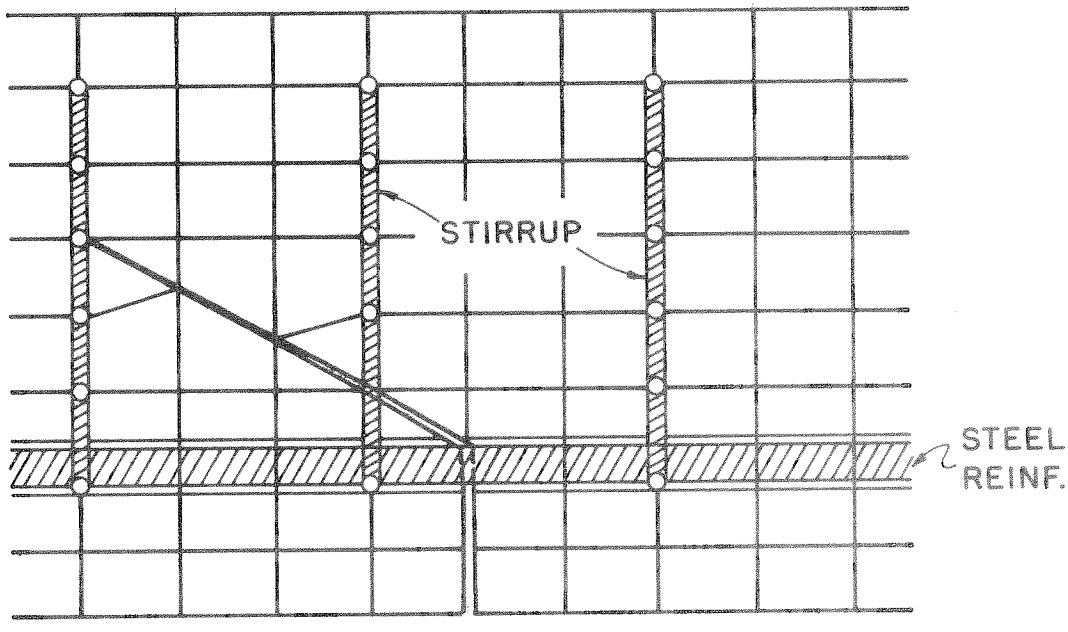


FIG. 2.6 WEB REINFORCEMENT REPRESENTATION

gage length is no longer constant, but depends upon the spacing of the nodal points in the original layout of the finite elements. This, again, is merely a simplified assumption for the convenience of carrying out the computer analysis.

In general practice, the web reinforcement is bent around the longitudinal steel bars. To reflect this situation, the one-dimensional stirrup bar elements were attached directly to the bottom nodes of the longitudinal steel reinforcement elements.

Similar to the case of longitudinal reinforcement, the web reinforcement was assumed to be uniformly distributed over the beam width. Thus the cross-sectional area of the one-dimensional bar elements was obtained by dividing the actual total cross-sectional area of the stirrups by the width of the beam.

## 2.3 Remarks on the Types of Finite Element Used

Questions often arise in the interpretation of the final results obtained from the finite element analysis. Among many considerations, one important point must be recognized is the type of finite element used. In the earlier work by Ngo and Scordelis [15], constant strain triangular elements were used, Fig. 2.7(a). While this type of element is very simple to form, a fine mesh is necessary in order to obtain an accurate result, due to the inherent nature of the constant strain field within each element. Nilson [16] employed a quadrilateral element which consists of four constant strain triangles, Fig. 2.7(b). By taking the average values of these four subelements, the results are improved. In the present investigation, a quadrilateral element consisting of two constrained linear strain triangles,

Fig. 2.7(c), was used. This type of refined element produces much more accurate results, especially for the shearing stress, and also the formation time within the computer is not excessive.

Undoubtedly, other more refined finite elements will be experimented with in future research. However, a balance must be achieved between the desirable accuracy and the computational effort. Refined elements yield more accurate results for the same mesh size but tend to increase the computer running time. Selection of the proper types of element to be used is one of the important problems to be decided upon when performing a finite element analysis.

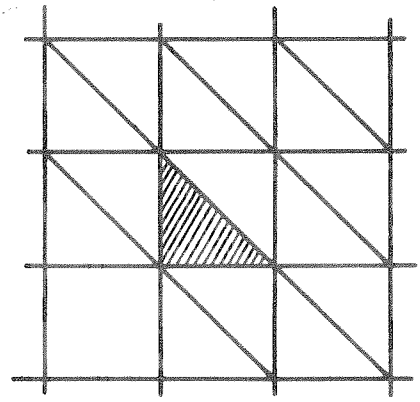

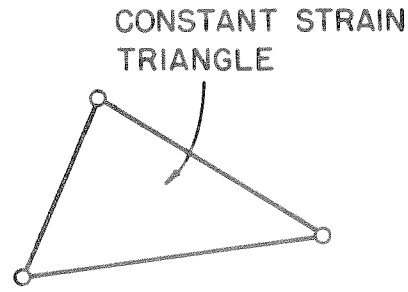


(a) CONSTANT STRAIN TRIANGLE

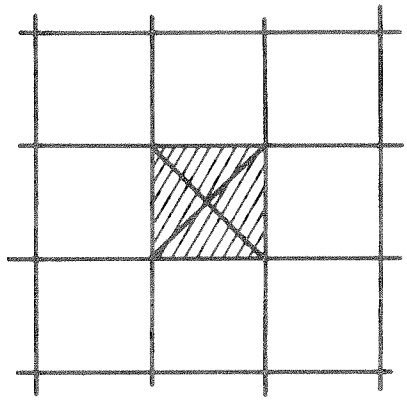

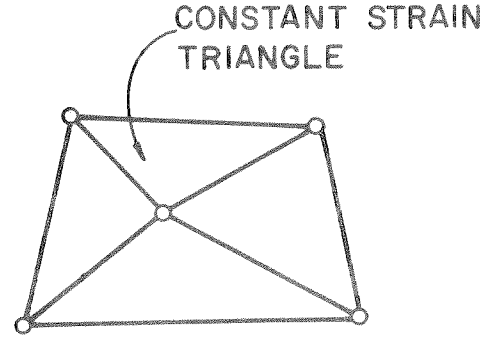


(b) QUADRILATERAL ELEMENT

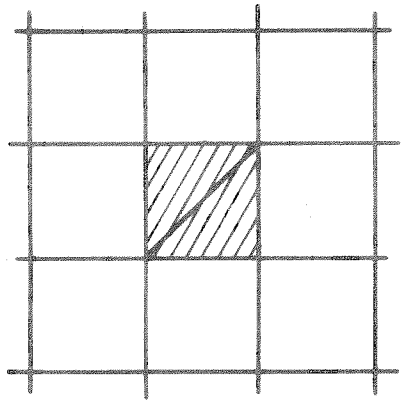

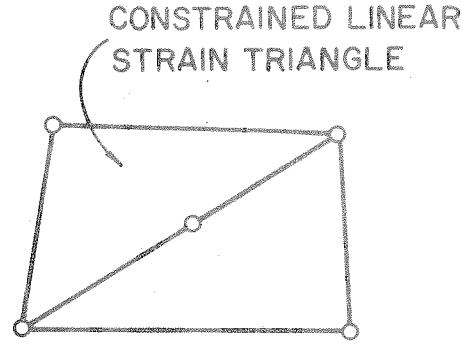


(c) QUADRILATERAL ELEMENT

FIG. 2.7 TYPE OF FINITE ELEMENT USED

# 3. SELECTION OF BEAM SPECIMENS

## 3.1 General Consideration

It is obvious that due to the limitation of linearity and the various constraints imposed in the analytical model used, no detailed quantitative comparison with actual experimental results is possible. However, if the specimens selected for analysis closely resemble those used in an experimental study, important qualitative information about the behavior of the beams can be obtained. Therefore, it is highly desirable to select a specimen which closely simulates a beam tested in a laboratory. For the present purposes of analysis, the main concern in selecting beam specimens is that the beam dimensions, amount of steel reinforcement, and predominant crack pattern is similar to that of the test beams.

## 3.2 Selected Beam Specimens

The beams selected for the present investigation correspond to Beam XOB-1 and Beam XB-1 tested by Bresler and Scordelis [7]. The actual beam dimensions are shown in Fig. 3.1. These two beams have identical concrete dimensions and main longitudinal reinforcement. The only difference is that Beam XB-1 has web reinforcement, while Beam XOB-1 has not. The beams are simply supported and subjected to a concentrated load at the midspan.

## 3.3 Predefined Crack Pattern

By examining the experimental cracking history of Beam XOB-1, as shown in Fig. 3.2, it can be seen that a predominant diagonal crack has taken place. Such a diagonal crack was also visible in the case of Beam XB-1, Fig. 3.3. Even though the crack patterns of

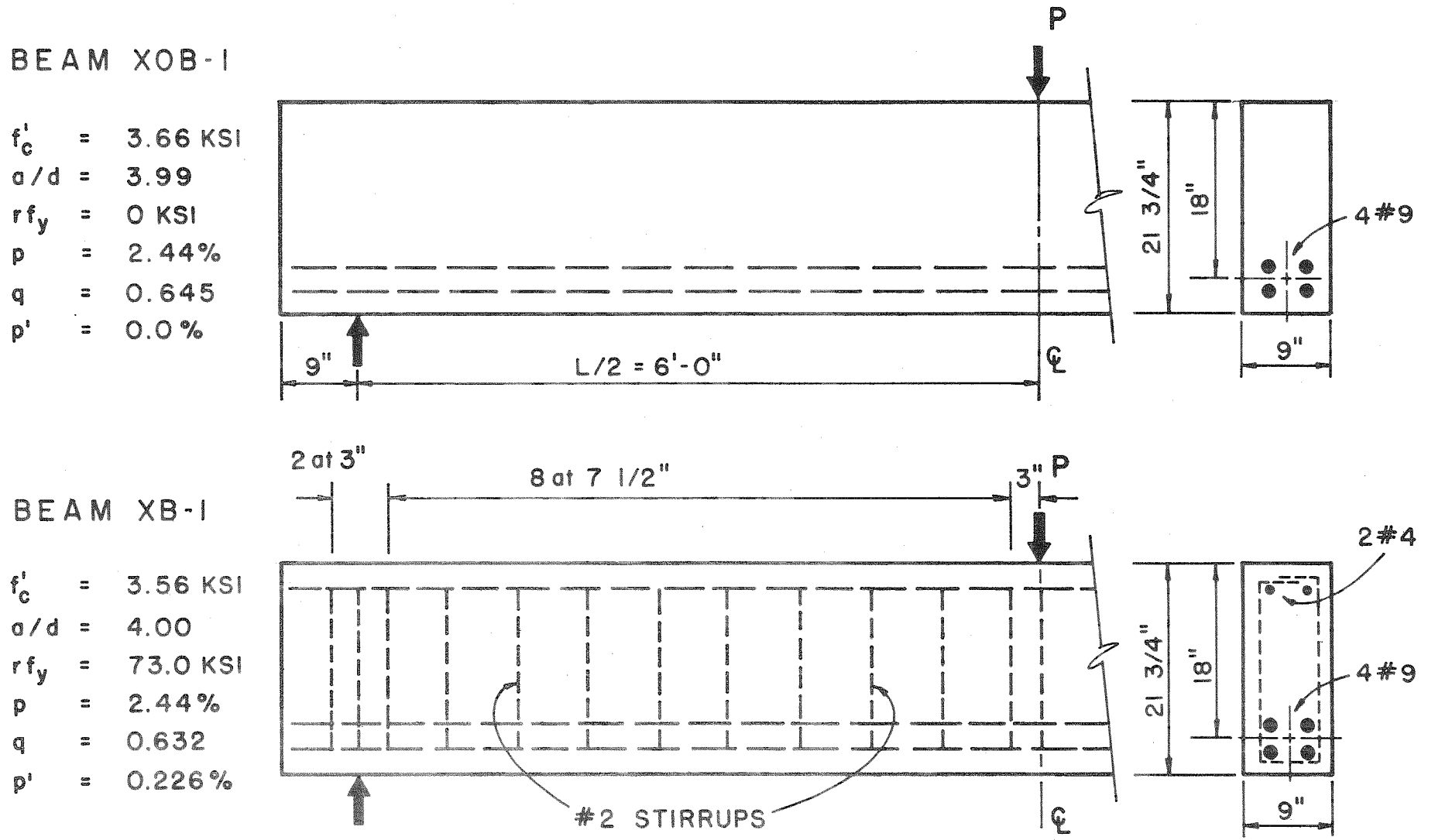


FIG. 3.1 SERIES X BEAM DIMENSIONS AND PROPERTIES
AFTER BRESLER AND SCORDELIS [7]

these two beams are not identical, because of the influence of web reinforcement in one of the beams, only the predominant diagonal crack was included in the analytical model for the present studies. Furthermore, the curved diagonal crack was idealized into three linear segments as shown in Fig. 3.4. Note that symmetry of the beam and the cracks were assumed, thus only half of the beam had to be analyzed, as presented in the subsequent sections.

## 3.4 Discussion

The main idea behind the selection of the beam specimens for the present study is simplicity. Simplicity is aimed at not only for the sake of ease in modeling, but also for the ease in interpreting the final results in terms of the predominant behavior involved. Therefore, some idealizations were necessary.

The drastic transformation of the crack pattern from the real beams to the analytical model cannot be considered as a divorce from reality. In the first place, a crack of this nature is not at all unusual for reinforced concrete beams having a shear span to depth ratio, a/d, greater than 2.5. Secondly, the study is confined to the question of what effects does a diagonal crack have as it gradually develops. Therefore, such an idealization is not unreasonable.

It is more important to keep in mind that each crack does not develop independently of other cracks. This aspect was not included in the present study. But it should be noted that it presents no additional conceptual difficulty in the analytical method employed.

It is also quite possible to approximate the shape of the curved diagonal crack to any desired accuracy. But this would generally require a finer mesh layout. Consequently, the computational effort would be sharply increased. More discussion on the finite element modeling of the beam specimens will be presented in the next chapter.

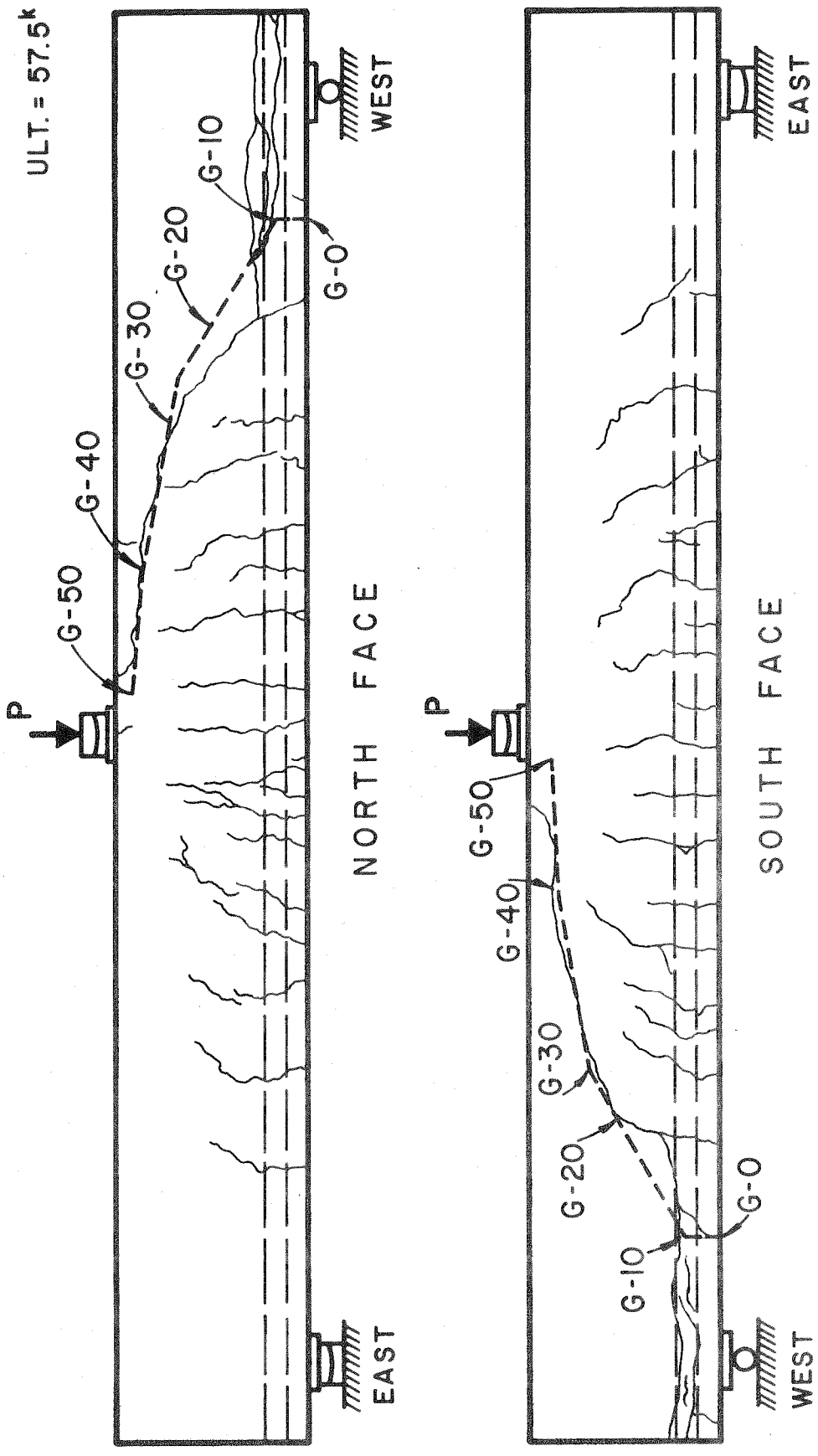


FIG. 3.2 CRACK PATTERN OF BEAM XOB-1
AFTER BRESLER AND SCORDELIS [7]

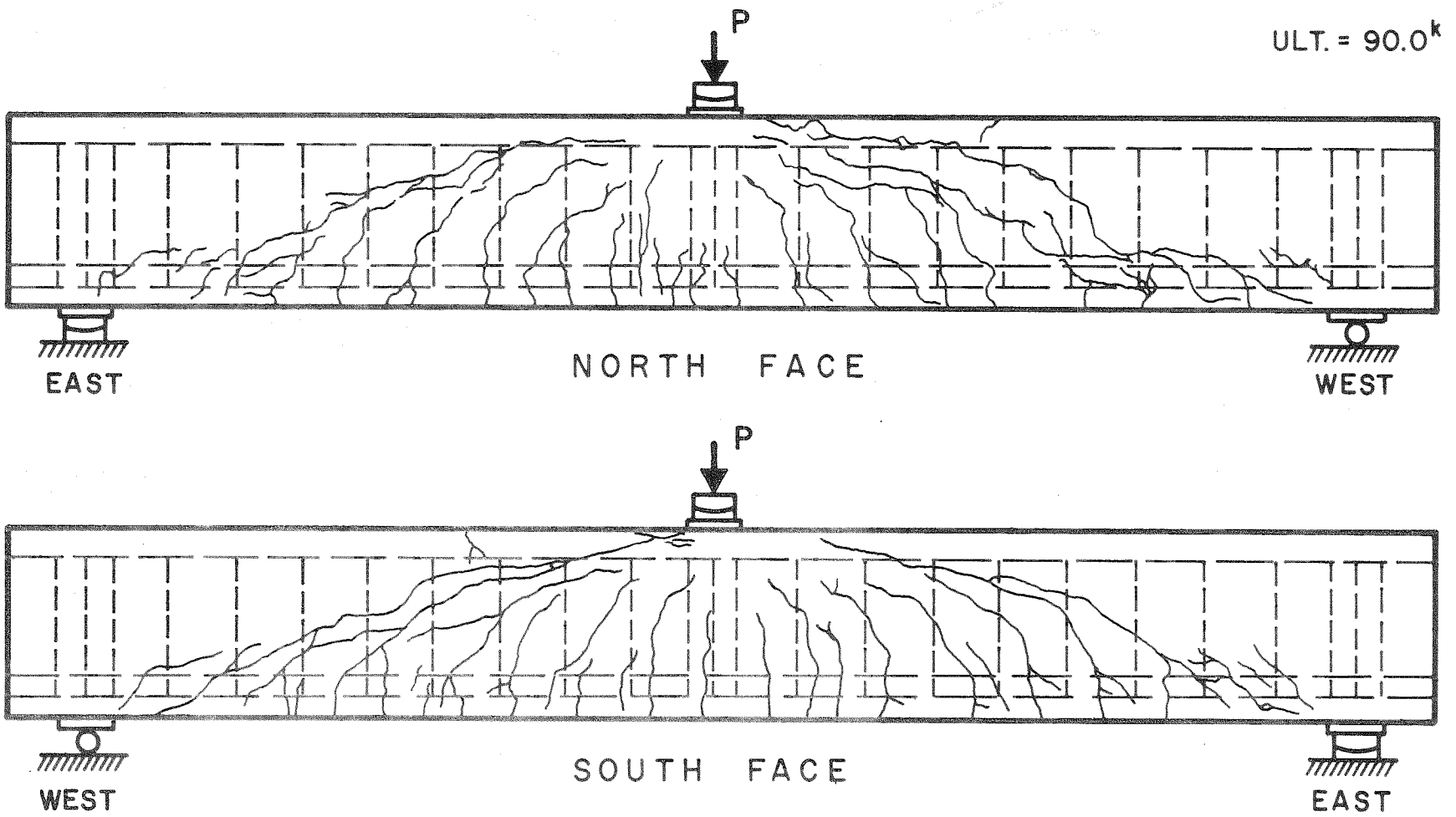


FIG. 3.3 CRACK PATTERN OF BEAM XB-1
AFTER BRESLER AND SCORDELIS [7]

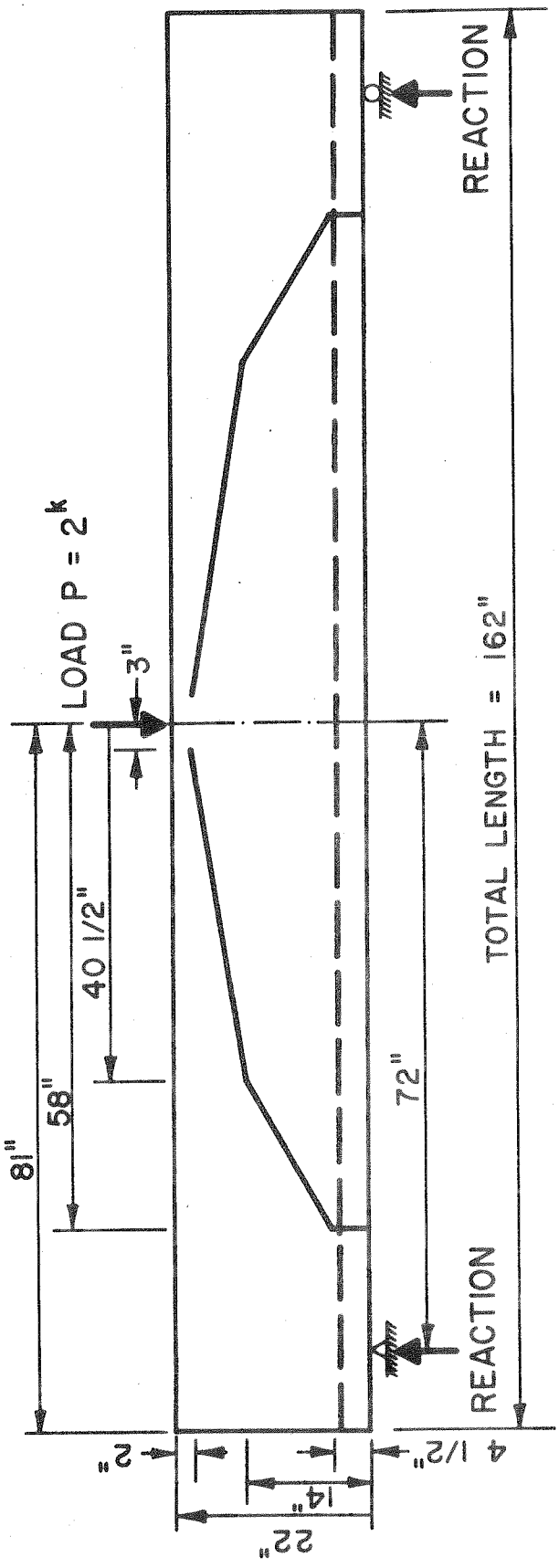


FIG. 3.4 IDEALIZED CRACK PATTERN

# 4. SPECIMEN IDEALIZATION AND DESIGNATION

## 4.1 General Finite Element Layout

After the beam dimensions and the crack pattern have been chosen, the next step required for the computer analysis is to layout the finite element mesh on the reinforced concrete beam. The general layout of the mesh used is shown in Fig. 4.1. Due to the symmetry of the beam geometry and the assumed crack pattern, only half of the beam was actually used for analysis. Appropriate boundary conditions were imposed at the line of symmetry to maintain the symmetrical condition.

In general, the finite element mesh size is dictated by the accuracy desired and the economy in computational effort. The selection of the present finite element layout was based upon past experience. It is believed that the mesh size used produces an adequate degree of accuracy without excessive computational effort.

## 4.2 Simulation of Crack Propagation

It was assumed that the crack developed in several stages, before it arrived at the final stage shown in Fig. 4.1. In other words, the crack was assumed to be propagating along a predefined path. To simulate this phenomenon, the linkage element, originally developed to simulate bond, was used.

Linkage elements were placed along the length of the crack, which connected the nodes on both sides across the crack. They were oriented in such way that one of the axes was parallel and the other one perpendicular to the crack. When the stiffnesses of the linkage elements were given a very high value, the crack would essentially

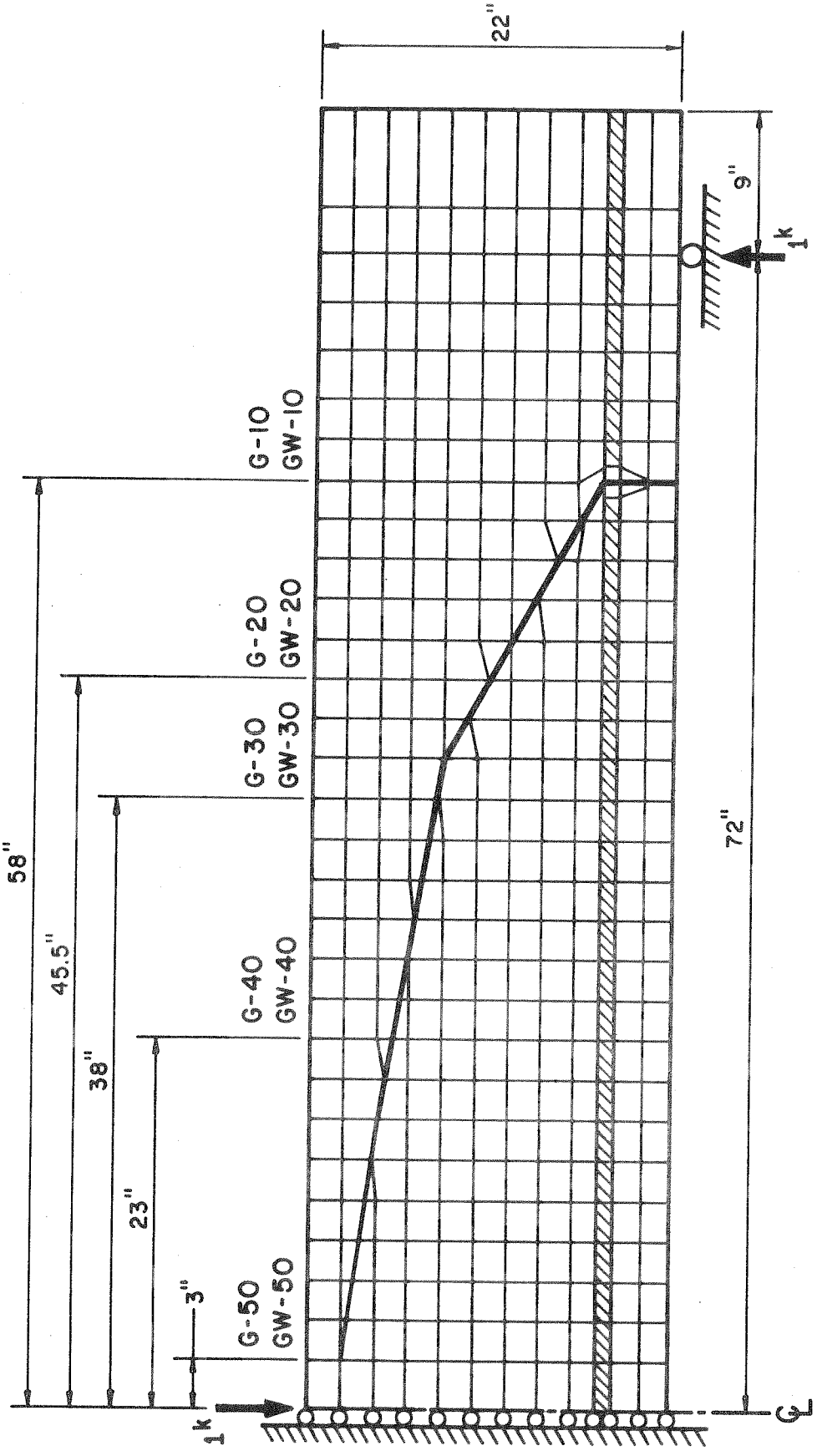


FIG. 4.1 GENERAL FINITE ELEMENT LAYOUT

be closed, i.e., the displacements of the nodes across the crack were almost identical. Conversely, if the stiffnesses of the linkage elements were set equal to zero, the crack would then open freely. In the case where the effect of the aggregate interlock was included in the analysis, a stiffness value was assigned in the direction parallel to the crack path, and a zero stiffness value was assigned in the perpendicular direction. In this way, the nodes across the crack can move freely in the direction perpendicular to the crack, but are somewhat restrained in the direction parallel to the crack, to simulate the effect of aggregate interlocak existing in a real beam.

By varying the stiffness value in the linkage elements, it was possible to stimulate the crack propagation without redefining the finite element mesh layout or renumbering of the nodal points.

In the present study, the cracking was arbitarily divided into six stages. Each new stage represented a deeper crack penetration. A computer analysis was performed for the beam at each stage of cracking. This can be regarded for purposes of analysis as six different beam types. Beams of each type were analyzed with and without stirrups and also under other special conditions as described below.

## 4.3 Beams of G-Series

The first series of beams analyzed are designated as the G-Series in this report. No web reinforcement was used in this series. No aggregate interlock was assumed. In order to identify the beams at the various stages of cracking, a trailing two-digit number was

added to signify the extent of cracking. Hence Beam G-00 would denote the initially uncracked beam, and Beam G-50 the most intensively cracked one. These beams are schematically shown in Fig. 4.2. These beams are identical to Beam XOB-1 tested by Bresler and Scordelis, Fig. 3.1.

## 4.4 Beams of GW-Series

To examine the effect of web reinforcement, another series of beams were analyzed. This series is called the GW-Series. It consists of six beams which are identical to those of the G-Series, except for the added stirrups. The trailing two-digit numbers have the same significance as previously defined. These beams are shown in Fig. 4.3. The location of the stirrups is shown in Fig. 4.4. These beams are identical to Beam XB-1 tested by Bresler and Scordelis, Fig. 3.1. No aggregate interlock was assumed.

No new layout of the finite element mesh was necessary for this series, because the original mesh was so proportioned that it fitted the stirrup spacing. One-dimensional bar elements were simply attached to the nodes where a stirrup existed. Details of the typical stirrup connections are shown in Fig. 4.5. Note that the one-dimensional bar elements were not connected to the nodes at the cracks, nor at the top of the main longitudinal tension steel reinforcement.

## 4.5 Special Beams of G-Series

Additional analyses were made to investigate the effects of aggregate interlock, splitting along the longitudinal reinforcement, and increase of shear span. These analyses were carried out with

little or no alteration of the finite element mesh layout used previously. On all of these special beams, a diagonal crack equivalent to G-30 was assumed. Hence they are called Beam GI-30, GS-30, and GE-30 for a beam with aggregate interlock, horizontal splitting, and extended shear span, respectively.

### 4.5.1 Beam GI-30

In this beam, aggregate interlock was simulated along the crack length, except for the vertical portion below the longitudinal reinforcement, Fig. 4.6. The omission of the aggregate interlock in the lower portion of the crack was intended to simulate the fact that the crack width at that particular portion might have been large enough to render the aggregate interlock ineffective. At the same time, it simplified the interpretation of the final results.

### 4.5.2 Beam GS-30

Splitting along the longitudinal reinforcement would generally occur when the dowel shear force is excessive. To study the effect of this splitting, Beam G-30 was modified to become Beam GS-30 in which some of the finite elements were connected in a different fashion as shown in Fig. 4.7. While the present arrangement of splitting might not be the most desirable, it at least fulfilled two fundamental requirements: (1) the separation of concrete elements along the splitting region; and (2) the increase of the steel element flexibility at the dowel section due to larger effective dowel length. Furthermore, no new layout of the finite element mesh was required under the present arrangement.

### 4.5.3 Beam GE-30

The question concerning the effect of increasing shear span on the reinforced concrete beam behavior has long been of interest to researchers. In the present investigation, such a study was easily included by simply extending the length of the beam as shown in Fig. 4.8. This extended beam is denoted as Beam GE-30. The shear span of this beam was increased by 18 inches, and had a total length of 90 inches.

## 4.6 Elastic Constants Used in Finite Element Analysis

The basic elastic constants used in the present investigation are listed in the following table for the various elements.

Table 4.1 Basic Elastic Constants Used in Finite Element Analysis For a Unit Thickness of One Inch

| Element | $E_c$ or $K_h$ | $E_T$ or $K_V$ | $\nu$ |
|---|---|---|---|
| Concrete | 3000 ksi | 3000 ksi | 0.17 |
| Modified concrete at the level of reinforcement | 1665 ksi | 1665 ksi | 0.17 |
| Modified steel for longitudinal reinforcement | 13350 ksi | 13350 ksi | 0.25 |
| Modified steel for stirrup | 333 kpi | 333 kpi | 0.25 |
| Bond link | 4900 kpi | $10^7$ kpi | |
| Link along the crack | 1000 kpi | 0 | |

$E_c$ = Modulus of elasticity in compression

$E_T$ = Modulus of elasticity in tension

$K_h$ = Horizontal stiffness of linkage element

$K_V$ = Vertical stiffness of linkage element

$\nu$ = Poisson ratio

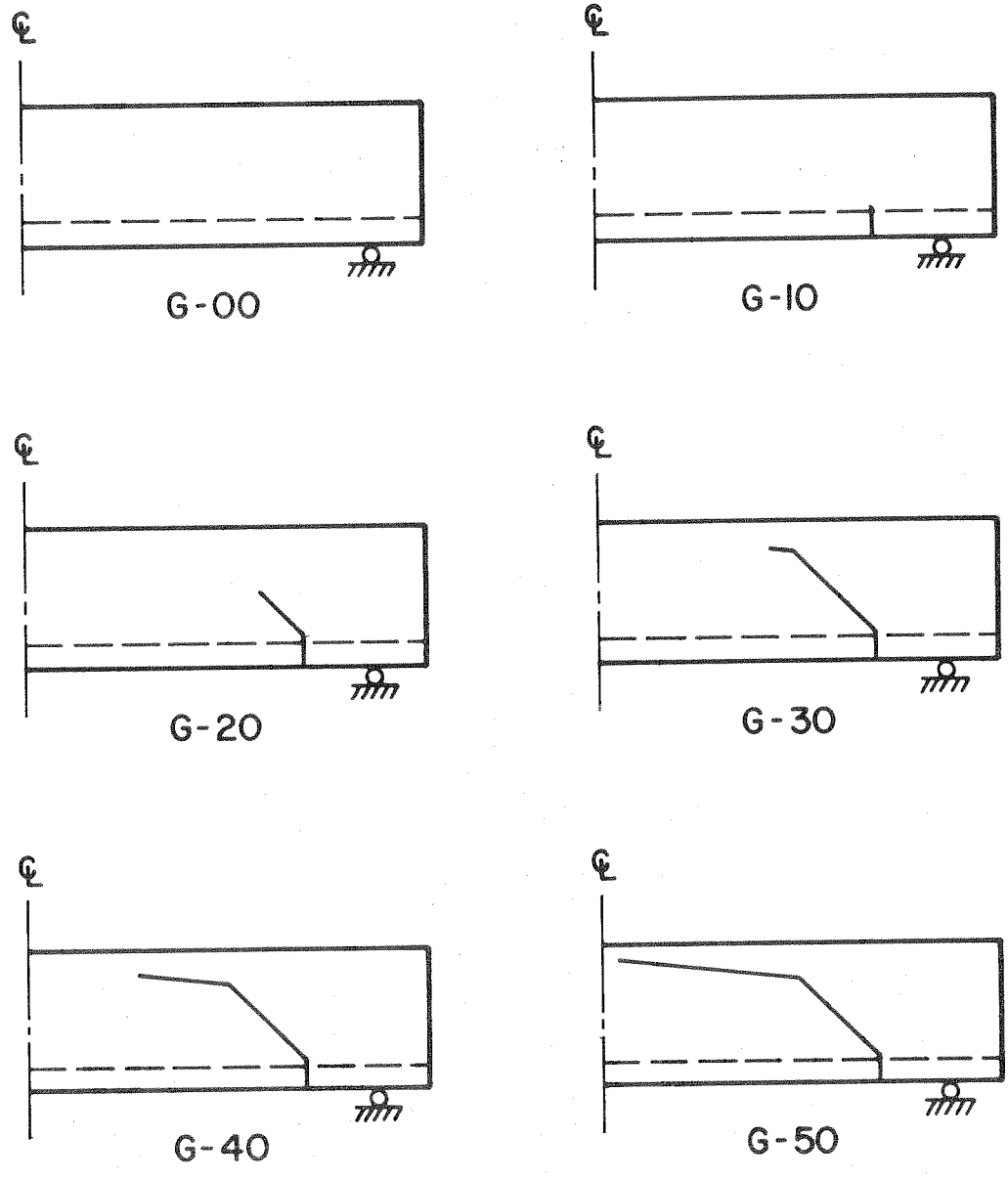


FIG. 4.2 BEAMS OF G SERIES

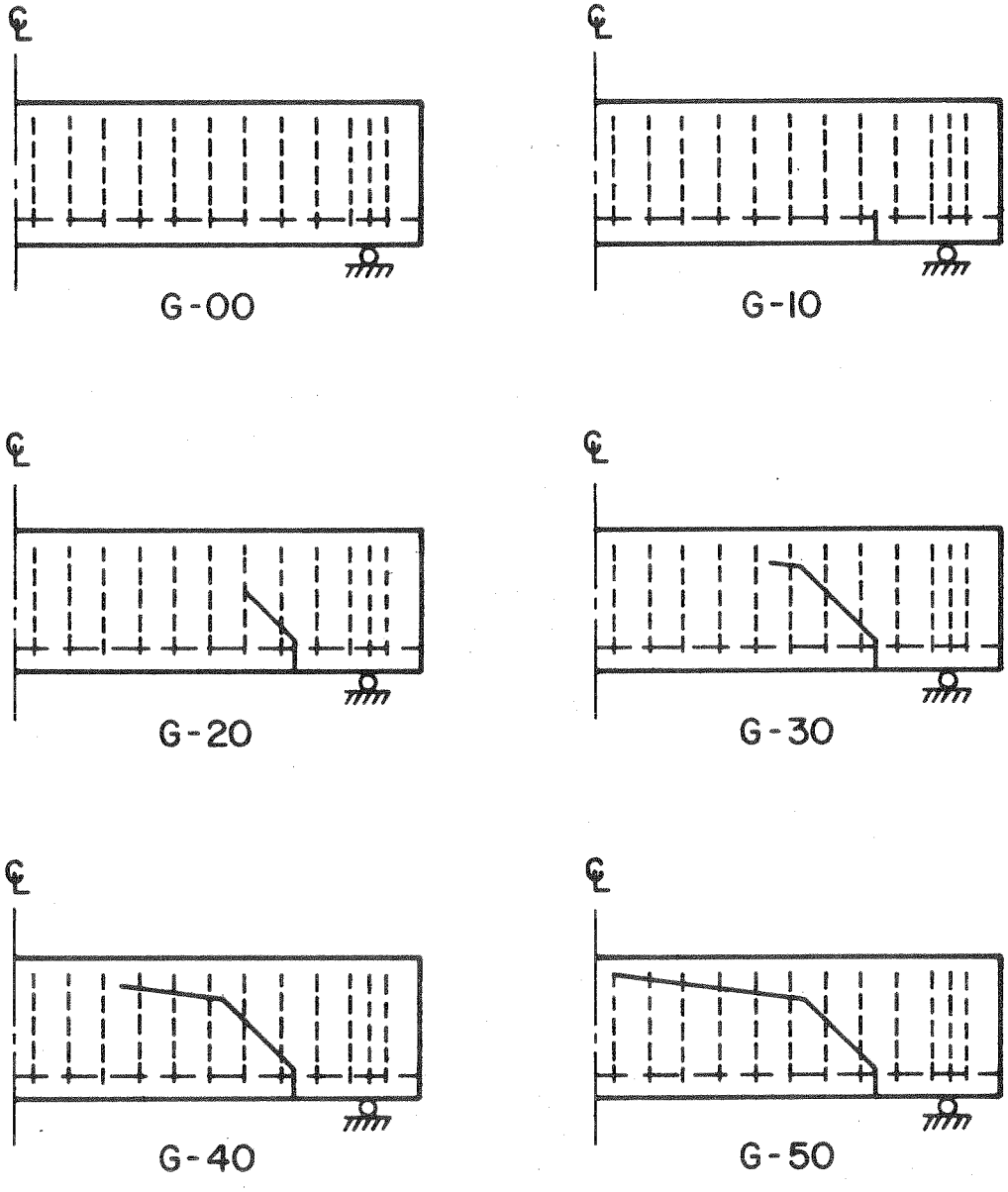


FIG. 4.3 BEAMS OF GW SERIES

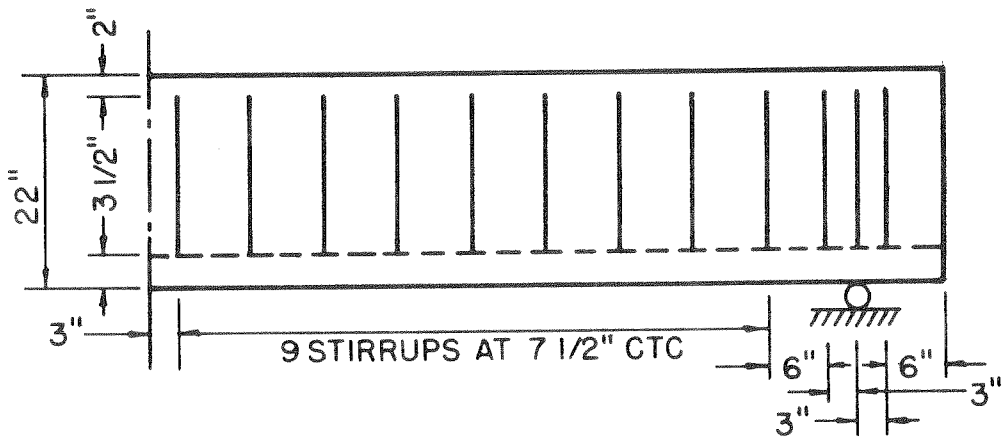


FIG. 4.4 STIRRUP SPACINGS

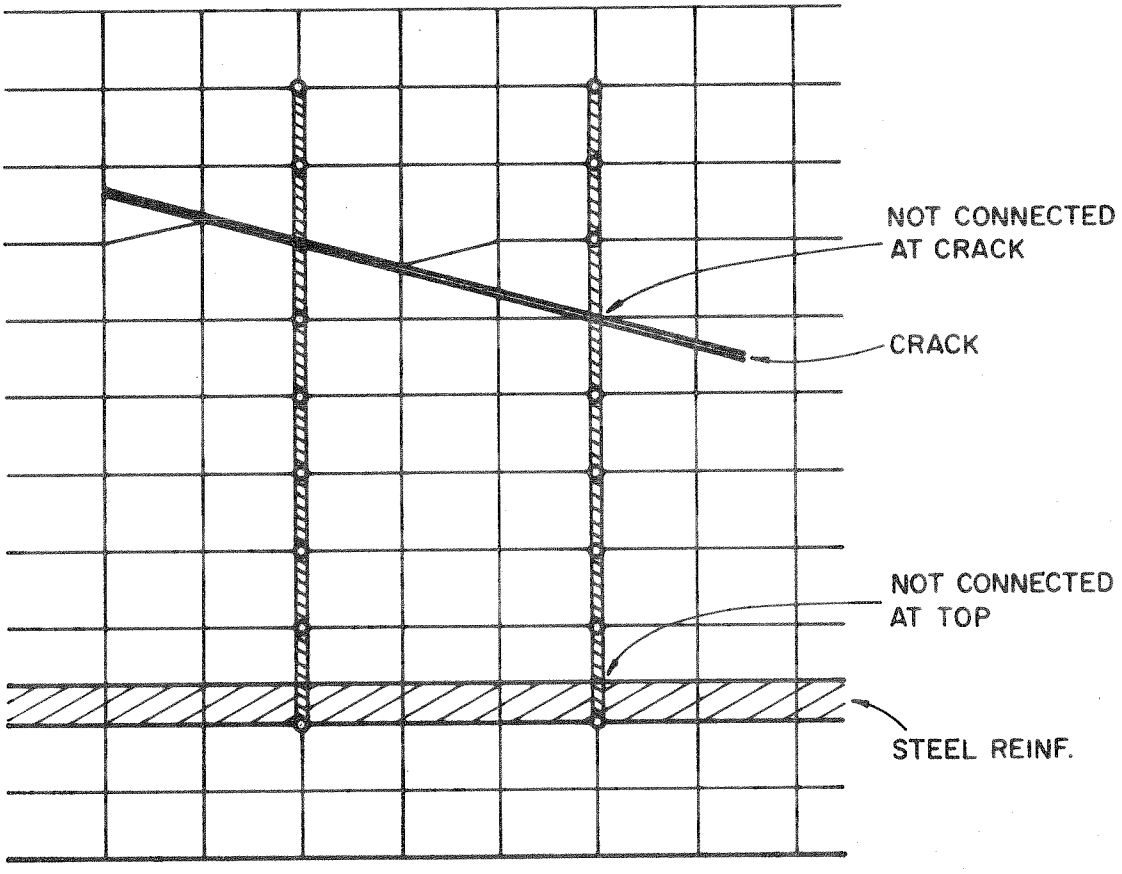


FIG. 4.5 DETAIL OF TYPICAL STIRRUP CONNECTION

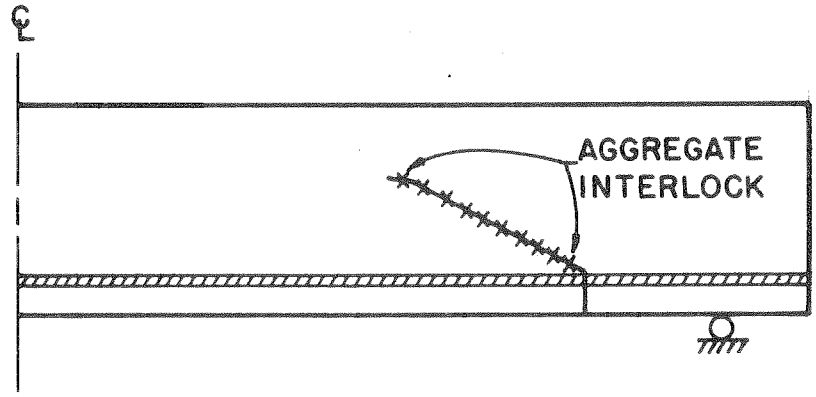


FIG. 4.6 BEAM GI - 30

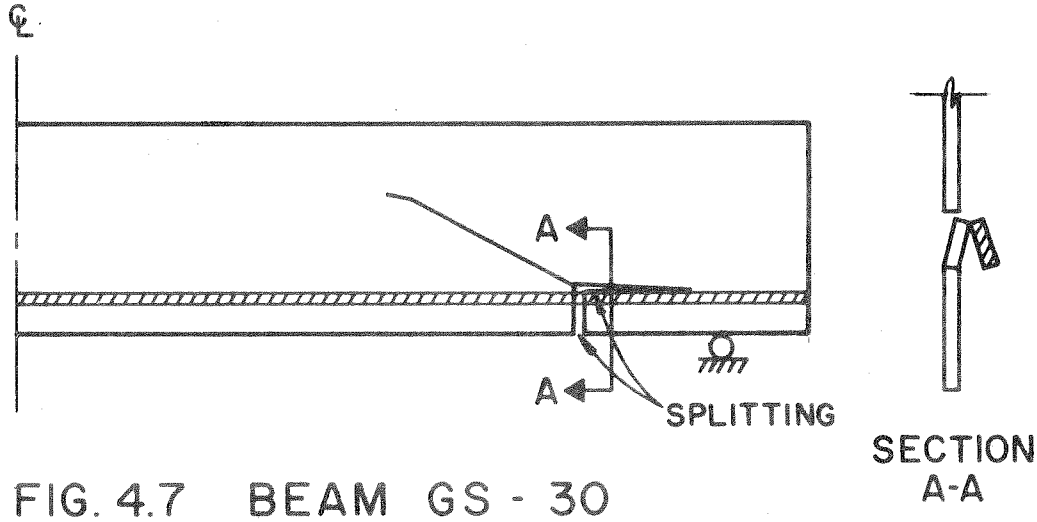


FIG. 4.7 BEAM GS - 30

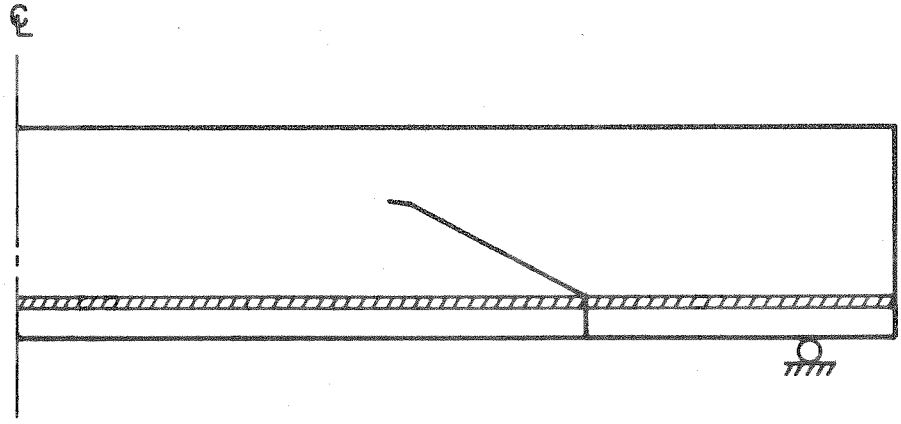


FIG. 4.8 BEAM GE - 30

# 5. PRESENTATION OF RESULTS AND DISCUSSION

## 5.1 Introduction

One of the advantages in employing the finite element method for the investigation of reinforced concrete beams is that it yields a wide range of information from a single computer analysis. In this chapter, essential results of all the beams analyzed will be presented. They consist of the following:

a) Longitudinal normal stress distributions in concrete

b) Shear stress distributions in concrete

c) Tensile forces in longitudinal steel reinforcement

d) Transverse shear forces in longitudinal steel reinforcement

e) Dowel tensions and dowel shears

f) Forces in bond link elements

g) Forces in stirrups

h) Principal tension stresses.

## 5.2 Longitudinal Normal Stress Distributions in Concrete

The distributions of longitudinal normal stress in the concrete are plotted at a number of selected sections along the length of the beam. The beams of G-Series are shown in Fig. 5.1, except for Beam G-30. Similarly, the beams of GW-Series are shown in Fig. 5.2, except for Beam GW-30. These two beams, G-30 and GW-30, are shown together with Beam GI-30 and Beam GS-30 in Fig. 5.3 where the variation of the normal stresses can be compared readily, since they all have the same degree of cracking. Beam GE-30 has a different span length, thus it is shown separately in Fig. 5.7(a). The normal stress distributions of Beam G-00 and Beam GW-00 are not shown, because their behavior closely

follows what would be predicted by the beam theory for an uncracked beam. Their stress distributions are almost identical to each other.

Similarity of the normal stress distributions between the G- and GW-Series at early stages of cracking can be observed by comparing the results in Fig. 5.1 and Fig. 5.2. This indicates that the web reinforcement has little effect on the normal stress distribution in the concrete when the depth of the diagonal crack penetration is small. In fact, it can be seen that the interference due to cracking is not pronounced when the crack is at a lower intensity. In the regions away from the zones near the crack and the loading and supporting points, the normal stresses vary in a linear manner as would be predicted by the elementary theory for an uncracked beam. This is true for the beams in both G- and GW-Series. But when the cracking has become more intensified, the normal stress distributions begin to deviate more and more from linearity. Furthermore, the results for the beams in the two series differ from each other as the crack progresses.

As the diagonal crack penetrates deeper into the compressive zone of the concrete beams, the compressive stress at the top fiber decreases for the beams of G-Series, but not for the GW-Series. This situation is best displayed in Beam G-50 and Beam GW-50, as shown in Fig. 5.1 and Fig. 5.2, respectively. This different pattern of stress distribution under an intensive diagonal cracking condition, as exemplified by these two beams, may be attributed to "arch action." The beams may be visualized as composed of two parts: an "arch," portion (A), and a "beam," portion (B), as depicted in Fig. 5.8. In the case of Beam G-50, where there is no web reinforcement the "arch" acts as if there is a hinge under the applied load, because of the relatively small zone of concrete

remaining intact. The negative bending moment along the "arch" produced by this action would reduce the compressive stress at the top fiber, see Fig. 5.8(a). This situation, however, is different when the web reinforcement is added in the case of Beam GW-50, see Fig. 5.8(b). Conceptually, the stirrup forces represent a distributed load along the "arch," which would tend to cause a larger compressive stress at the top fiber.

Kani proposed a "principle of arch supports" to explain the function of web reinforcement [19]. The beam was visualized as composed of a series of concrete arches, Fig. 5.9(a). The web reinforcement is then thought of as providing the support for the hanging arches, Fig. 5.9(b). The present investigation is not intended to verify Kani's theory. But the difference in the patterns of normal stress distribution, exhibited in Beam G-50 and Beam GW-50, provides a justification for the concept of "arch support."

The portion of the beam below the diagonal crack, portion (B) in Fig. 5.8, acts as a tapered "beam" member. When there is no web reinforcement, this tapered "beam" member is supported by the dowel action of the longitudinal steel reinforcement, see Fig. 5.10(a). When web reinforcement was used, the "beam" was supported at several intermediate points by the stirrups, in addition to the dowel support. Therefore, the normal stresses in this portion of the beams have a smaller magnitude for GW-Series than for G-Series.

Not much difference in the longitudinal stress distribution exists among the beams of G-30, GS-30, GI-30, and GW-30, Fig. 5.3, except that for Beam GS-30, a higher normal stress is observed near the crack tip and a slight deviation of the pattern of stress distribution at Section (E) where the crack begins to curve. These localized effects

are due to the additional rotation induced by the horizontal splitting. Beam GE-30, Fig. 5.7(a), also conforms to the normal trend of longitudinal stress distributions found in Beam G-30.

## 5.3 Shear Stress Distributions in Concrete

The shear stress distributions in the concrete are plotted at the same sections where longitudinal normal stress distributions were taken. The beams of G-Series are shown in Fig. 5.4, and GW-Series in Fig. 5.5, except for Beam G-30 and Beam GW-30, which are shown together with GI-30 and GS-30 in Fig. 5.6. The shear stress distributions of Beam GE-30 are shown separately in Fig. 5.7(b). Again, results for Beam G-00 and GW-00 are not shown for exactly the same reasons as in the case of longitudinal stress distributions. The shear stress distributions of these two beams conform very closely to elementary theory for uncracked beams and show no difference between them. For the cracked beams shown, the deviation from a parabolic shear stress distribution occurs only at the sections where the crack appears. This deviation becomes more pronounced when the crack becomes more intensified. At the same time, the pattern of the shear stress distributions for corresponding beams in the G-Series and the GW-Series less and less resemble each other as the crack progresses. Beam G-50 and Beam GW-50 clearly illustrate this fact. In other words, the web reinforcement plays more and more an important role when the crack progresses deeper and deeper into the compressive zone.

Discontinuity in the shear stress distributions would naturally occur at the crack. Note that because the crack is inclined, the vertical shear stress does not vanish at this location. On the contrary, the magnitude of the shear stress is generally increased. Observe also

that there is a tendency for the shear stress to shift down to the "beam" portion of the specimens. Such shifting is more for the beams of G-Series than for GW-Series. This phenomenon, again, might be explained by the "arch" and "beam" actions, as in the case of longitudinal stress. Take Beam G-50 and Beam GW-50, for example. The shear force carried by the "arch," portion (A) in Fig. 5.8, must be less for beams of G-Series than for GW-Series. On the other hand, the shear force carried by the "beam," portion (B) in Fig. 5.8, is bigger for beams of G-Series than for GW-Series.

High shear concentrations near the loading and supporting points were observed. These are the results of an elasticity solution provided by the finite element method. The distribution of the shear stress near these two points, sections (A) and (F) in both Fig. 5.4 and Fig. 5.5, are seen to be relatively undisturbed by cracking for the beams of GW-Series, but not so for G-Series. This suggests that the effect of web reinforcement is to help in distributing the shear forces along the shear span and to confine the interference on stress distributions due to cracking.

No great difference in magnitudes and patterns of shear stress distributions exists among the beams of G-30, GI-30, and GW-30, Fig. 5.6, but drastic changes occur in Beam GS-30. The splitting along the longitudinal reinforcement has altered the shear path. In this case, the portion of the concrete beam above the crack has to carry a higher shear force, because the portion below the crack has been rendered ineffective in carrying shear by the splitting. The shear stress distributions in Beam GE-30, Fig. 5.7(b), is similar in pattern to those of Beam G-30, as expected.

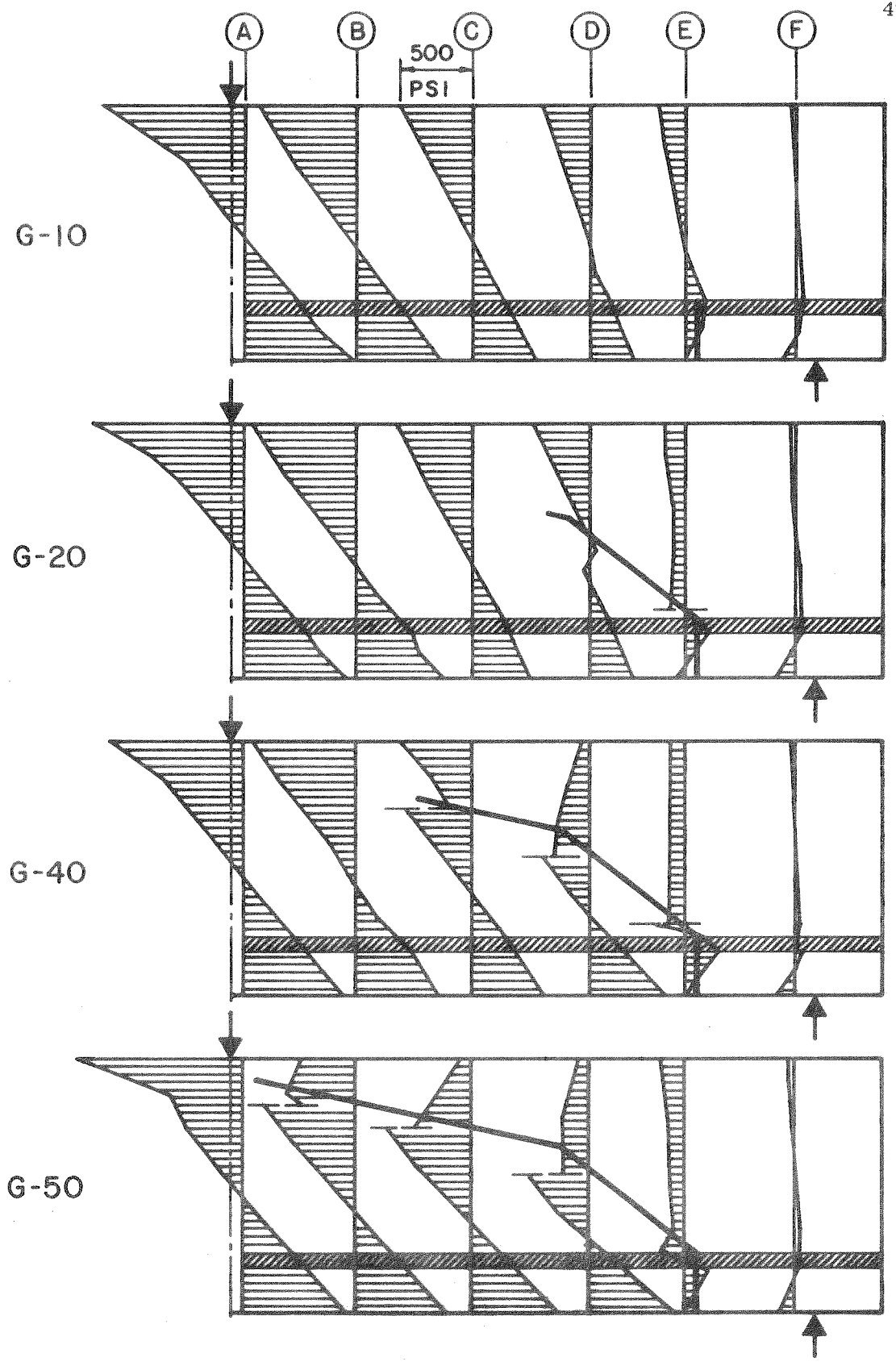


FIG. 5.1 LONGITUDINAL STRESSES IN CONCRETE FOR G-SERIES BEAMS

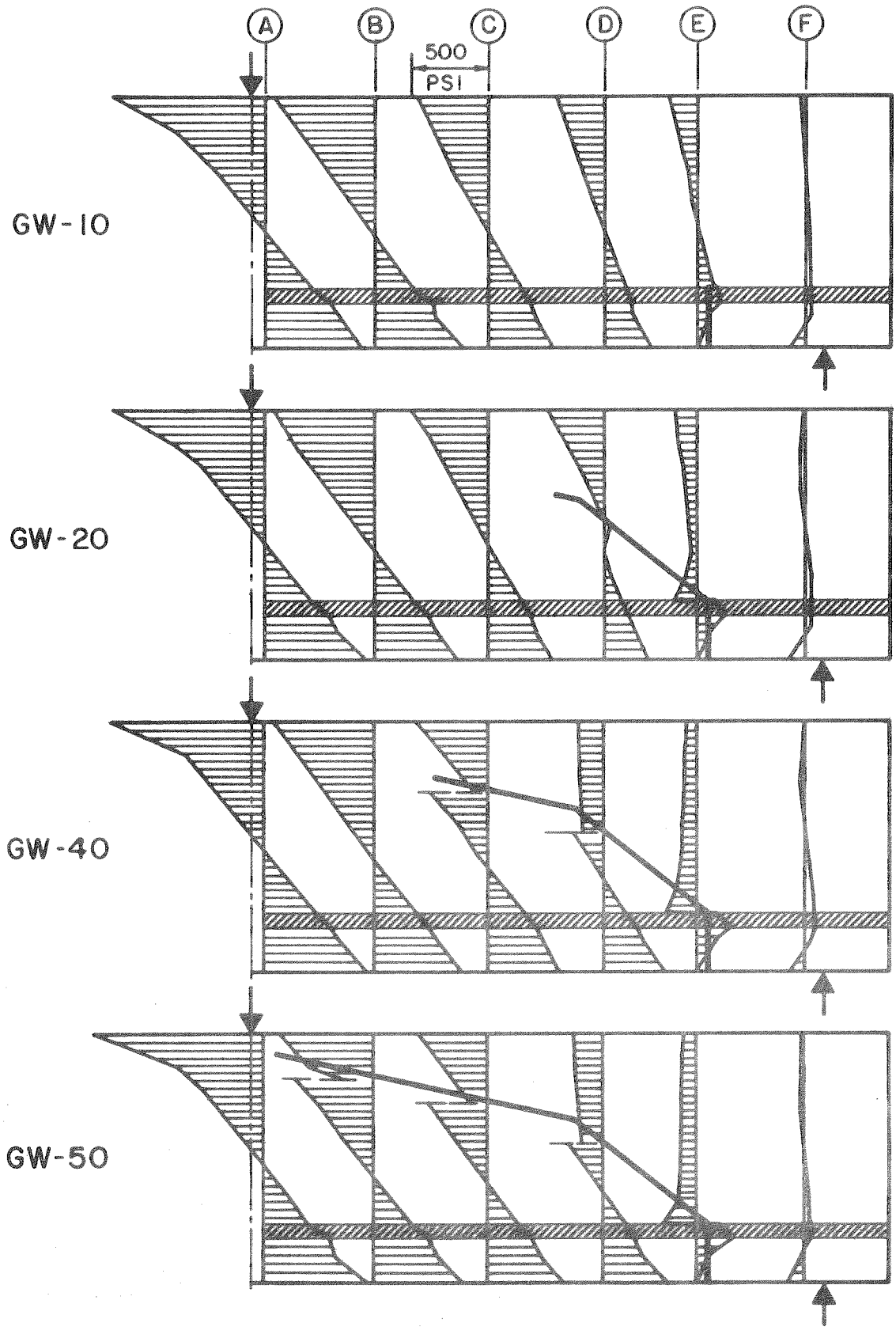


FIG. 5.2 LONGITUDINAL STRESSES IN CONCRETE FOR GW-SERIES BEAMS

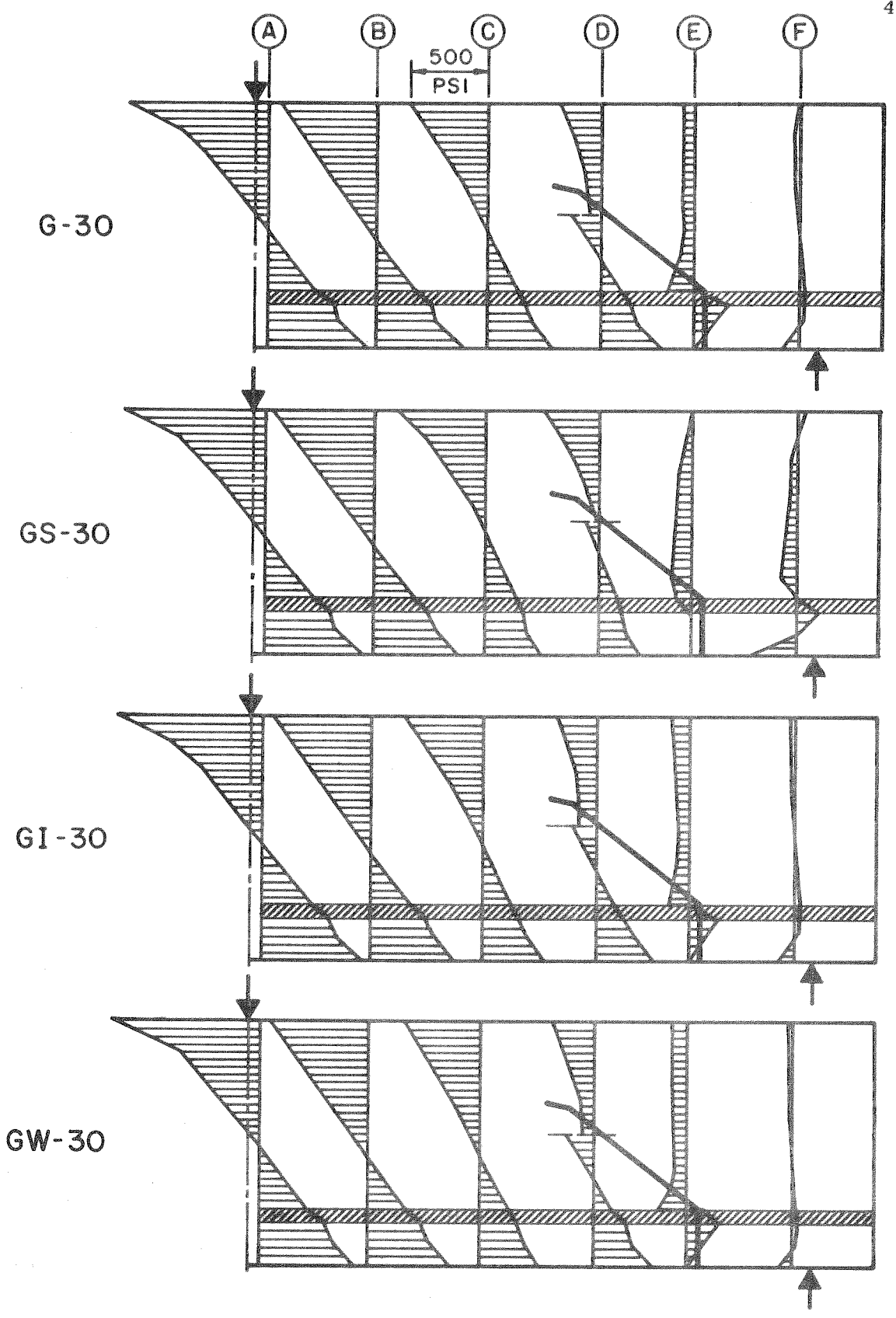


FIG. 5.3 LONGITUDINAL STRESSES IN CONCRETE FOR G-30 SERIES BEAMS

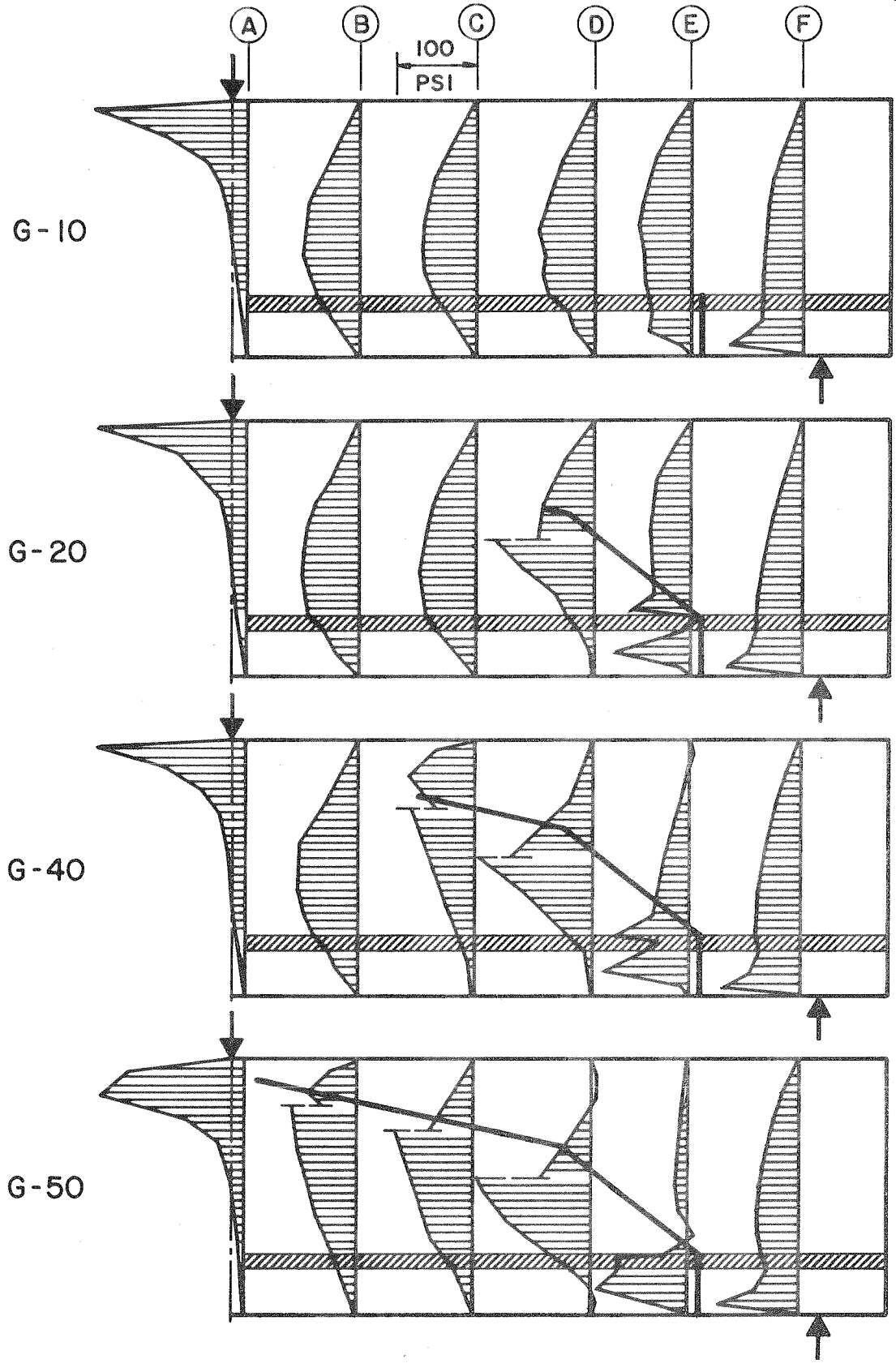


FIG. 5.4 SHEAR STRESSES IN CONCRETE FOR G-SERIES BEAMS

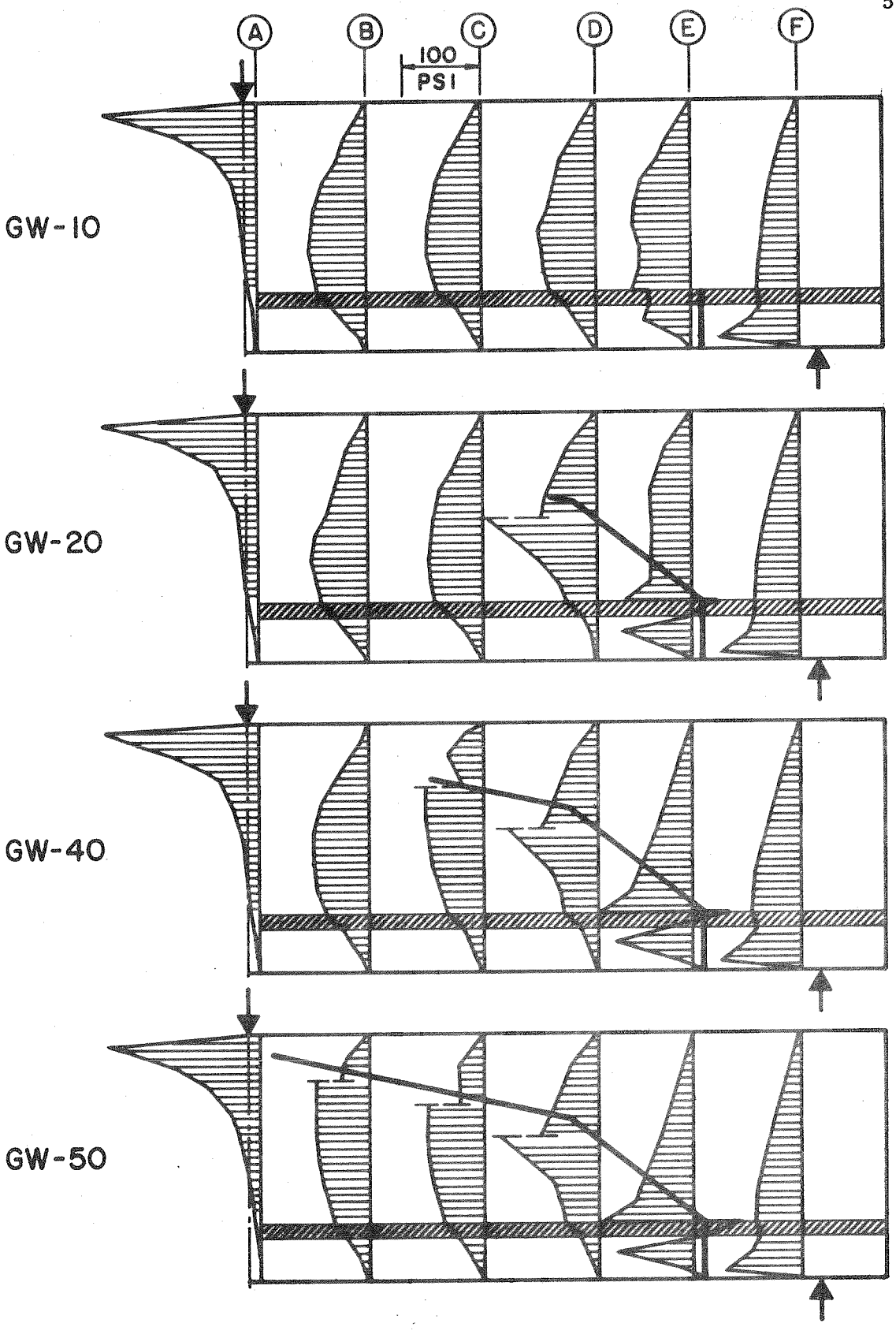


FIG. 5.5 SHEAR STRESSES IN CONCRETE FOR GW-SERIES BEAMS

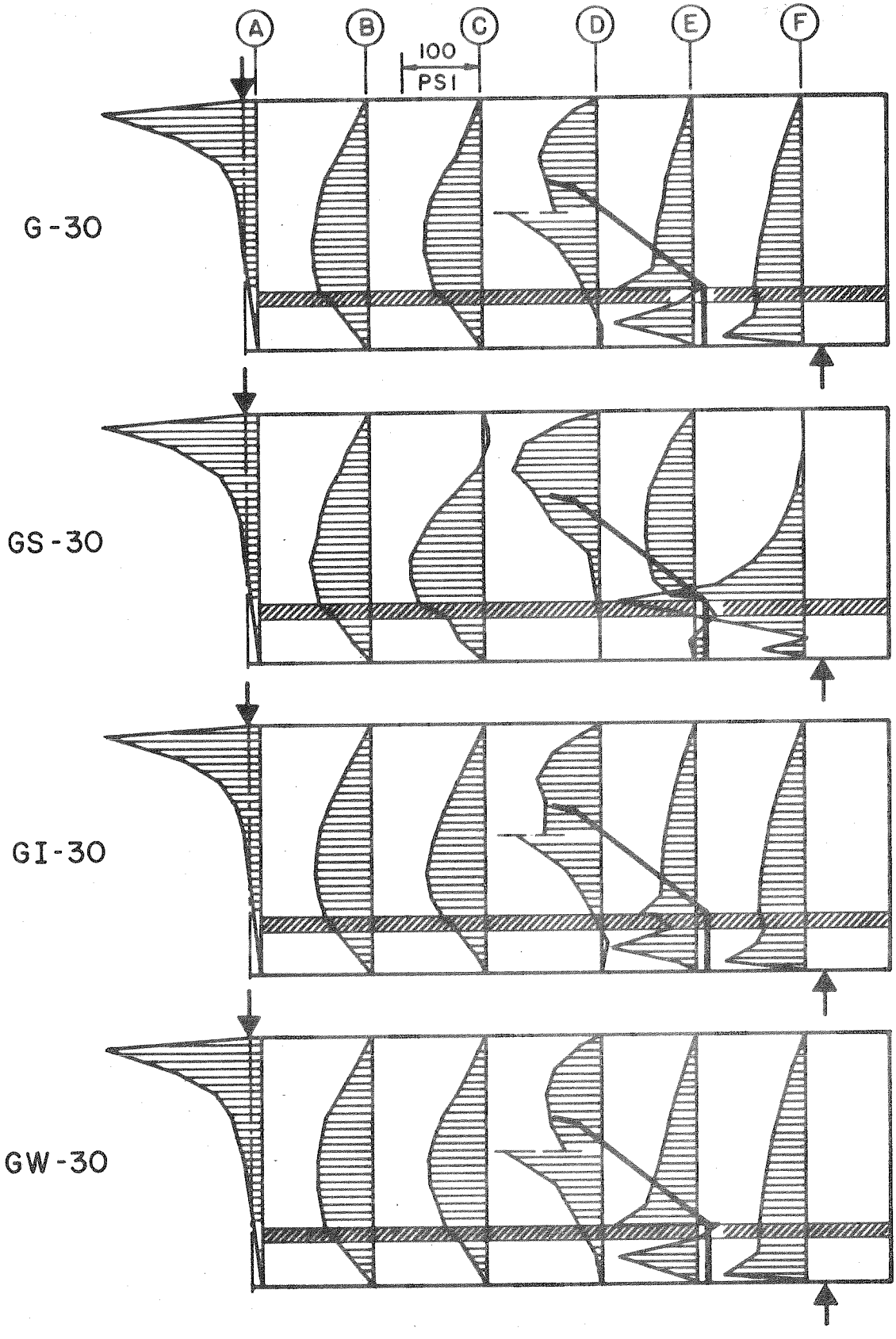


FIG. 5.6 SHEAR STRESSES IN CONCRETE FOR G-30 SERIES BEAMS

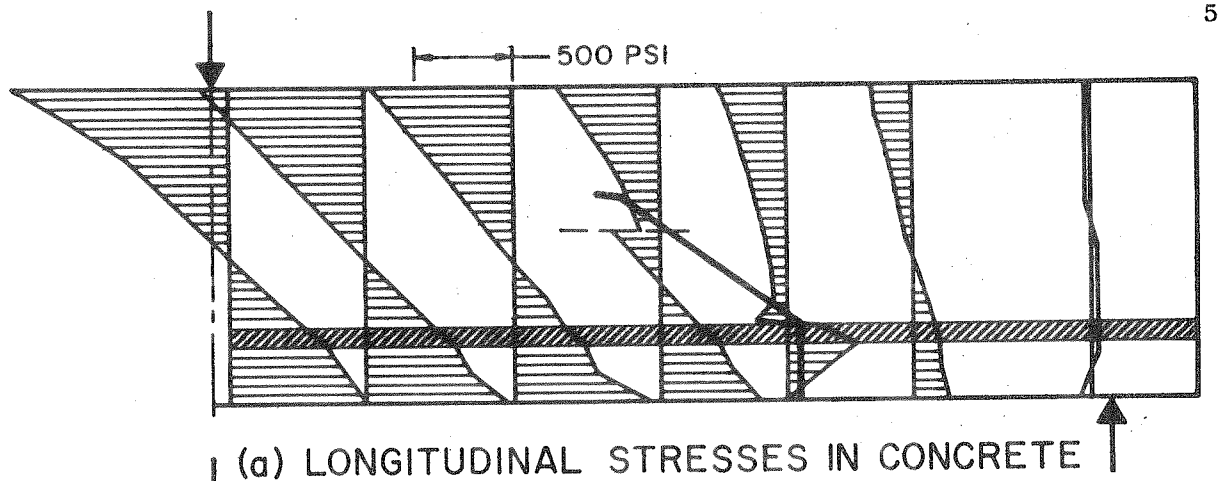


(a) LONGITUDINAL STRESSES IN CONCRETE

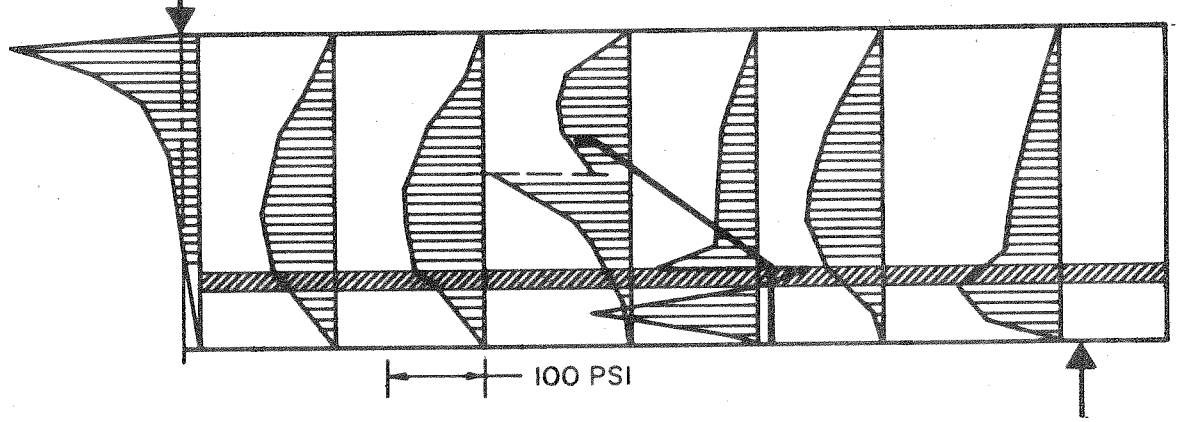


(b) SHEAR STRESSES IN CONCRETE

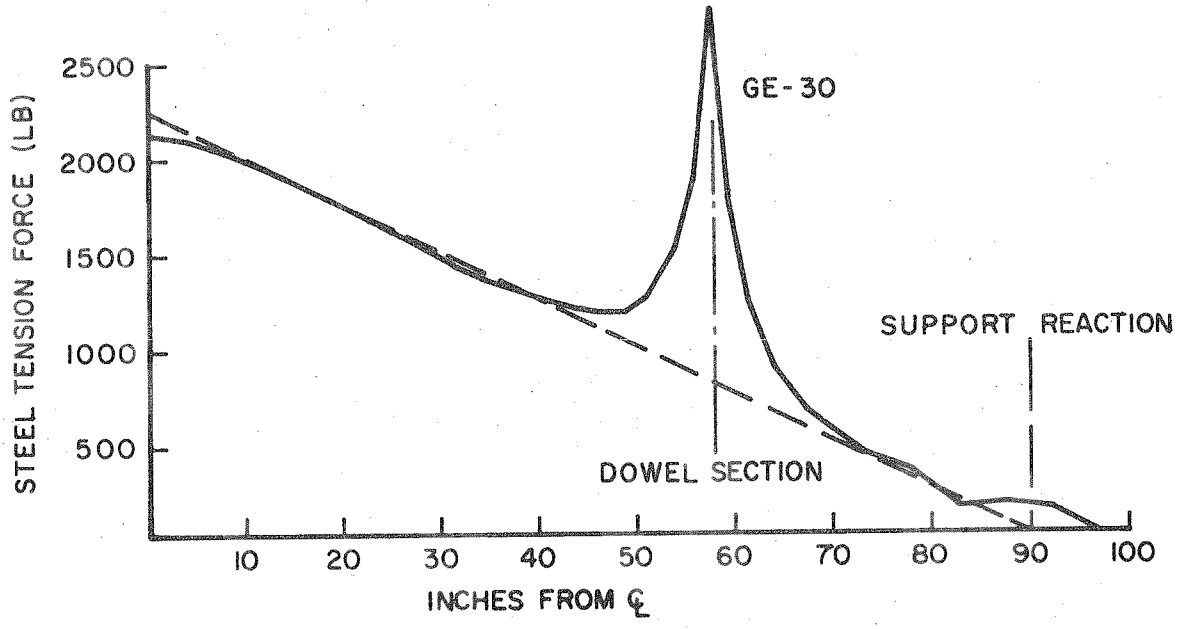


(c) STEEL TENSION FORCE IN LONGITUDINAL REINFORCEMENT

FIG. 5.7 CONCRETE AND STEEL STRESSES FOR BEAM GE-30

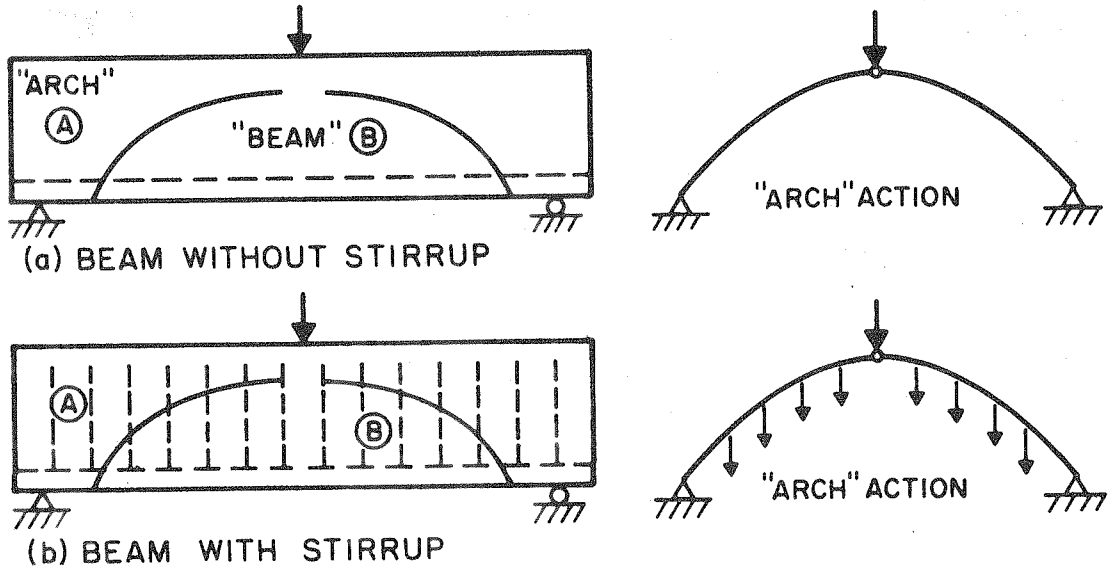


FIG. 5.8 CONCEPTUAL "ARCH" ACTION

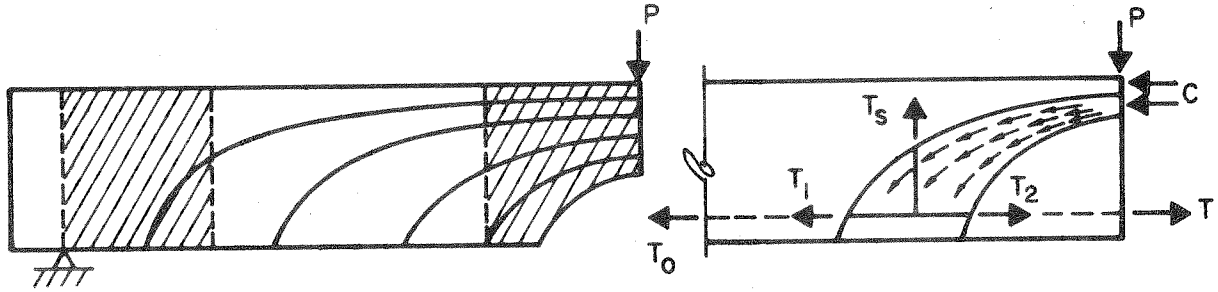


FIG. 5.9 KANI'S ARCH SUPPORT THEORY

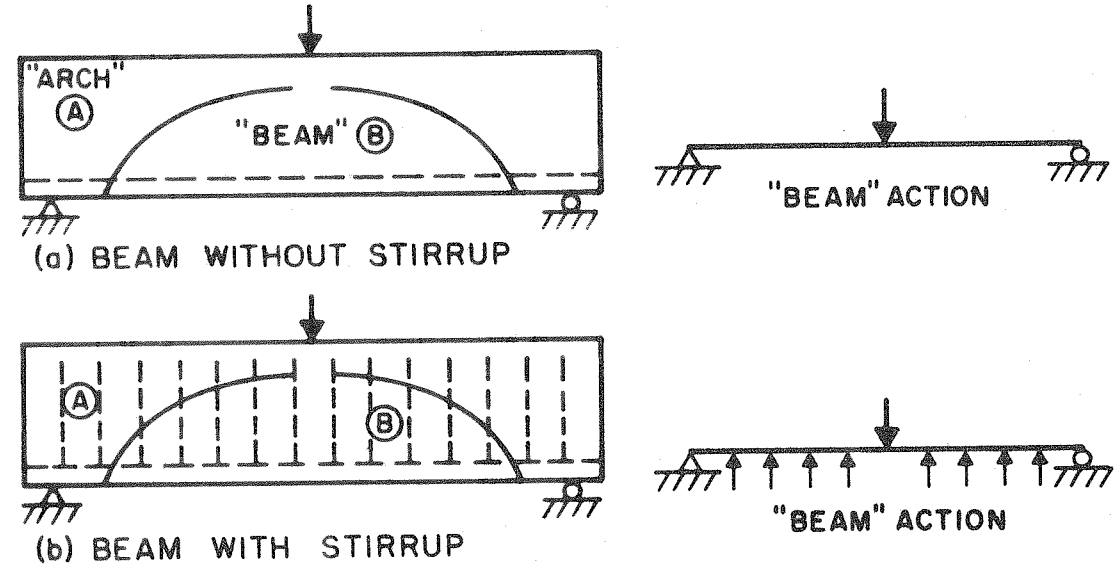


FIG. 5.10 CONCEPTUAL "BEAM" ACTION

## 5.4 Tensile Forces in Longitudinal Steel Reinforcement

Tensile forces in the longitudinal steel reinforcement are shown in Fig. 5.11 for the beams of G-Series. In order to provide a means for comparison, the theoretical value calculated for an uncracked beam is also presented. The tensile forces for the beams of GW-Series are not shown because they are almost identical to those of G-Series, except at the dowel section. The magnitudes of the tensile forces at the dowel section are shown in Fig. 5.17 for the beams of both series.

It can be seen in Fig. 5.11 that in the region where no crack exists, the steel force agrees closely with the theoretical value for an uncracked beam. The increase or decrease of steel tensile force along the span is mainly due to the adjustment of the T-C couple in maintaining moment equilibrium, Fig. 5.12. The steel tensile force at the dowel section, called dowel tension, is seen to be affected most acutely, since all of the tensile force must be carried by the steel alone at that section while at other sections the concrete and steel share the tensile force.

It is interesting to note that the tensile force in the steel at the dowel section has a smaller magnitude for Beam G-50. This appears to be surprising at first sight, because this dowel tension increases as the crack propagates in all the beams from G-10 to G-40. An examination of the moment equilibrium about the tension steel at the dowel section for the concrete block depicted in Fig. 5.12 reveals that the difference of the moment due to normal forces, $M_n$, and the moment due to shear, $M_s$, is equal to the moment due to reaction force, $M_r$, which is a constant in this particular case:

$$M_n - M_s = M_r = \text{constant}, \qquad (5.1)$$

or

$$C\,y - S\,x = P\,g.$$

In the finite element analyses it was found that the vertical moment arm, y, stayed at a fairly constant value. On the other hand, the shear force, S, in the concrete block at the crack tip decreases as the crack progresses, because of the continuous reduction in the concrete block block size, Fig. 5.13(a). The product S x, which equals $M_s$, would have a curved shape as shown qualitatively in Fig. 5.13(b) for the variation of S vs x shown in Fig. 5.13(a). The plot of the values for $M_n$ should also have the same shape as $M_s$, because the difference of $M_n$ and $M_s$ is constant. Since the moment arm, y, has a fairly constant value, the magnitude of the compressive force, C, hence the tensile force, T, should have a variation closely resembling that of $M_n$, i.e., C and T increase up to a certain point and decrease subsequently, which results in a drop of dowel tension for Beam G-50.

Figure 5.14 shows the tensile force variation along the shear span for beams G-30, GW-30, GI-30, and GS-30. The first three beams of this group behave in a very similar manner. But Beam GS-30 exhibits a high tensile steel force within the end block where splitting occurs. This high tensile force is due to the loss of concrete strength in carrying tension, and due to the shift of the compressive force resultant, which in turn reduces the moment arm of the T-C couple. Note the reversal of stress, from compressive to tension at the top fiber of Beam GS-30 at section (F) in Fig. 5.3.

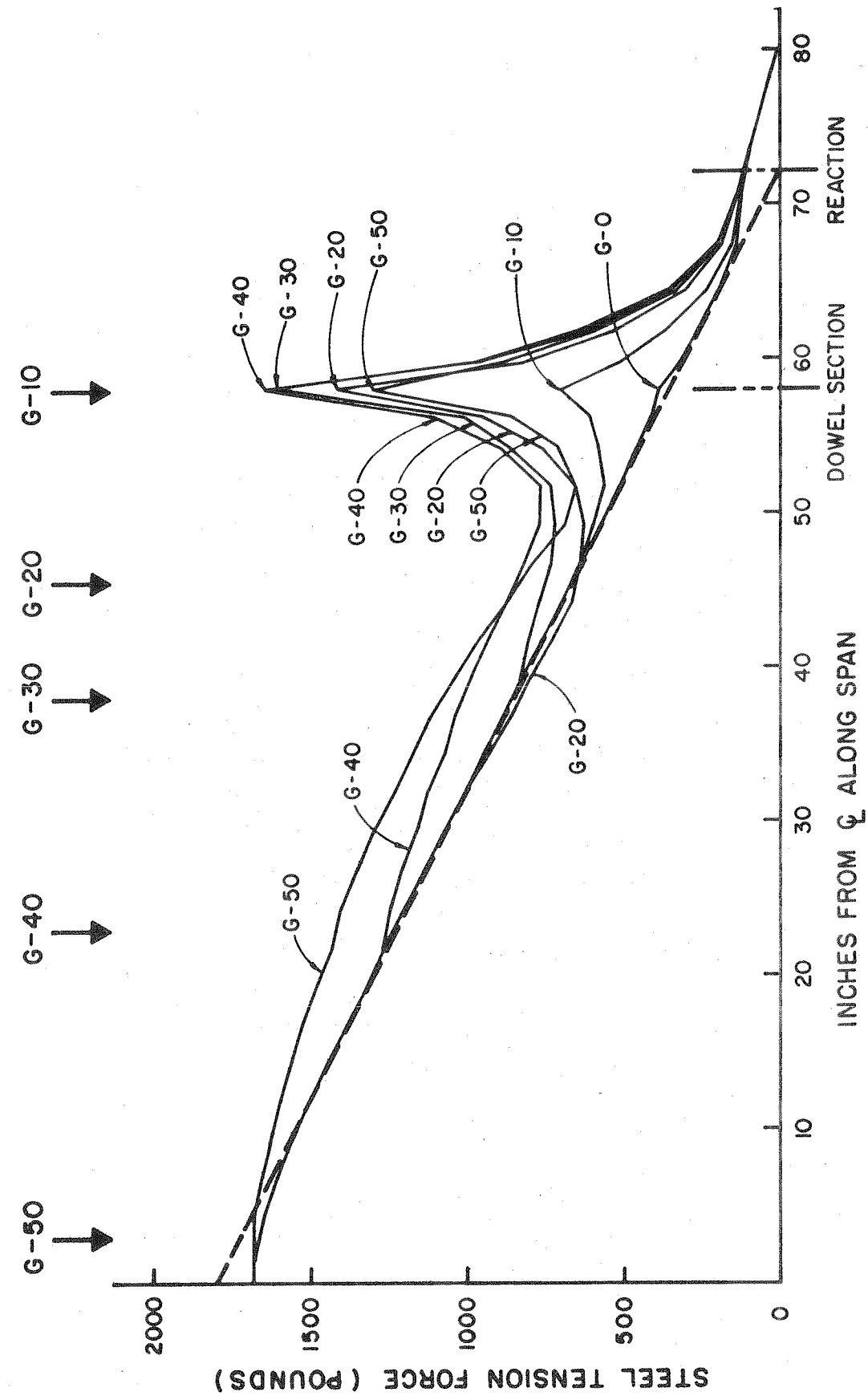


FIG. 5.11 VARIATION ALONG THE SPAN OF TENSILE FORCE IN MAIN REINFORCEMENT

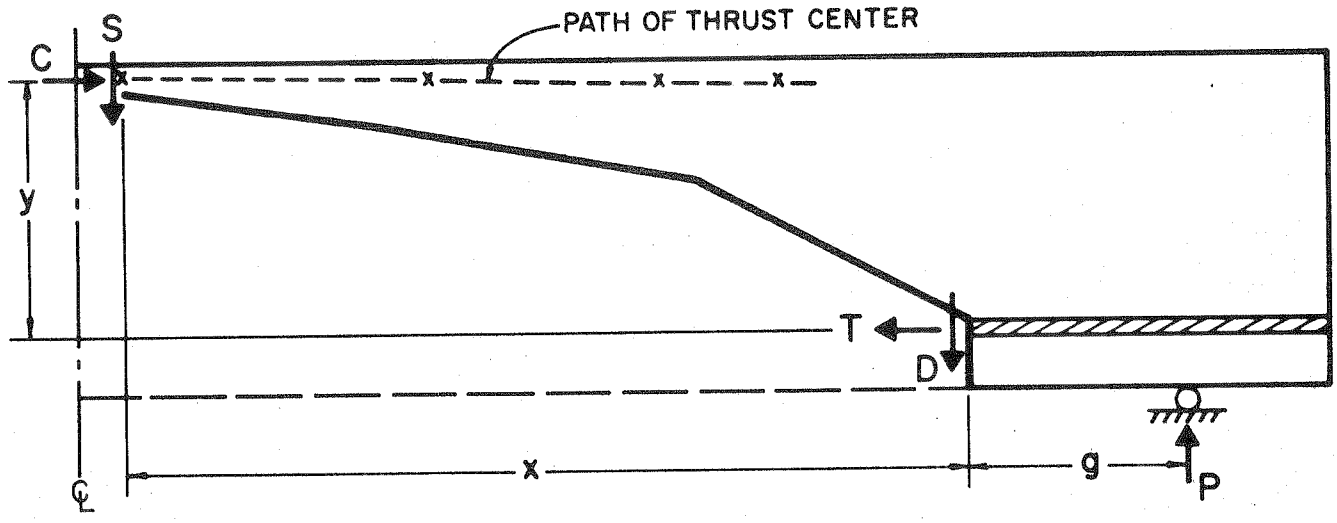


FIG. 5.12 EQUILIBRIUM BLOCK FORCES

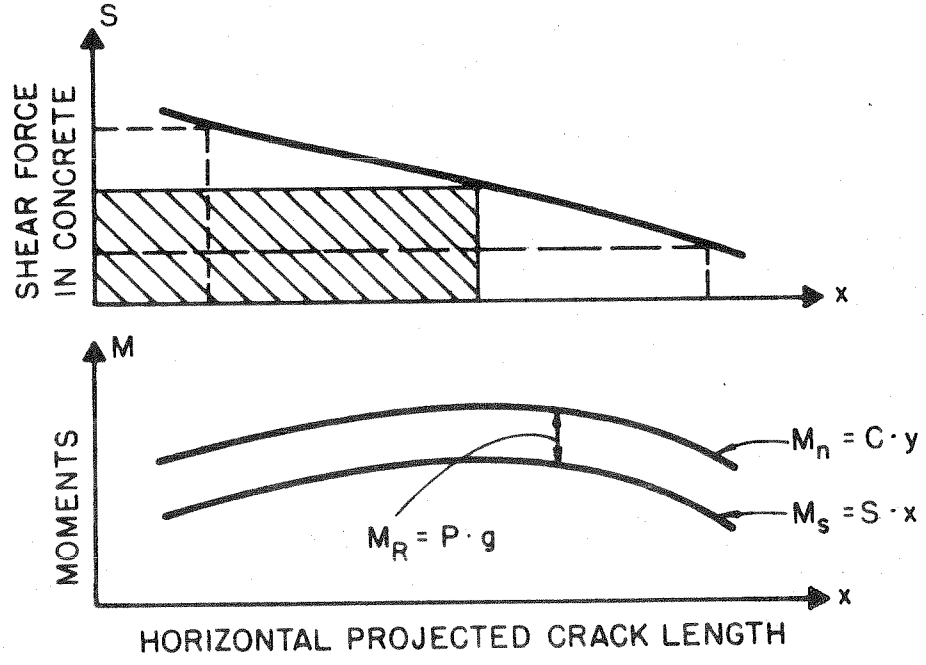


FIG. 5.13 SCHEMATIC REPRESENTATION OF VARIATION OF MOMENTS AS FUNCTION OF HORIZONTAL PROJECTED CRACK LENGTH

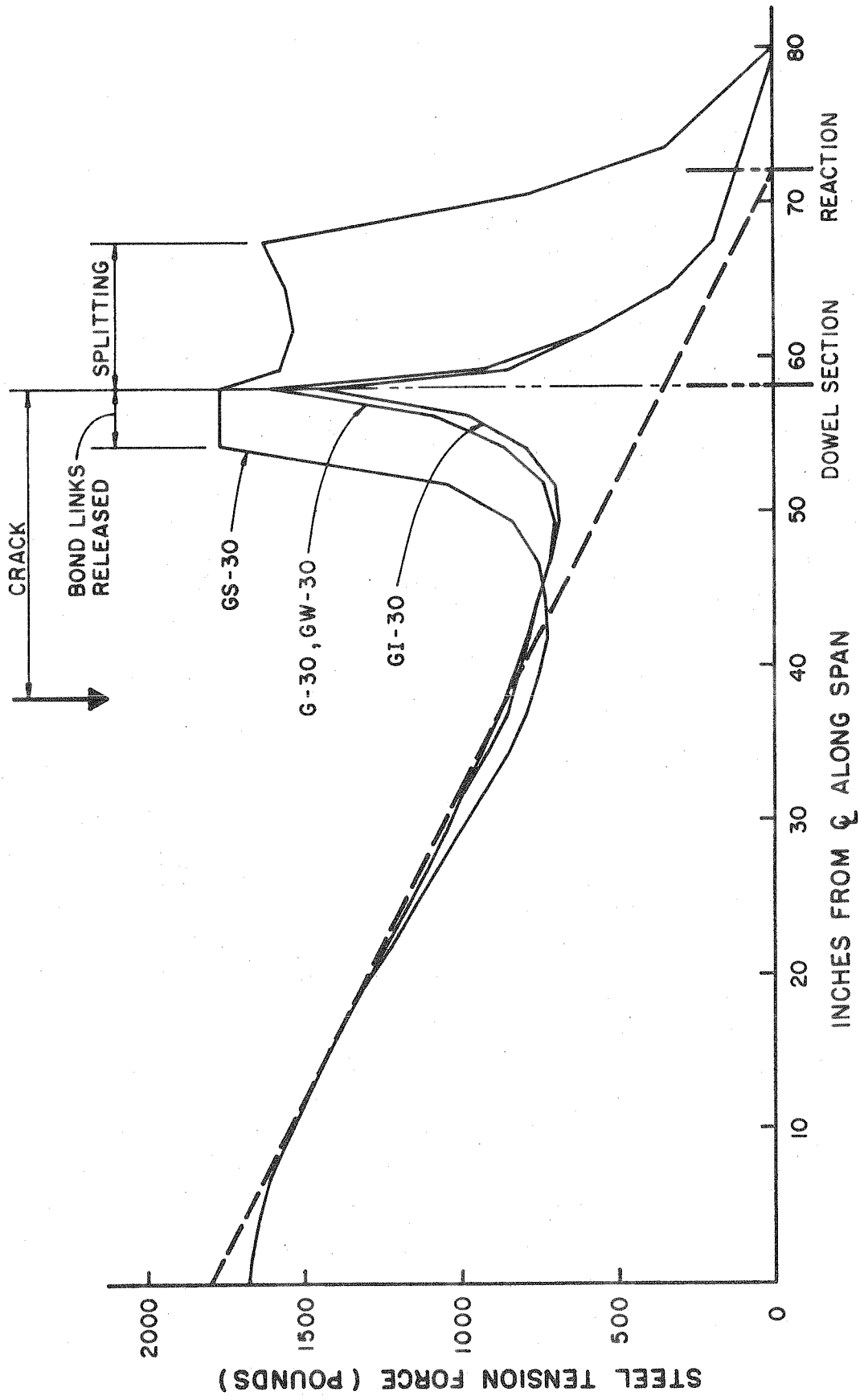


FIG. 5.14 VARIATION ALONG THE SPAN OF TENSILE FORCE IN MAIN REINFORCEMENT

## 5.5 Transverse Shear Forces in Longitudinal Steel Reinforcement

The finite element model presently employed is also capable of providing the transverse forces existing in the longitudinal reinforcement. As in the case of tensile forces, the beams of G- and GW-Series have a very similar pattern of longitudinal variation of these shear forces for the same stage of cracking, except at the dowel section where a marked difference in magnitude occurs. Since the state of forces at the dowel section is of particular interest, such shear forces, called dowel shears, will be presented separately in the next section. To illustrate how these transverse shear forces may vary longitudinally, the values for beams of G-30, GW-30, GI-30, and GS-30 are plotted in Fig. 5.15.

It can be seen that the magnitudes of the shear forces are relatively small in the regions away from the dowel section. Therefore, the shear forces in the longitudinal reinforcement are generally of no major concern in considering the beam strength, except at the dowel section where these shear forces have an important consequence.

Special attention is called to the different magnitudes of the dowel shear forces for the various beams in Fig. 5.15. In constrast to the general belief that aggregate interlock should reduce the dowel shear, Beam GI-30 has the highest value. This increase of dowel shear can be explained by the relative movements of the two concrete blocks found in the finite element analysis and schematically shown in Fig. 5.16(a). As a result of such movements, the force components due to the aggregate interlock are as shown in Fig. 5.16(b), which, in effect, increases the dowel shear and reduces the dowel

tension to maintain proper force equilibrium, see Fig. 5.17 and Fig. 5.18.

The fact that the dowel shear of GW-30 is smaller than that of G-30 in Fig. 5.15 requires little explanation. It is obvious that the web reinforcement of Beam GW-30 has taken part at the total shear force. The even smaller value for Beam GS-30 can be thought of as the consequence of the reduction in the dowel stiffness in resisting shear due to the horizontal splitting. In other words, the effective dowel length (see Section 2.2.5) has been increased. This drop of dowel shear is accompanied by an increase in the dowel tension, see Fig. 5.17 and Fig. 5.18.

## 5.6 Dowel Tensions and Dowel Shears

The longitudinal tensile and transverse shearing forces in the longitudinal steel reinforcement at the dowel section, called dowel tension and dowel shear respectively, are affected considerably by the cracking conditions in the beam specimens. To show this influence, the dowel tension and dowel shear are plotted against the projected horizontal length of the crack in Fig. 5.17 and Fig. 5.18, for all the beams analyzed except Beam GE-30 which cannot be compared because of its elongated span length. Henceforth, Beam GE-30 will not be discussed any further.

From Fig. 5.17, it is observed that the dowel tensions have similar magnitudes for the beams of G- and GW-Series in the early and intermediate stages of cracking. The values, however, depart from each other for the corresponding beams in the two Series as the crack progresses further. The dowel tension of the G-Series begins to

decrease after the horizontal crack length reaches 30 inches, while the GW-Series maintains an approximately constant value. On the other hand, the dowel shear, Fig. 5.18, increases linearly for G-Series, but levels off with a much lower value for GW-Series, after Beam GW-30. For instance, the dowel shear of Beam GW-40 is only about half of Beam G-40.

As pointed out previously, the dowel tension of Beam GS-30 is higher than Beam GI-30, while the reverse is true for the dowel shear. All these variations of dowel tension and dowel shear, shown in Fig. 5.17 and Fig. 5.18, can be explained by the equilibrium requirements for a block, such as the one shown in Fig. 5.12.

Figures 5.17 and 5.18 clearly demonstrate the fact that the behavior of the dowel section is, indeed, a function of many factors. Here, a few of the important parameters affecting this behavior, namely, the crack length, the web reinforcement, the aggregate interlock, and the horizontal splitting, have been clearly illustrated.

## 5.7 Forces in Bond Link Elements

Because of the structure of the bond link used in the finite element analyses, the horizontal and vertical forces existing in the bond link element permit different interpretations for physical meaning. Therefore, they are presented separately. The horizontal bond forces, in pounds per linear inch of the longitudinal reinforcement, are shown in Fig. 5.19 for the beams of G-Series. Since the results for the beams of GW-Series are very similar to those of the G-Series, they are omitted from this report. For comparison purposes, the horizontal bond link forces for beams of G-30, GW-30, GI-30, and

GS-30 are shown in Fig. 5.20.

In both Fig. 5.19 and Fig. 5.20, it can be seen that the horizontal bond forces are very small over the length of the beams except near the dowel section. Furthermore, the pull-out effect, represented by the negative horizontal bond force on the left of the dowel section and the positive bond force on the right, is confined to a rather narrow region. If the model used in this investigation to represent bond in reinforced concrete beams could be considered realistic, then the horizontal bond force distributions obtained would be of considerable interest.

The half century old question of bond as related to the "arch action" in reinforced concrete beams has been again brought up recently by Swamy, Andriopoulos, and Adepegba [20]. In order to have true arch action, a uniform tensile force corresponding to an end-to-end break of bond must exist. Swamy, Andriopoulos, and Adepegba did not find this situation in their experimental investigation of the tensile strain in steel. Complete loss of bond is believed to be rather unlikely for most reinforced concrete beams. The results shown in Fig. 5.19 and Fig. 5.20 could be used to verify this claim. Local destruction of bond is, however, quite possible at the region near the dowel section. Also note that the zone of high horizontal bond force is not greatly changed by the intensity of the cracking. This further suggests that the destruction of bond has a limited spread, even though the beams have a substantial diagonal crack.

The vertical bond link forces furnished by the computer output of the present investigation have no counterpart in known experimental data. In fact, it might be extremely difficult to obtain measurements

of this sort experimentally. In general, these vertical bond forces are small in magnitude, except at the dowel section where they become appreciable. As an illustration, the total vertical bond forces for the beams of G-30, GW-30, GI-30, and GS-30 are shown in Fig. 5.21. The significance of the vertical bond forces is twofold. First, it may initiate or amplify the bond destruction. Second, it may create a horizontal splitting, or the so-called "press down" effect, when the vertical bond force is excessive and the concrete surrounding the steel bars is too weak to sustain this vertical force.

A reinforcing steel bar embedded in concrete and subjected to a vertical load can be considered as a problem of beam on elastic foundation. Viewed from this light, similar wave forms and damping of the amplitudes are visible in Fig. 5.21. It is also known from the beam on elastic foundation problem that the wave length is dependent only on the foundation modulus. In Fig. 5.21, it can be seen that all the beams have approximately the same wave length. This fact might be used to estimate the effective foundation modulus, and to give a better evaluation of the effective dowel length in future beam modeling.

## 5.8 Forces in Stirrups

The maximum forces in each stirrup in the beams of the GW-Series are tabulated in Fig. 5.22. These values usually occur in the segment of stirrup crossing the crack. For ease of visualization, the variations of such stirrup forces for each cracking stage are shown graphically by a set of curves in the same figure.

Note that even though the external shear value was constant within the shear span for all the beam specimens, the stirrup forces are not at all constant, which is somewhat inconsistent to the general belief in practice. Under most present day codes, the stirrups are designed assuming an equal stress in all stirrups crossing a crack. Kani [19] has shown that there are two zones of ineffective web reinforcement; one near the loading point, and the other near the support, shaded areas in Fig. 5.9. The results shown in Fig. 5.22 also indicate near-zero forces in these two zones. Needless to say, much more detailed analytical investigations must be carried out to provide theoretical support to Kani's theory. But one can agree that the function of the web reinforcement and the philosophy behind its design, as re-examined by Kani, certainly deserve further deliberation, and the finite element method employed in this report could be used for this purpose.

## 5.9 Principal Tensions

The magnitude of the principal tension is often used as a cracking criteria. For this reason, the contours of the principal tensions are plotted for the beams of G-30, GW-30, GS-30, and GI-30 in Fig. 5.23 and Fig. 5.24. Since the state of the stress in the regions near the head of the crack and near the dowel section are of special interest, maximum values of the principal tensions in these two regions are plotted in Fig. 5.25 and Fig. 5.26.

No large deviation in the patterns of the principal tensile stress contours can be observed among the beams of G-30, GW-30, and GI-30. Beam GS-30, however, has a moderately high principal tension in the

concrete below the horizontal splitting. At the same time, it has a much higher principal tension near the head of the crack, see Fig. 5.25. This is, again, due to the larger degree of rotation permitted by the horizontal splitting.

The values of maximum principal tensions near the head of the crack have a tendency to decrease as the crack progresses and penetrates deeper into the compressive zone, Fig. 5.25. This is particularly true for the beams of GW-Series. For the beams of G-Series, there is a period of constant maximum principal tension before a decrease in value takes place. It can also be seen in Fig. 5.25 that the values for the beams of GW-Series are smaller than those of G-Series.

The curves plotted for the maximum principal tension in the dowel region, Fig. 5.26, have some interesting characteristics. They show, for the beams of G-Series, a linear increase of maximum principal tension with respect to the projected horizontal crack length, whereas for the beams of GW-Series, the maximum principal tension reaches a flat plateau.

In a real beam, due to the material nonlinearity and other factors, the variation of maximum principal tension near the head of the crack and near the dowel section may not be identical to those presented in Fig. 5.25 and Fig. 5.26. However, the trend is clear, indicating that beams with web reinforcement have a definite advantage over beams without web reinforcement with respect to the magnitude of the maximum principal tensile stresses developed as the diagonal crack propagates. The web reinforcement, besides the other

functions it performs, has the additional benefit of containing the maximum principal tensile stress near the head of the crack and near the dowel region at a lower magnitude. This advantage has not been clearly recognized or demonstrated previously in reinforced concrete beam studies.

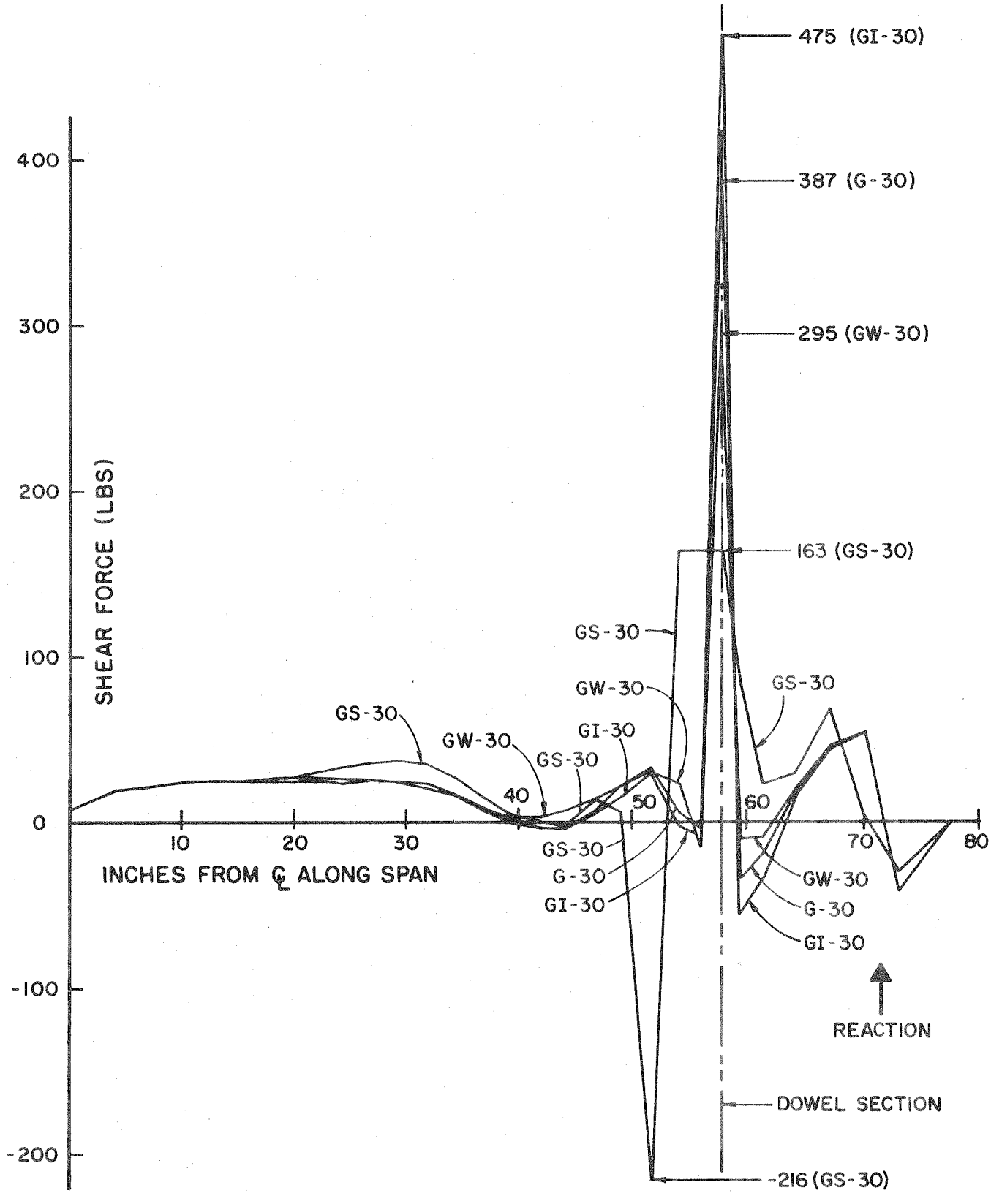


FIG. 5.15 VARIATION ALONG THE SPAN OF TRANSVERSE SHEAR FORCES IN MAIN REINFORCEMENT

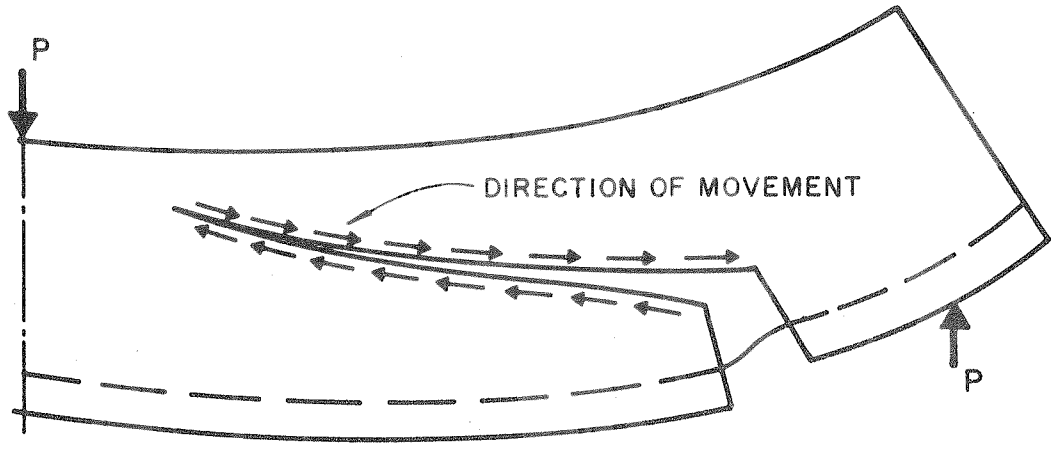


(a) RELATIVE MOVEMENTS ALONG THE CRACK

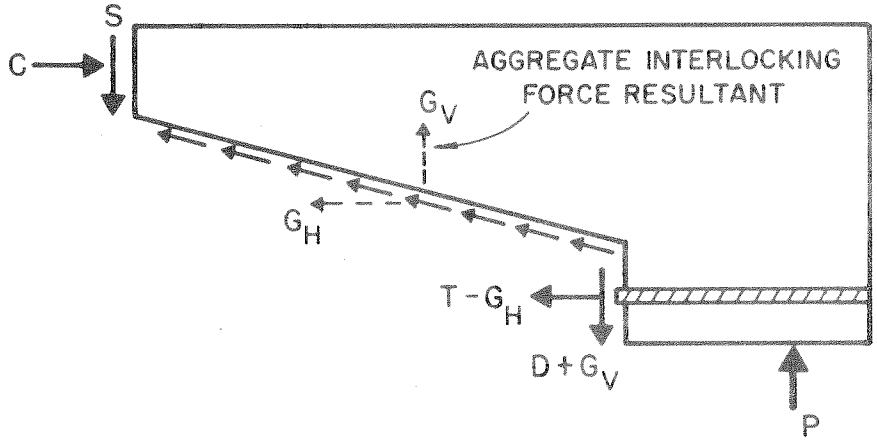


(b) EQUILIBRIUM UNDER AGGREGATE INTERLOCKING

FIG. 5.16 RELATIVE MOVEMENTS AND FORCE EQUILIBRIUM UNDER THE CONDITION OF AGGREGATE INTERLOCKING

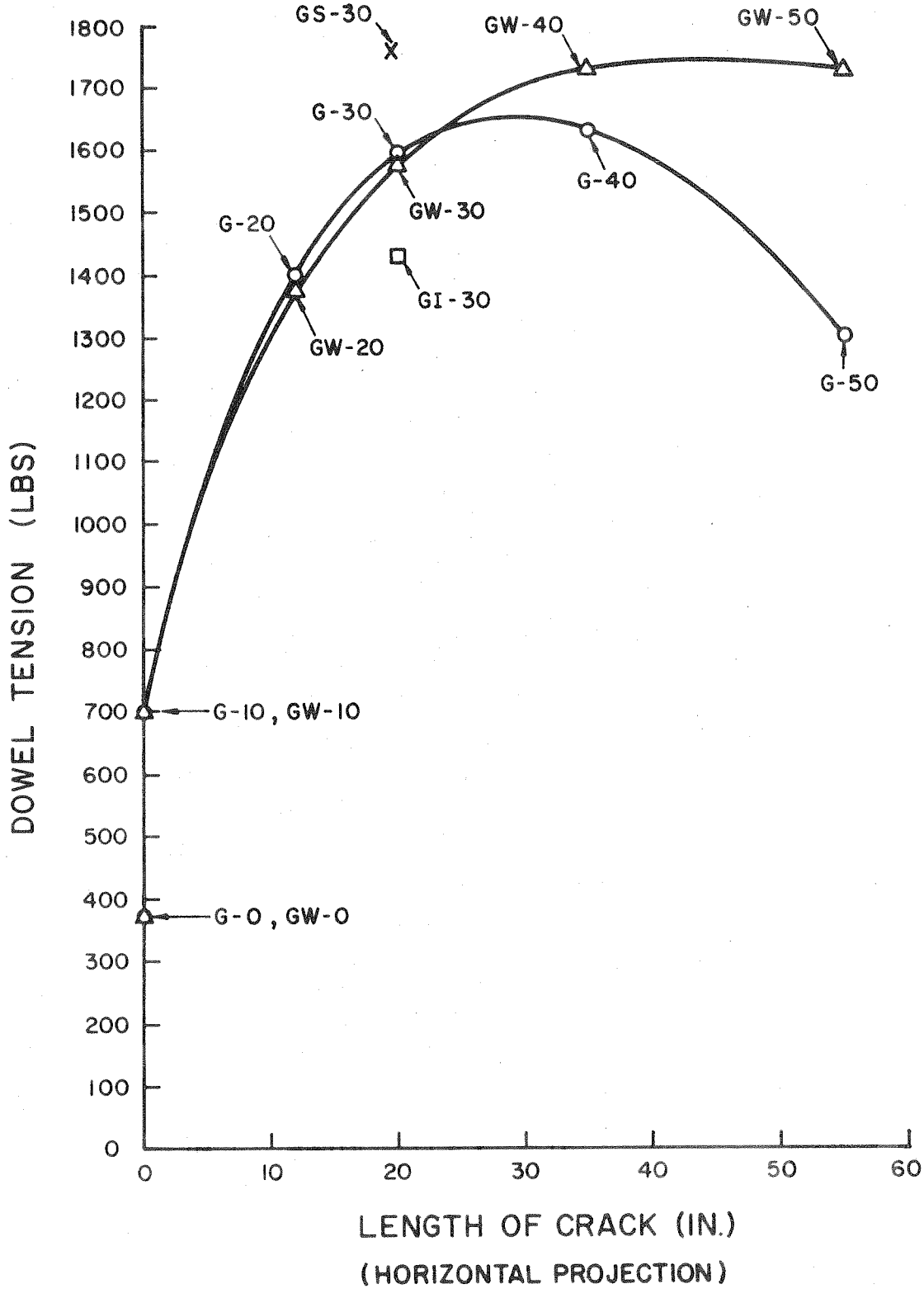


FIG. 5.17 VARIATION OF DOWEL TENSION VS. CRACK LENGTH

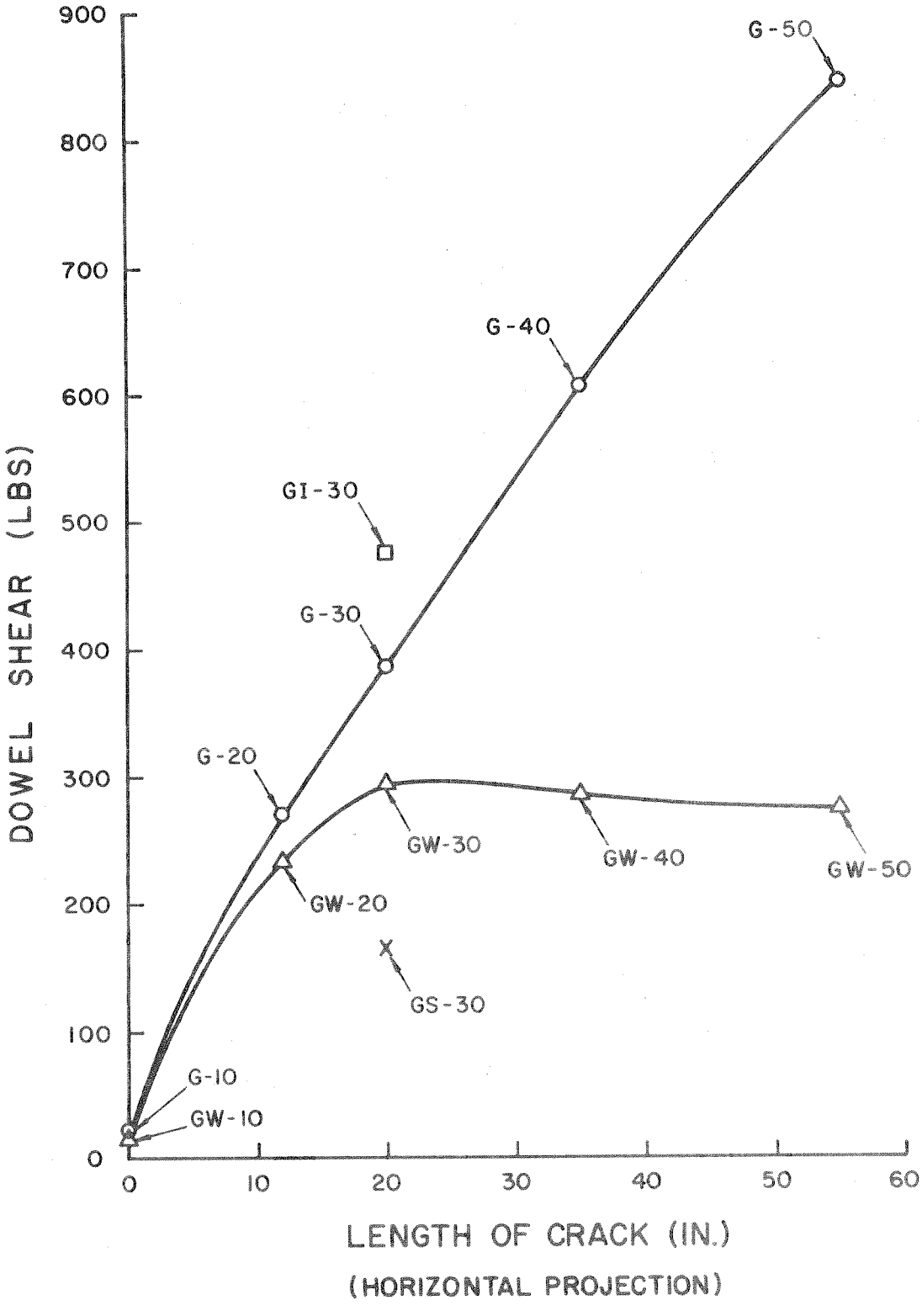


FIG. 5.18 VARIATION OF DOWEL SHEAR VS. CRACK LENGTH

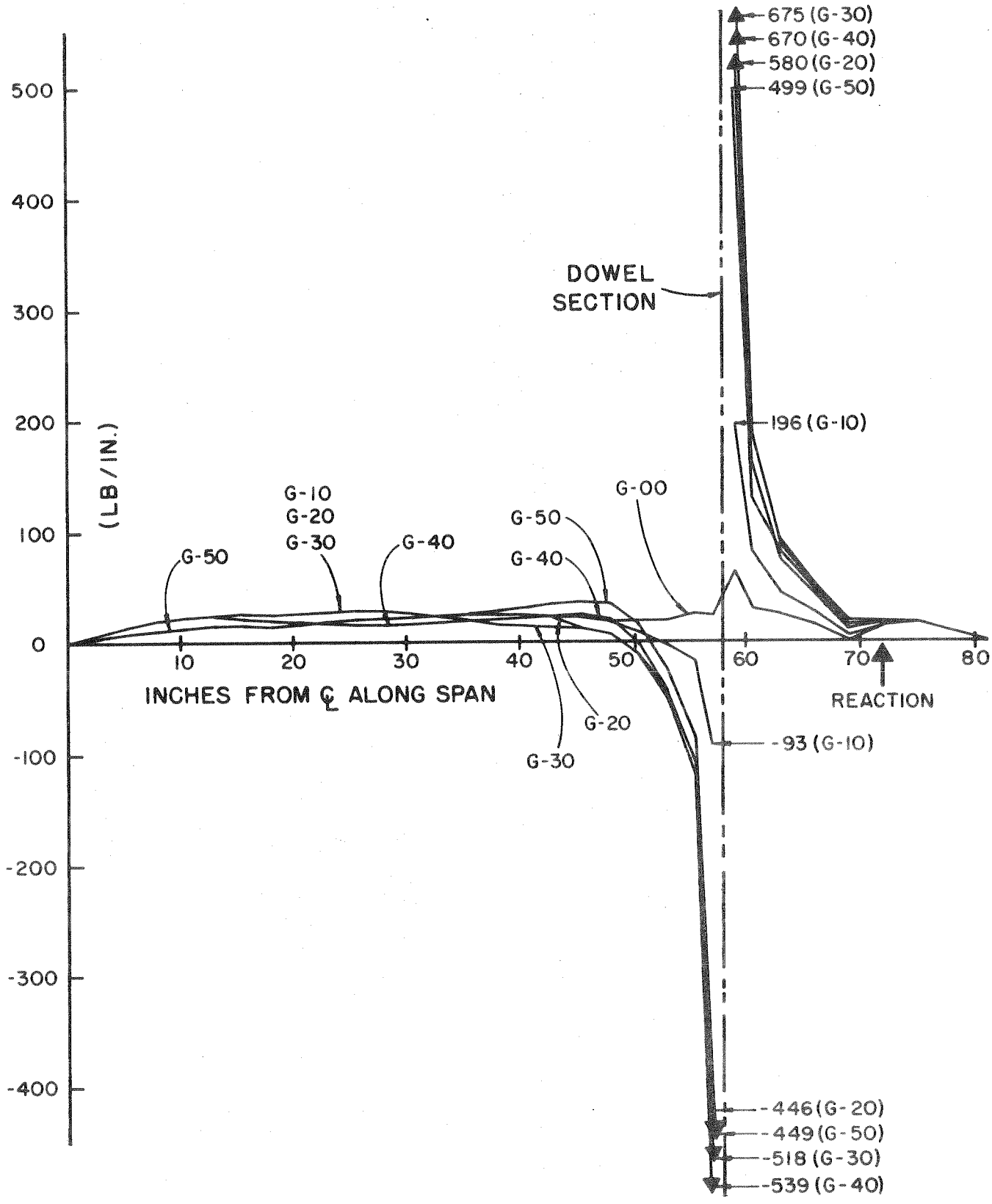


FIG. 5.19 VARIATION ALONG THE SPAN OF HORIZONTAL BOND FORCE FOR BEAMS OF G-SERIES

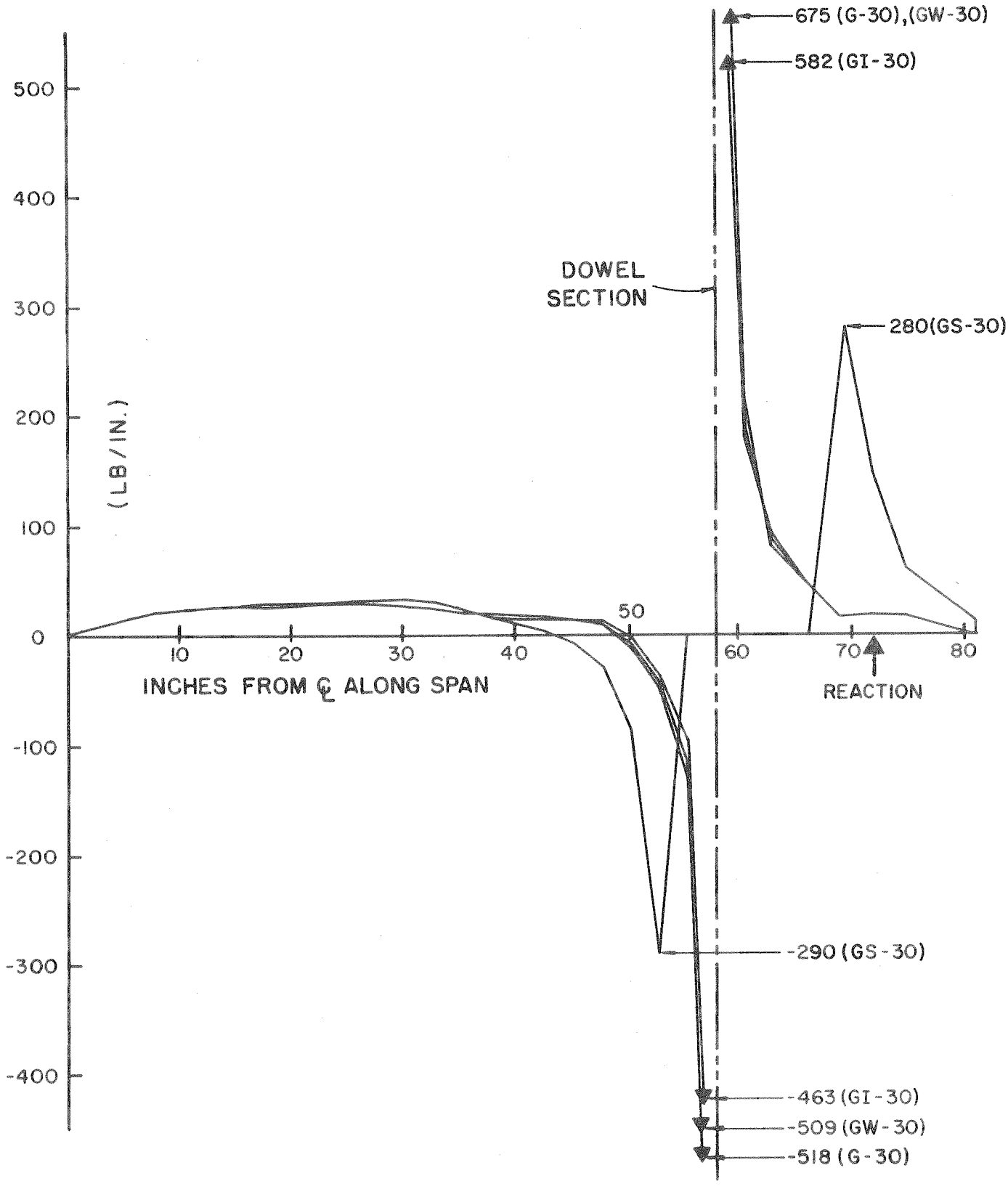


FIG. 5.20 VARIATION ALONG THE SPAN OF HORIZONTAL BOND FORCE FOR BEAMS OF G-30 SERIES

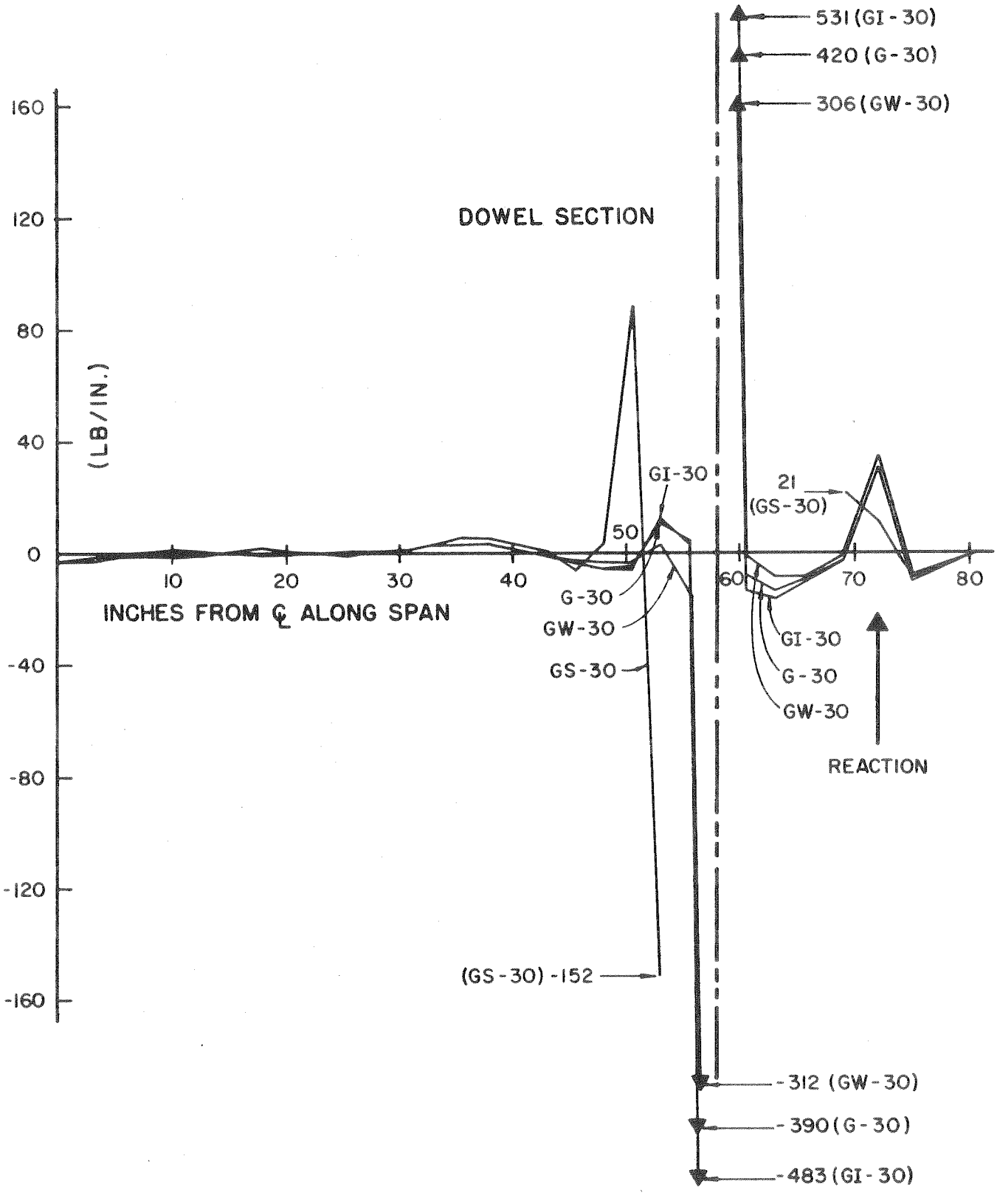


FIG. 5.21 VARIATION ALONG THE SPAN OF VERTICAL BOND FORCE FOR BEAMS OF G-30 SERIES

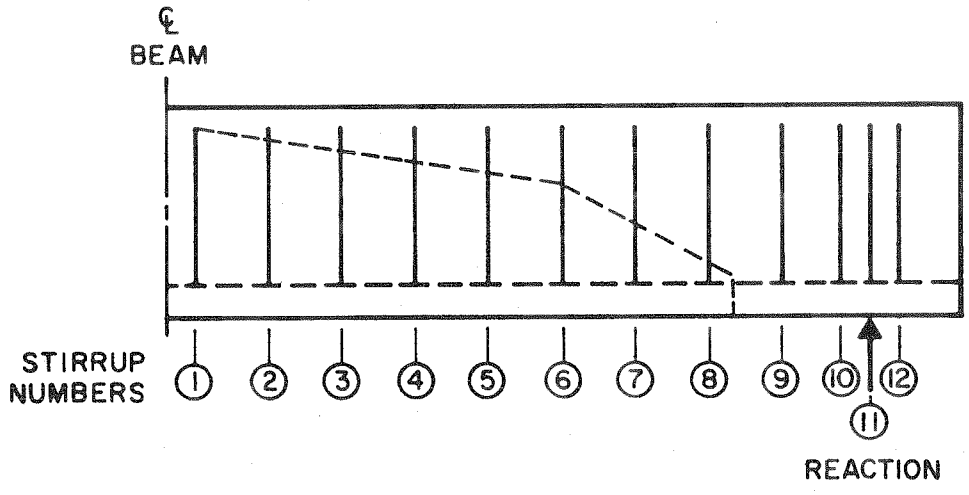


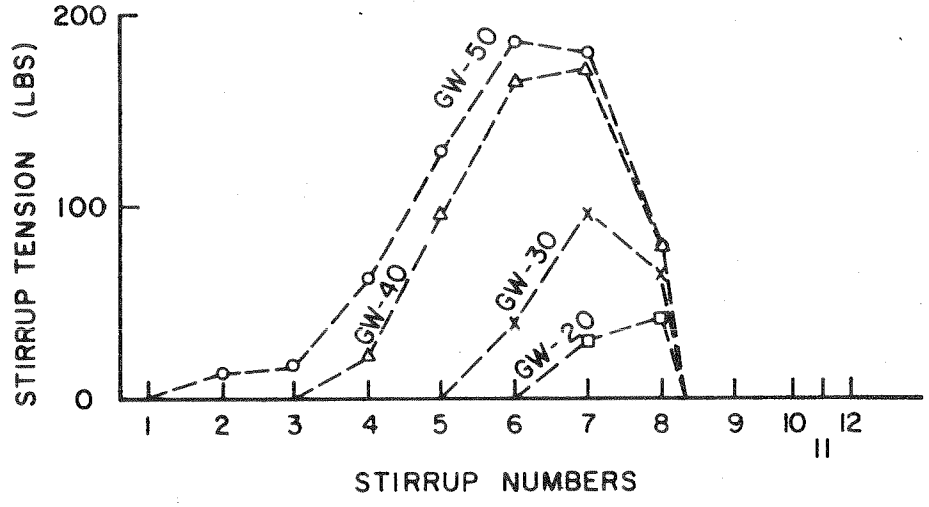


| STIRRUP NO. | 1 | 2 | 3 | 4 | 5 | 6 | 7 | 8 | 9 | 10 | 11 | 12 |
|---|---|---|---|---|---|---|---|---|---|---|---|---|
| GW-50 | 0.8 | 12.4 | 15.5 | 61.3 | 129.3 | 185.0 | 180.0 | 81.4 | – | | | |
| GW-40 | | | – | 23.9 | 98.7 | 166.6 | 172.3 | 81.5 | – | | | |
| GW-30 | | | | | – | 39.1 | 94.6 | 65.6 | – | | | |
| GW-20 | | | | | | – | 30.0 | 42.2 | – | | | |
| GW-10 | | | | | | – | – | – | – | | | |
| GW-00 | | | | | | – | – | – | – | | | |

FIG. 5.22 STIRRUP FORCES FOR GW-SERIES BEAMS

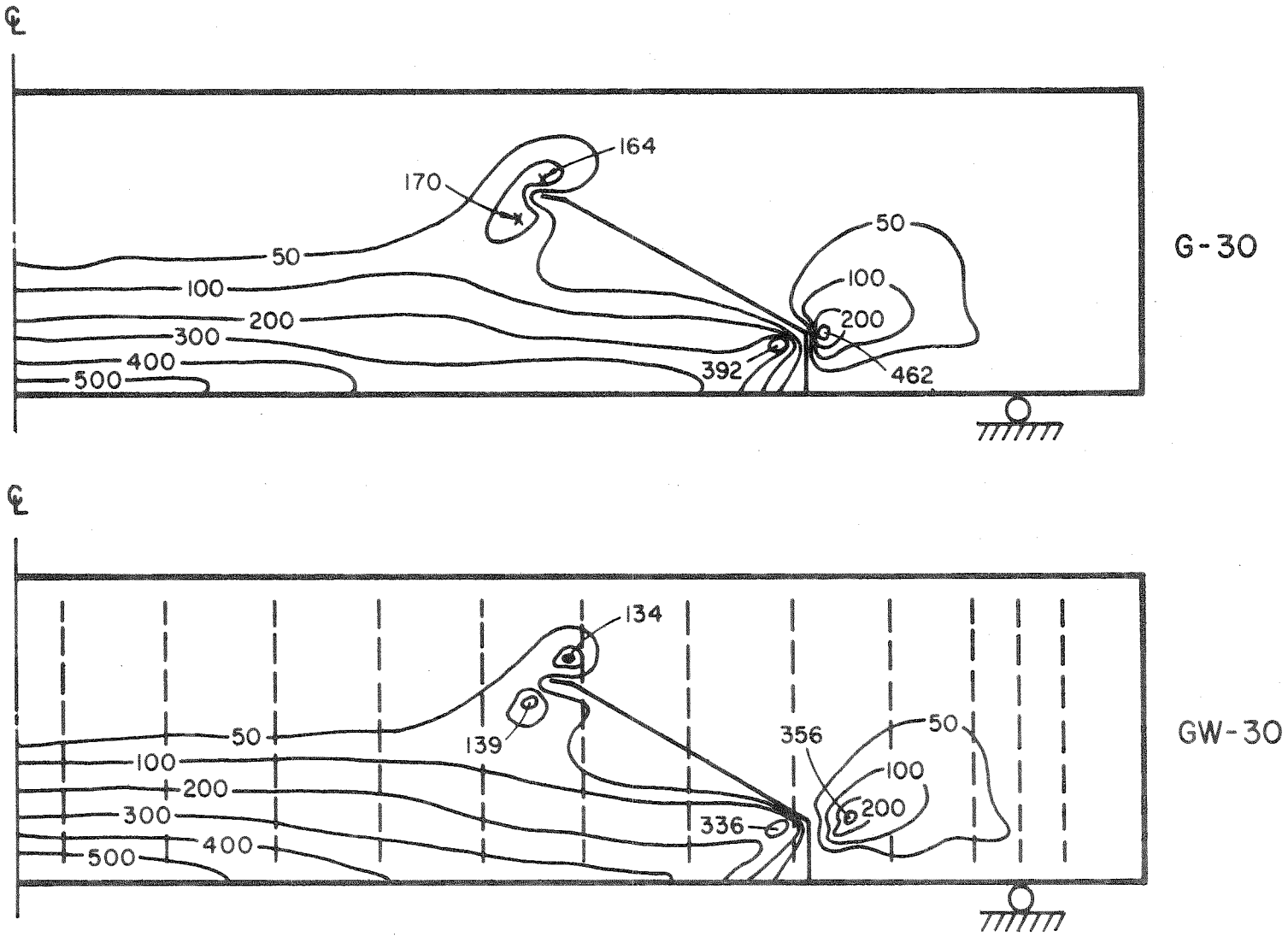


FIG. 5.23 PRINCIPAL TENSILE STRESS CONTOURS

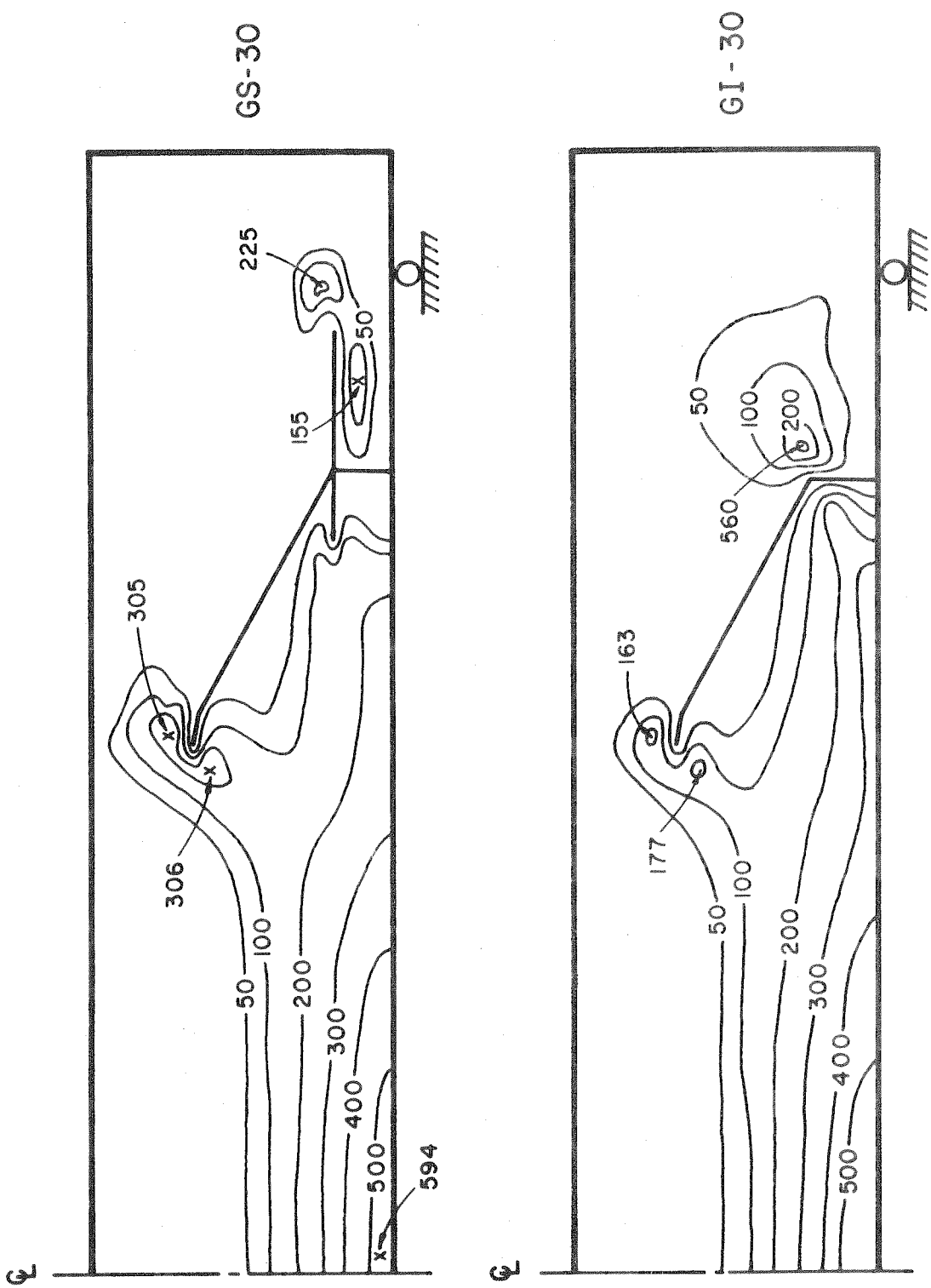


FIG.5.24 PRINCIPAL TENSILE STRESS CONTOURS

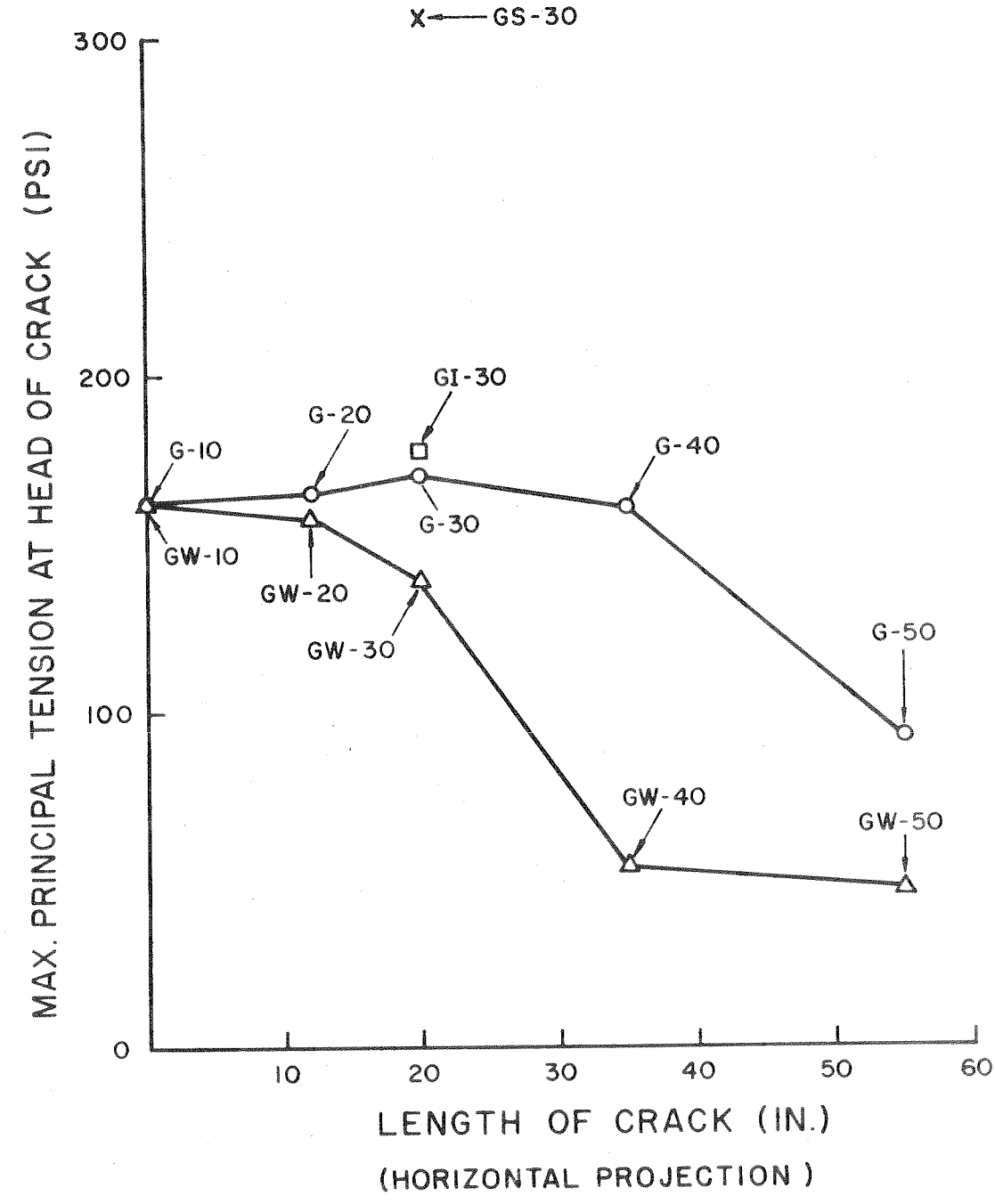


FIG. 5.25 VARIATION OF PRINCIPAL TENSILE STRESS AT THE HEAD OF CRACK VS. CRACK LENGTH

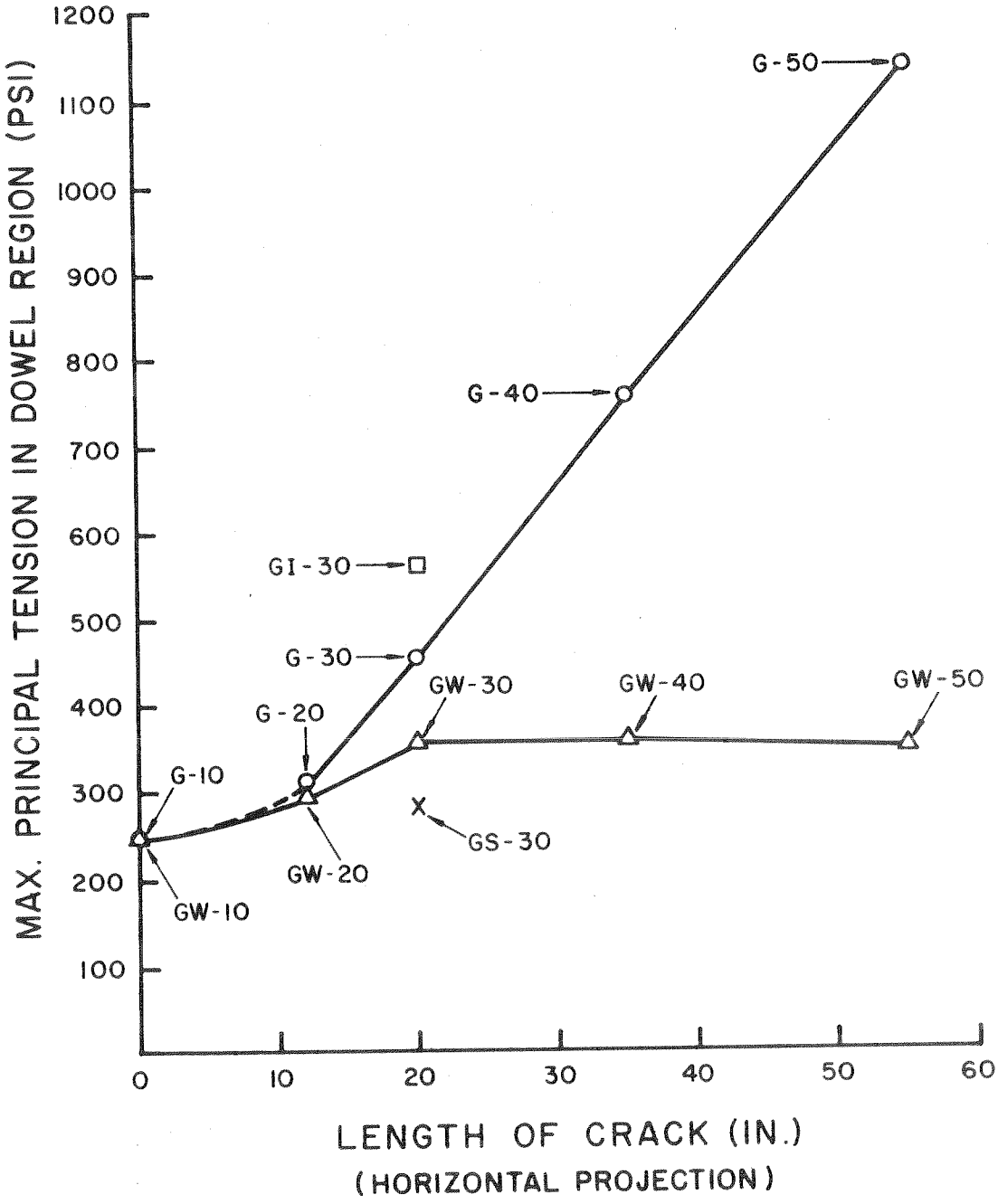


FIG. 5.26 VARIATION OF PRINCIPAL TENSILE STRESS AT DOWEL REGION VS. CRACK LENGTH

# 6. SUMMARY AND CONCLUSION

## 6.1 General Remarks

This exploratory investigation, even though confined to a linear elastic analysis of an artificial model with a single diagonal crack has demonstrated several points of importance:

a) When cracking is at an early stage, the distributions of normal and shearing stresses at a section are almost identical for beams with and without web reinforcement.

b) When the cracking becomes intensive, the longitudinal normal stress at the top fiber of concrete beams decreases for beams without web reinforcement, but increases for beams with web reinforcement. At these cracking stages, a downward shift of the shear stress distributions is observed. This shifting is more for beams without web reinforcement than for beams with web reinforcement. All of this behavior can be explained by the concepts of "arch" action and "beam" action.

c) Horizontal splitting causes the largest stress redistribution. In particular, it reduces significantly the dowel shear.

d) The longitudinal tensile force in the steel reinforcement deviates from the value obtained from beam theory mostly within the region where the crack occurs, especially near the dowel section. This high tensile force at the dowel section does not increase continuously, however, as the diagonal crack progresses. It drops in magnitude at the

most intensive cracking stage.

e) The effect of the aggregate interlock along the crack length was detrimental for the case studied, instead of beneficial as generally believed. It caused an increase instead of a decrease in the dowel shear.

f) Vertical and horizontal forces in the bond link elements have a high magnitude only near the dowel section, with a limited spread. This implies that a complete end-to-end break of bond is unlikely for most reinforced concrete beams.

g) Web reinforcement functions only when there is a crack crossing the web reinforcement. But even at the most intensive stage of cracking, such as Beam GW-50 in this investigation, there are two zones where the web reinforcement is ineffective: one near the applied loading, and one near the support.

h) The magnitude of maximum principal tension in the region near the head of the crack and near the dowel section is smaller for beams with web reinforcement than for those without web reinforcement and this difference becomes greater and greater as the diagonal crack propagates into the compression zone.

## 6.2 A Cyclic Effect of Diagonal Cracking, Aggregate Interlocking, and Horizontal Splitting

From the results of the present investigation, a novel and important relationship involving diagonal cracking, aggregate interlocking, and horizontal splitting can be postulated, which, in part, may shed some light on the behavior of a reinforced concrete beam subjected to shear. Diagonal cracking and horizontal splitting often occur in beams without web reinforcement, see Fig. 3.2. But the inter-

relationship between these two is not clearly understood. An attempt is made below, based on the knowledge gained in the present study, to explain why diagonal cracking is often accompanied by horizontal splitting near the support.

Cracking, particularly of the diagonal type, is inevitable for beams of normal dimensions, because of the weak tensile strength of the concrete. Once the crack starts, dowel action takes place. One of the important features of the dowel action is the dowel shear which helps to carry part of the total shear force. As the external applied load increases, the diagonal crack propagates, which in turn reduces the size of the concrete block above the crack in resisting the shear and also the longitudinal normal compressive forces. Thus the shear force taken by the dowel has to increase. What has been commonly neglected is the effect of aggregate interlock existing along the crack length. This effect of aggregate interlocking has been shown in the example studied in this report to be detrimental in the sense that it increases the dowel shear, even though it reduces somewhat the tensile force in the longitudinal reinforcement. Unless the concrete surrounding the reinforcing bar is strong enough to resist the dowel shear force, horizontal splitting along the longitudinal reinforcement naturally occurs. The effect of this horizontal splitting is to release some of the shear force back to the concrete block, and, at the same time, it increases the tensile force in the longitudinal steel reinforcement. If equilibrium can be attained with this stress redistribution, then the external applied load can be increased, which will start the cycle over once again, by inducing deeper diagonal cracking into the concrete beam. This cycle

is repeated until finally failure occurs either near the head of the concrete block or near the dowel section. The cyclic effect is best summarized in Fig. 6.1.

## 6.3 Suggested Future Studies

There is no doubt that the finite element method of analysis of reinforced concrete beams provides a powerful and relatively economical means of investigation. More detailed studies with refined procedures are certainly possible, and should be pursued, with the hope of arriving at a rational theory for both the analysis and design of reinforced concrete members commonly employed in various types of structures.

The work presented in this report merely marks the beginning of possible studies of this type. The many inherent limitations in the present analytical model cannot be overemphasized, and many improvements need to be incorporated in future studies. Nevertheless, valuable insight into the response of a reinforced concrete beam with a diagonal tension crack has been gained. To make the findings in the present report even more valuable to the engineering profession, the following questions are of immediate interest:

a) Does the material nonlinearity, neglected in the present study, have an important or negligible effect on the beam behavior?

b) What is the influence of multiple cracks occurring in a progressive manner with an accompanying stress redistribution rather than a single pre-defined crack as used in the present study?

c) Can the cyclic effect of the diagonal cracking, aggregate interlocking, and horizontal splitting prove to be a fundamental relationship of reinforced concrete beams, which is capable of offering a rational explanation for the behavior of beams without web reinforcement?

These questions may well be answered by future finite element investigations of reinforced concrete beams.

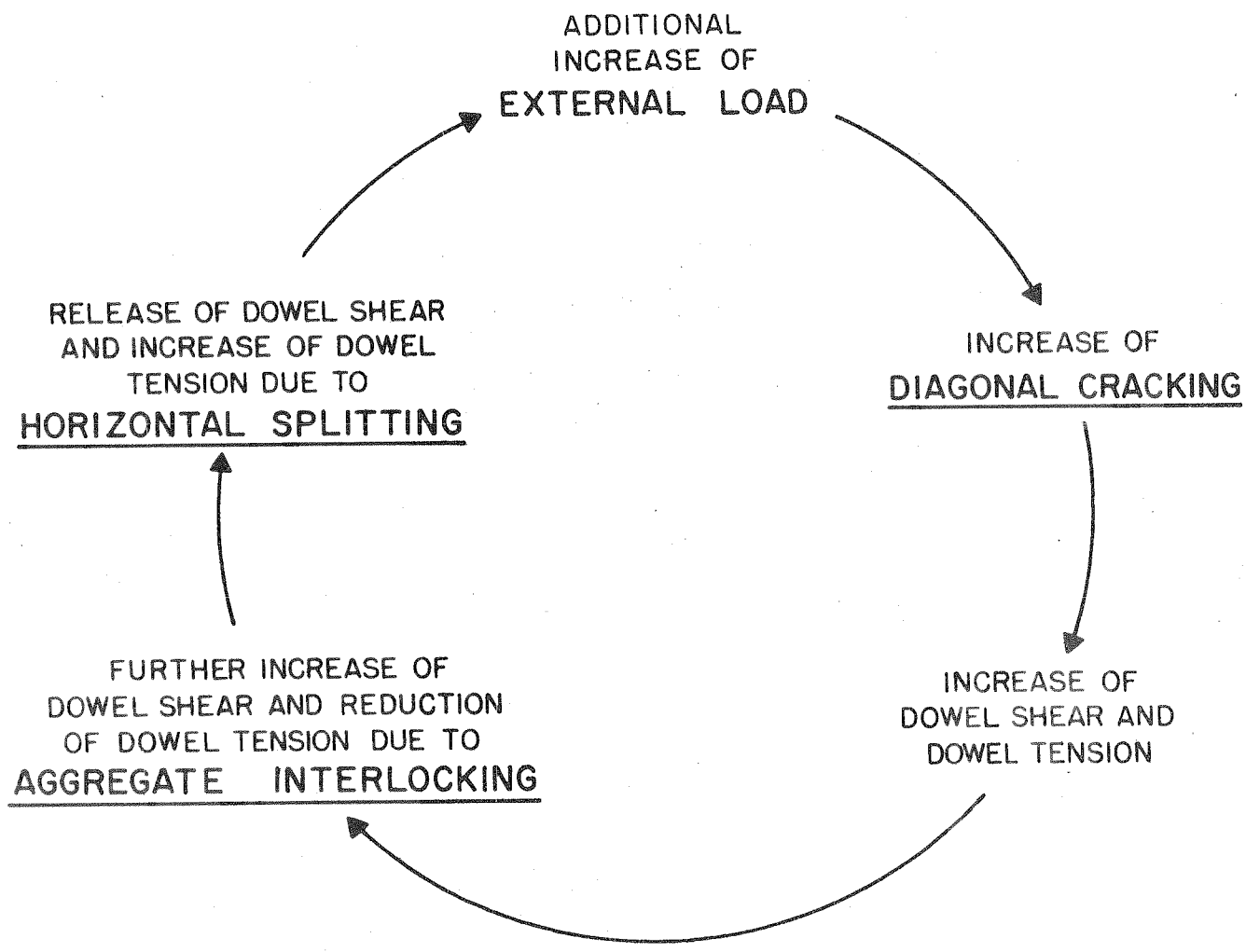


FIG. 6.1 CYCLIC EFFECT OF DIAGONAL CRACKING, AGGREGATE INTERLOCKING AND HORIZONTAL SPLITTING

## 7. ACKNOWLEDGEMENTS

This research investigation was sponsored by the National Science Foundation under Grant GK-1809 and their support is gratefully acknowledged. The Computer Center of the University of California at Berkeley provided facilities for the computer work.

A number of graduate students participated in the computer analyses, data reduction and plotting of results. Special thanks in this respect go to L. N. Davis and C. Y. Liaw.

## 8. REFERENCES


1. ACI-ASCE Committee 326, "Shear and Diagonal Tension," ACI Journal, Proceedings, v. 59, January, February, March 1962, pp. 1-30, 277-334, and 352-396.

2. Bresler, B., and MacGregor, J. G., "Review of Concrete Beams Failing in Shear," Journal of the Structural Division, ASCE, v. 93, no. ST1, Feb. 1967, pp. 343-372.

3. Acharya, D. N., and Kemp, E. O., "Significance of Dowel Forces on the Shear Failure of Rectangular Beams Without Web Reinforcement," ACI Journal, Proceedings, v. 62, no. 10, Oct. 1965, pp. 1265-1278.

4. Bresler, B., and Pister, K. S., "Strength of Concrete Under Combined Stress," ACI Journal, Proceedings, v. 30, Sept. 1958, pp. 321-345.

5. Krefeld, W. J., and Thurston, C. W., "Contribution of Longitudinal Steel to Shear Resistance of Reinforced Concrete Beams," ACI Journal, v. 63, no. 3, March 1966, pp. 325-344.

6. MacGregor, J. G., and Walters, J. R. V., "Analysis of Inclined Cracking Shear in Slender Reinforced Concrete Beams," ACI Journal, Proceedings, v. 64, no. 10, Oct. 1967, pp. 644-653.

7. Bresler, B., and Scordelis, A. C., "Shear Strength of Reinforced Concrete Beams -- Series II," Institute of Engineering Research, Report No. 64-2, University of California, Berkeley, Dec. 1964, 62 pp.

8. Taylor, H. P. J., "Shear Stresses in Reinforced Concrete Beams Without Shear Reinforcement," Technical Report, TRA 407, Cement and Concrete Association, London, Feb. 1968, 23 pp.

9. Reeves, J. S., "The Strength of Concrete Under Combined Direct and Shear Stress," Technical Report, TRA/365, Cement and Concrete Association, London, Nov. 1962, 11 pp.

10. Fenwick, R. C., and Paulay, T., "Mechanisms of Shear Resistance of Concrete Beams," Journal of the Structural Division, ASCE, v. 94, no. ST10, Oct. 1968, pp. 2325-2350.

11. Gergely, P., "Splitting Cracks Along the Main Reinforcement in Concrete Members," Dept. of Structural Engineering, Cornell University, Ithaca, April 1969, 51 pp.

12. Zienkiewicz, O. C., and Cheung, Y. K., "The Finite Element Method in Structural and Continuum Mechanics," McGraw-Hill Co. Ltd., 1967, 272 pp.

13. Wilson, E. L., "Finite Element Analysis of Two-Dimensional Structures," Report 63-2, Dept. of Civil Engineering, University of California, Berkeley, June 1963, 72 pp.

14. Sandhu, R. W., Wilson, E. L., and Raphael, J. M., "Two-Dimensional Stress Analysis with Incremental Construction and Creep," SESM 67-34, Dept. of Civil Engineering, University of California, Berkeley, Dec. 1967, 50 pp.

15. Ngo, D., and Scordelis, A. C., "Finite Element Analysis of Reinforced Concrete Beams," ACI Journal, Proceedings, v. 64, no. 3, March, 1967, 152-163 pp.

16. Nilson, A. H., "Nonlinear Analysis of Reinforced Concrete by Finite Element Method," ACI Journal, Proceedings, v. 65, no. 9, Sept. 1968, pp. 757-766.

17. Franklin, H. A., "Nonlinear Analysis of Reinforced Concrete Frames and Panels," SESM 70-5, Dept. of Civil Engineering, University of California, Berkeley, March 1970, 259 pp.

18. Bresler, B., and Bertero, V., "Influence of Load History on Cracking in Reinforced Concrete," Report to California Division of Highways, Dept. of Civil Engineering, Division of Structural Engineering and Structural Mechanics, University of California, Berkeley, Aug. 1966, 20 pp.

19. Kani, G. N. J., "A Rational Theory For the Function of Web Reinforcement," ACI Journal, Proceedings, v. 66, no. 3, March 1969, pp. 185-197.

20. Swamy, R. N., Andriopoulos, A., and Adepegba, D., "Arch Action and Bond in Concrete Shear Failures," Journal of the Structural Division, ASCE, v. 96, no. ST6, June 1970, pp. 1069-1091.